

# Technical Program for Long-Term Management of Canada's Used Nuclear Fuel – Annual Report 2019

NWMO-TR-2020-01

December 2020

**J. Chen, M. Behazin, J. Binns, K. Birch, A. Blyth, A. Boyer, S. Briggs, J. Freire-Canosa, G. Cheema, R. Crowe, D. Doyle, J. Giallonardo, M. Gobien, R. Guo, M. Hobbs, M. Ion, J. Jacyk, H. Kasani, P. Keech, E. Kremer, C. Lawrence, A. Lee, H. Leung, K. Liberda, T. Liyanage, C. Medri, M. Mielcarek, L. Kennell-Morrison, A. Murchison, N. Naserifard, A. Parmenter, M. Sanchez-Rico Castejon, U. Stahmer, Y. Sui, E. Sykes, M. Sykes, T. Yang, X. Zhang**

Nuclear Waste Management Organization

**nwmo**

NUCLEAR WASTE  
MANAGEMENT  
ORGANIZATION

SOCIÉTÉ DE GESTION  
DES DÉCHETS  
NUCLÉAIRES



**Nuclear Waste Management Organization**

22 St. Clair Avenue East, 4<sup>th</sup> Floor

Toronto, Ontario

M4T 2S3

Canada

Tel: 416-934-9814

Web: [www.nwmo.ca](http://www.nwmo.ca)

# **Technical Program for Long-Term Management of Canada's Used Nuclear Fuel – Annual Report 2019**

**NWMO-TR-2020-01**

December 2020

**J. Chen, M. Behazin, J. Binns, K. Birch, A. Blyth, A. Boyer, S. Briggs, J. Freire-Canosa, G. Cheema, R. Crowe, D. Doyle, J. Giallonardo, M. Gobien, R. Guo, M. Hobbs, M. Ion, J. Jacyk, H. Kasani, P. Keech, E. Kremer, C. Lawrence, A. Lee, H. Leung, K. Liberda, T. Liyanage, C. Medri, M. Mielcarek, L. Kennell-Morrison, A. Murchison, N. Naserifard, A. Parmenter, M. Sanchez-Rico Castejon, U. Stahmer, Y. Sui, E. Sykes, M. Sykes, T. Yang, X. Zhang**

Nuclear Waste Management Organization

### Document History

|                                       |   |       |               |
|---------------------------------------|---|-------|---------------|
| Title:                                | Technical Program for Long-Term Management of Canada's Used Nuclear Fuel – Annual Report 2019   |       |               |
| Report Number:                        | NWMO-TR-2020-01   |       |               |
| Revision:                             | R000  | Date: | December 2020 |
| Nuclear Waste Management Organization |   |       |               |
| Authored by:                          | J. Chen, M. Behazin, J. Binns, K. Birch, A. Blyth, A. Boyer, S. Briggs, J. Freire-Canosa, G. Cheema, R. Crowe, D. Doyle, J. Giallonardo, M. Gobien, R. Guo, M. Hobbs, M. Ion, J. Jacyk, H. Kasani, P. Keech, E. Kremer, C. Lawrence, A. Lee, H. Leung, K. Liberda, T. Liyanage, C. Medri, M. Mielcarek, L. Kennell-Morrison, A. Murchison, N. Naserifard, A. Parmenter, M. Sanchez-Rico Castejon, U. Stahmer, Y. Sui, E. Sykes, M. Sykes, T. Yang, X. Zhang |       |               |
| Reviewed by:                          | P. Gierszewski  |       |               |
| Approved by:                          | D. Wilson   |       |               |



**ABSTRACT**

**Title:** Technical Program for the Long-Term Management of Canada's Used Nuclear Fuel – Annual Report 2019

**Report No.:** NWMO-TR-2020-01

**Author(s):** J. Chen, M. Behazin, J. Binns, K. Birch, A. Blyth, A. Boyer, S. Briggs, J. Freire-Canosa, G. Cheema, R. Crowe, D. Doyle, J. Giallonardo, M. Gobien, R. Guo, M. Hobbs, M. Ion, J. Jacyk, H. Kasani, P. Keech, E. Kremer, C. Lawrence, A. Lee, H. Leung, K. Liberda, T. Liyanage, C. Medri, M. Mielcarek, L. Kennell-Morrison, A. Murchison, N. Naserifard, A. Parmenter, M. Sanchez-Rico Castejon, U. Stahmer, Y. Sui, E. Sykes, M. Sykes, T. Yang, X. Zhang

**Company:** Nuclear Waste Management Organization

**Date:** December 2020

**Abstract**

This report is a summary of activities and progress in 2019 for the Nuclear Waste Management Organization's Technical Program. The primary purpose of the Technical Program is to support the implementation of Adaptive Phased Management (APM), Canada's approach for the long-term management of used nuclear fuel.

The work continued to develop the repository design; to understand the engineered barrier, geological and other processes important to the safety case; and to assess the candidate siting areas.

NWMO continued to participate in international research activities, including projects associated with the Mont Terri Underground Rock Laboratory, the SKB Äspö Hard Rock Laboratory, the Greenland ICE Project, the OECD (Organisation for Economic Co-operation and Development) Nuclear Energy Agency and BIOPROTA.

NWMO's technical program supported technical presentations at national and international conferences, issued 12 NWMO technical reports and published 18 journal articles.

In 2019, NWMO released a summary of its research and development program, RD2019.



## TABLE OF CONTENTS

|   | <u>Page</u> |
|---|-------------|
| <b>ABSTRACT</b> .....   | iv          |
| <b>1. INTRODUCTION</b> .....  | <b>1</b>    |
| <b>2. OVERVIEW OF NWMO TECHNICAL PROGRAMS</b> .....                               | <b>3</b>    |
| <b>3. REPOSITORY ENGINEERING</b> .....  | <b>5</b>    |
| <b>3.1 USED FUEL TRANSPORTATION</b> .....   | <b>5</b>    |
| 3.1.1 Used Fuel Transportation System Development .....                           | 5           |
| <b>3.2 USED FUEL CONTAINER (UFC)</b> .....  | <b>6</b>    |
| 3.2.1 UFC Design .....  | 7           |
| 3.2.2 UFC Serial Production Campaign .....  | 8           |
| 3.2.3 UFC Manufacturing .....   | 10          |
| 3.2.4 UFC Non-Destructive Examination .....                                       | 20          |
| 3.2.5 UFC Testing.....  | 20          |
| 3.2.6 Fuel Integrity during Closure Welding of the UFC .....                      | 22          |
| <b>3.3 SITE AND REPOSITORY</b> .....  | <b>23</b>   |
| 3.3.1 Sealing for Decommissioning and Closure.....                                | 23          |
| 3.3.2 Underground Ventilation System.....   | 25          |
| 3.3.3 Excavated Rock Management Area.....   | 27          |
| 3.3.4 Life Cycle Cost Estimation .....  | 27          |
| <b>4. BUFFER AND SEALING SYSTEMS</b> .....  | <b>28</b>   |
| <b>4.1 EMPLACEMENT EQUIPMENT</b> .....  | <b>28</b>   |
| <b>4.2 EMPLACEMENT EQUIPMENT TESTING</b> .....                                    | <b>28</b>   |
| 4.2.1 Background.....   | 28          |
| 4.2.2 Buffer Box Stacking Trial.....  | 33          |
| 4.2.3 Stacking Trial #2 .....   | 35          |
| <b>4.3 MATERIAL STUDIES</b> .....   | <b>36</b>   |
| 4.3.1 Used Fuel Container Corrosion Studies .....                                 | 36          |
| 4.3.2 Internal Corrosion of UFC .....   | 39          |
| 4.3.3 Microbial Studies.....  | 40          |
| 4.3.4 Bentonite .....   | 41          |
| 4.3.5 Corrosion Modelling .....   | 41          |
| <b>4.4 OTHERS</b> .....   | <b>42</b>   |
| 4.4.1 Reactive Transport Modelling of Concrete-Bentonite Interactions .....       | 42          |
| 4.4.2 Gas-Permeable Seal Test (GAST).....   | 42          |
| 4.4.3 DECOVALEX.....  | 43          |
| 4.4.4 Shaft Seal Properties .....   | 49          |
| 4.4.5 Thermo-hydro-mechanical Modelling of NWMO Placement Room.....               | 50          |
| <b>5. GEOSCIENCE</b> .....  | <b>51</b>   |
| <b>5.1 GEOSPHERE PROPERTIES</b> .....   | <b>51</b>   |
| 5.1.1 Geological Setting and Structure - Bedrock Geology of Southern Ontario..... | 51          |
| 5.1.2 Hydrogeological Properties .....  | 56          |
| 5.1.3 Hydrogeochemical Conditions.....  | 57          |
| 5.1.4 Groundwater and Porewater Compositions.....                                 | 58          |
| 5.1.5 Measuring pH in Highly Saline Groundwaters .....                            | 58          |

|            |   |            |
|------------|---|------------|
| 5.1.6      | Transport Properties of the Rock Matrix.....                                | 63         |
| 5.1.7      | Geomechanical and Thermal Properties.....                                   | 68         |
| <b>5.2</b> | <b>LONG TERM GEOSPHERE STABILITY.....</b>                                   | <b>77</b>  |
| 5.2.1      | Long Term Climate Change – Glaciation.....                                  | 77         |
| 5.2.2      | Groundwater System Stability.....   | 78         |
| 5.2.3      | Seismicity.....   | 79         |
| 5.2.4      | Geomechanical Stability of the Repository.....                              | 82         |
| 5.2.5      | Geoscientific Studies in Support of Geosynthesis.....                       | 87         |
| <b>6.</b>  | <b>REPOSITORY SAFETY.....</b>   | <b>89</b>  |
| <b>6.1</b> | <b>WASTE INVENTORY.....</b>   | <b>89</b>  |
| 6.1.1      | Physical Inventory.....   | 89         |
| 6.1.2      | Radionuclide Inventory.....   | 90         |
| 6.1.3      | Chemical Composition.....   | 90         |
| 6.1.4      | Irradiation History.....  | 90         |
| <b>6.2</b> | <b>WASTEFORM DURABILITY.....</b>  | <b>91</b>  |
| 6.2.1      | Used Fuel Dissolution.....  | 91         |
| 6.2.2      | Solubility.....   | 92         |
| <b>6.3</b> | <b>BIOSPHERE.....</b>   | <b>93</b>  |
| 6.3.1      | General Approach – Post-closure Biosphere Modelling and Data.....           | 93         |
| 6.3.2      | Participation in BIOPROTA.....  | 93         |
| <b>6.4</b> | <b>SAFETY ASSESSMENT.....</b>   | <b>94</b>  |
| 6.4.1      | Pre-closure Safety.....   | 94         |
| 6.4.2      | Post-closure Safety.....  | 97         |
| <b>6.5</b> | <b>MONITORING.....</b>  | <b>99</b>  |
| 6.5.1      | Knowledge Management.....   | 99         |
| <b>7.</b>  | <b>SITE ASSESSMENT.....</b>   | <b>100</b> |
| <b>7.1</b> | <b>IGNACE.....</b>  | <b>100</b> |
| 7.1.1      | Geological Investigation.....   | 100        |
| 7.1.2      | Environmental Assessment.....   | 103        |
| <b>7.2</b> | <b>SOUTH BRUCE/HURON-KINLOSS.....</b>                                       | <b>104</b> |
|            | <b>REFERENCES.....</b>  | <b>105</b> |
|            | <b>APPENDIX A: NWMO TECHNICAL REPORTS AND REFEREED JOURNAL ARTICLES ...</b> | <b>116</b> |
| <b>A.1</b> | <b>NWMO TECHNICAL REPORTS.....</b>  | <b>117</b> |
| <b>A.2</b> | <b>REFEREED JOURNAL ARTICLES.....</b>                                       | <b>119</b> |

**LIST OF TABLES**

|  | <b><u>Page</u></b> |
|--|--------------------|
| Table 3-1: 2019 UFC Serial Production Results.....                       | 9                  |
| Table 6-1: Typical Physical Attributes Relevant to Long-term Safety..... | 89                 |

**LIST OF FIGURES**

|   | <b><u>Page</u></b> |
|---|--------------------|
| Figure 1-1: Illustration of a Deep Geological Repository Reference Design .....   | 2                  |
| Figure 1-2: Interested Community Status as of 31 December 2019 .....  | 2                  |
| Figure 3-1: Interim Storage Facilities and Potential Siting Areas .....   | 5                  |
| Figure 3-2: Illustration of the Used Fuel Container Reference Design .....  | 7                  |
| Figure 3-3: Prototype 2018 UFC Insert Design.....   | 9                  |
| Figure 3-4: Machined Copper Coated Upper Hemispherical Head for UFC Serial Production...  | 10                 |
| Figure 3-5: UFC Weld Cross-Section Showing Unfused Region at Weld Root.....   | 12                 |
| Figure 3-6: Weld Cross-Section of LP-GMAW Sample Showing Wider Weld Root Region .....   | 13                 |
| Figure 3-7: Comparison of the Weld Joint in the Prior Design (Left) and the New Design (Right)<br>.....   | 13                 |
| Figure 3-8: Serial Production Hemi-Spherical Head .....   | 14                 |
| Figure 3-9: Nanovate™ Tank System (NTS).....  | 15                 |
| Figure 3-10: Lower Assembly Optimization Trial .....  | 16                 |
| Figure 3-11: Example of Two Sets of Laser/Particle Jet Relative Positions .....   | 17                 |
| Figure 3-12: Cold Spray Process Using Laser Assistance to Achieve the “Bond Layer” .....  | 18                 |
| Figure 3-13: Copper Particle after Impact on a Steel Surface Having a Temperature of 400°C. 18  |                    |
| Figure 3-14: Scanning Electron Micrographs of Cold-Sprayed Copper in the Axial Direction (Yu<br>et al. 2019) .....  | 19                 |
| Figure 3-15: Example of Hemispherical Head Copper Inspection Results from Zero Degree<br>Ultrasonic Probe.....  | 20                 |
| Figure 3-16: UFC Carbon Steel Material Tensile Test Rig With Heating Chamber And Video<br>Extensometer .....  | 21                 |
| Figure 3-17: UFC Carbon Steel Material Charpy Impact Test Rig .....   | 22                 |
| Figure 3-18: Generic Reference Placement Room Seal for Use in Sedimentary or Crystalline<br>Host Rocks Where Water Control or Gas Venting Is Not Required.....  | 23                 |
| Figure 3-19: Access Tunnel and Ramp Sealing System Concept for Use in Sedimentary or<br>Crystalline Rock .....  | 24                 |
| Figure 3-20: Phased Approach to Closure .....   | 25                 |
| Figure 3-21: Ventilation Infrastructure locations for the Crystalline Repository Layout.....  | 26                 |
| Figure 3-22: APM DGR Design Development Ventilation System Fixed Installation Concepts<br>Surface Exhaust Ventilation Shaft - HEPA Filters General Arrangement - Plans ANS<br>Section .....   | 26                 |
| Figure 3-23: Excavated Rock Management Area Plan .....  | 27                 |
| Figure 4-1: HCB Block .....   | 29                 |
| Figure 4-2: Shaped HCB Block .....  | 29                 |
| Figure 4-3: Buffer Box Assembly.....  | 30                 |
| Figure 4-4: Vacuum Lift HCB .....   | 31                 |
| Figure 4-5: Vacuum Lift UFC.....  | 31                 |
| Figure 4-6: Simulated Emplacement Room with Faux Rock Walls Simulated Drill And Blast<br>Profile. (A) Exterior Steel Frame Approximately 3m X 3m X 15m in Size; (B) Interior With<br>Faux Rock Walls and (C) Actual Blast Profile from Underground Research Laboratory .... | 32                 |

|   |    |
|---|----|
| Figure 4-7: Buffer Box Attachment installed on Versa Lift 25/35.....  | 33 |
| Figure 4-8: Stacked Buffer Box Placement.....   | 34 |
| Figure 4-9: Stacked Buffer Boxes .....  | 34 |
| Figure 4-10: Stacked Buffer Boxes with Fork Pockets (Top assembly) .....  | 35 |
| Figure 4-11: (a) and (b) Schematics of Test Cells for Anoxic Copper Corrosion Investigations in Deionised and Brine Cells Respectively at CanmetMATERIALS; (c) Calculated Copper Corrosion Rates Based On Hydrogen Measurements for Two Deionised Cells and One Concentrated Brine Cell Over Approximately Four Years .....   | 37 |
| Figure 4-12: (a) Experimental Setup for all 18 Pressure Cells Connected to the HPLC Pump. (b) Custom Press Housed Inside an Anoxic Chamber Used to Compress Bentonite to the Desired Density and to Core Bentonite Plugs for Analysis. (c) Sectioned Bentonite Plug Following Removal from Pressure Cell. (d) Dismantled Pressure Cell Following and Experiment Prior to Sectioning ..... | 40 |
| Figure 4-13: Photos of the Test Modules Containing Copper Embedded in Bentonite Clay on the Immersion Platform (a) Prior to Immersion in the Pacific Ocean and (b) During Immersion at 95 m .....   | 41 |
| Figure 4-14: Three-dimensional Layout of the TED Experiment Indicating Heaters and Instrument Boreholes (Armand et al. 2017) .....  | 44 |
| Figure 4-15: Three-dimensional Layout of the ALC Experiment Indicating Heaters and Instrument Boreholes (Armand et al. 2017) .....  | 44 |
| Figure 4-16: Comparison of Temperatures, Pore Pressures, Displacements and Normal Stresses Calculated using the COMSOL Model and the Analytical Solution with a Biot Coefficient of 1.0 .....   | 45 |
| Figure 4-17: Comparison of Calibration COMSOL Model Temperatures (a) and Pore Pressures (b) with Measurement at Different Locations .....   | 45 |
| Figure 4-18: Interpretative Temperatures at Different Locations in the ALC Experiment using Parameters Determined from Calibration Modelling of the TED Experiment with Measurements .....  | 46 |
| Figure 4-19: Diagram of the Facilities of the Cigéo Project.....  | 47 |
| Figure 4-20: Model Geometry of the Base Case with 6 Placement Cells Presented in Detail ....  | 48 |
| Figure 4-21: Comparison of Temperature between Coupled THM COMSOL Model and the Accurate Results at Point P1 and Point P2.....  | 49 |
| Figure 4-22: Dry Densities at Full Water Saturation in the THM Model with Maximum Offset Geometry (Left) and THM Model with a Flux-Limited Water Inflow .....   | 50 |
| Figure 5-1: Published 3-D Model of the Paleozoic Bedrock of Southwestern and Southcentral Ontario, Surficial Sediment Cover Removed (from Carter et al., 2019).....   | 52 |
| Figure 5-2: Target Locations for Sample Collection and Structural Mapping .....   | 53 |
| Figure 5-3: Target Locations for Sample Collection and Structural Mapping .....   | 54 |
| Figure 5-4: Ce Anomaly Cross Plot for Different Types of Dolomite .....   | 55 |
| Figure 5-5: Isotope Diagram of Porewaters Extracted from Crystalline Rock .....   | 59 |
| Figure 5-6: Cuboidal Sample of the Lac Du Bonnet Granite from the Canadian Shield .....   | 64 |
| Figure 5-7: Schematic View of the Experimental Facility .....   | 64 |
| Figure 5-8: 2 SPNE SC/CE Model Simulation of Sorption of Se(-II) on MX-80 (Left) and Illite (Right) .....   | 66 |
| Figure 5-9: Correlation Between BET Surface Area and CEC (Expressed by Brobe Consumption).....  | 68 |
| Figure 5-10: Sample of the Dry Lac du Bonnet Granite Prepared for Uniaxial Testing .....  | 70 |
| Figure 5-11: New Shear Testing Equipment Integrated with Existing Laboratory Load Frame ..  | 72 |
| Figure 5-12: MoFrac-DFN transformed in PyRockMass Tool Being Developed as Part of Rock Mass Effective Properties project. ....  | 74 |
| Figure 5-13: One DFN realization with several values of Lc .....  | 75 |

|   |     |
|---|-----|
| Figure 5-14: Local Stress Tensors .....   | 76  |
| Figure 5-15: Seismograph Stations in Northern Ontario, 1995-2018 .....  | 80  |
| Figure 5-16: Earthquakes in Northern Ontario, 1982–2018 .....   | 80  |
| Figure 5-17: Map showing the locations of l'argile and McArthur lakes, Quebec .....   | 81  |
| Figure 5-18: (Left) Definition of EDZ Domains Using Discontinuum Model Indicators. (b) Sensitivity of EDZ Mode (Extension Vs Shear) and Extent, to Stress Level and Rock Properties.....  | 83  |
| Figure 5-19: Sensitivity of Discontinuum EDZ Development to Pre-existing Structure and Stress Ratio (Finite Element Discrete Element Hybrid Model). .....   | 84  |
| Figure 5-20: Progression from Laser Or 3D Photoscans Of Direct Shear Discontinuity Samples, through to Geometrically Realistic 3D Discontinuum Model ff Shear Test. ....  | 84  |
| Figure 5-21: (Top) Installation of Fibre-Optic Sensor for Full Sample Coverage of Lateral Strain - Strain Map At Yield For Limestone Sample Shown in the Middle Image. (Bottom) Strain Maps For Granite Samples at Different Stress Levels Showing Different Failure Modes Developing in the Test (from Platen Induced Chipping at Left, Spalling in the Middle and Shearing at Right). ..... | 85  |
| Figure 5-22: Map of Potential Petroleum Resources in Southern Ontario.....  | 88  |
| Figure 6-1: High Level Step-Wise Approach in Climate Change Impacts Study .....   | 96  |
| Figure 7-1: Borehole IG_BH02 Site, Summer 2019.....   | 100 |
| Figure 7-2: Examining Core from Ignace Boreholes .....  | 102 |
| Figure 7-3: Ignace Wabigoon - Location of Borehole Sites 1 to 6 and Area of Interest 1 and 2 .....  | 103 |

## 1. INTRODUCTION

The Nuclear Waste Management Organization (NWMO) is implementing Adaptive Phased Management (APM) for the long-term management of used nuclear fuel. This is the approach recommended in *“Choosing a Way Forward: The Future Management of Canada’s Used Nuclear Fuel”* (NWMO 2005) and selected by the Government of Canada in June 2007.

The technical objective of the APM approach is a Deep Geological Repository (DGR) that provides long-term isolation and containment, to ensure safety of people and the environment while the radioactivity in the used fuel decays.

The deep geological repository is a multiple-barrier system designed to safely contain and isolate used nuclear fuel over the long term. It will be constructed at a depth of approximately 500 metres, depending upon the geology of the site, and consist of a series of tunnels leading to a network of placement rooms where the used nuclear fuel will be contained using a multiple-barrier system. A conceptual design for a DGR is illustrated in Figure 1-1 for a generic rock setting (the design will be varied for actual crystalline or sedimentary rock conditions).

The NWMO is presently in the Site Selection phase. No site has been selected to host the DGR. The process for selecting a host community is described in *“Moving Forward Together: Process for Selecting a Site for Canada’s Deep Geological Repository for Used Nuclear Fuel”* (NWMO 2010). The steps for evaluating the geological suitability of willing and informed host communities consists of: a) initial screenings to evaluate the suitability of candidate sites against a list of preliminary screening criteria, using readily available information; b) preliminary assessments to further determine if candidate sites may be suitable for developing a safe used fuel repository; and c) detailed field investigations to confirm suitability of one site.

Initially, 22 communities had expressed interest in the program. By 2019 the number of communities engaged in the site selection process had been narrowed to three, Ignace, Huron-Kinloss and South Bruce, based on preliminary desktop assessments of potential geological suitability and potential for the project to contribute to community well-being. The status of each community as of December 2019 is shown in Figure 1-2. All reports completed are published on the NWMO’s site selection website ([http://www.nwmo.ca/sitingprocess\\_feasibilitystudies](http://www.nwmo.ca/sitingprocess_feasibilitystudies)).

The NWMO continues to conduct technical work to support design, site assessment and safety case for a DGR, in parallel with work to engage with and establish a partnership with communities. This report summarizes technical work conducted in 2019. In the near term, this information will support selection of a preferred site by 2023. In the longer term, this will support an impact assessment and licence application at the selected site. NWMO’s overall implementation plan is described in *Implementing Adaptive Phased Management 2019-2023* (NWMO 2019).

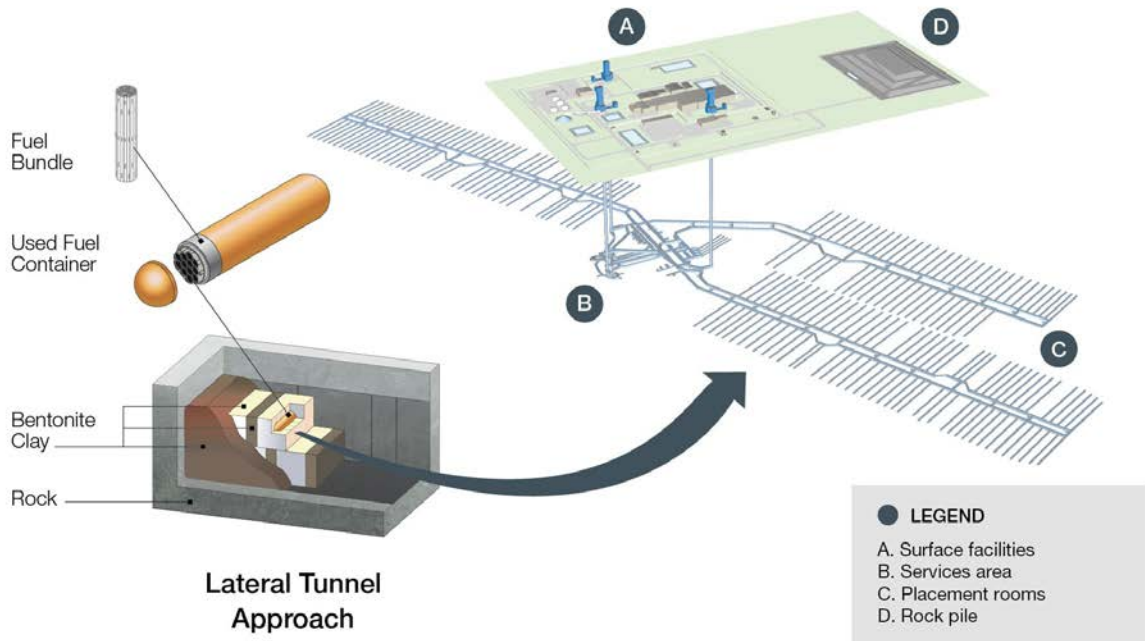


**Figure 1-1: Illustration of a Deep Geological Repository Reference Design**



**Figure 1-2: Interested Community Status as of 31 December 2019**

## 2. OVERVIEW OF NWMO TECHNICAL PROGRAMS

The APM Technical Program includes site investigations, preliminary design and proof testing, and developing the safety case for a used fuel DGR. Work conducted during 2019 is summarized in this report. Prior year work is summarized in Chen et al 2018.

The work is summarized in the following sections divided into Engineering, Geoscience, Repository Safety, and Site Assessment.

This work involved 18 universities, as well as a variety of industrial and governmental research partners. A list of the 2019 technical reports produced by NWMO is provided in Appendix A.1. Appendix A.2 provides a list of journal articles on work supported by NWMO.

An important aspect of the NWMO's technical program is collaboration with radioactive waste management organizations in other countries. In 2019, the NWMO had formal agreements with ANDRA (France), INER (Taiwan), KORAD (South Korea), NAGRA (Switzerland), NDA (United Kingdom), NUMO (Japan), ONDRAF (Belgium), POSIVA (Finland), and SKB (Sweden) to exchange information arising from their respective national programs to develop a deep geologic repository for nuclear waste.

Some of this collaboration is work undertaken at underground research facilities. In 2019, NWMO supported projects at the Mont Terri Underground Rock Laboratory in Switzerland, the SKB Äspö Hard Rock Laboratory in Sweden, the ONKALO facility in Finland, and the Grimsel Test Site (GTS) in Switzerland. These provide information in both crystalline (Äspö, ONKALO, GTS) and sedimentary (Mont Terri) geological environments.

NWMO was involved with the following joint experimental projects in 2019:

- POST Project (Fracture Parameterization for Repository Design & Post-closure Analysis) at Äspö and ONKALO;
- Full-scale In Situ System Test (FISST) demonstration project at ONKALO;
- Deep Borehole Experiment (DB, DB-A) at Mont Terri;
- Long-term Diffusion experiment (DR-B) at Mont Terri;
- Full Scale Emplacement Experiment (FE-G, FE-M) at Mont Terri;
- Hydrogen Transfer (HT) test at Mont Terri;
- Iron Corrosion – Bentonite (IC-A) test at Mont Terri;
- Long-term Pressure Monitoring (LP-A) at Mont Terri;
- Microbial Activity (MA) at Mont Terri;
- Materials Corrosion Test (MaCoTe) at GTS;
- Gas-Permeable Seal Test (GAST) at GTS;
- Enhanced Sealing Project (ESP) at Whiteshell Labs, Canada.

The NWMO also collaborated with NAGRA, SKB and POSIVA on an ice drilling project (ICE) to establish constraints on the impact of ice sheets on groundwater boundary conditions at the ice-bed contact.

The NWMO continued to participate in the international radioactive waste management program of the Organisation for Economic Co-operation and Development (OECD) Nuclear Energy Agency (NEA). Members of this group include the major nuclear energy countries, including waste owners and regulators. NWMO participated in the following NEA activities:

- Radioactive Waste Management Committee (RWMC);
- Integration Group for the Safety Case (IGSC);
- Working Group on the Characterization, the Understanding and the Performance of Argillaceous Rocks as Repository Host Formations (i.e., Clay Club);
- Expert Group on Geological Repositories in Crystalline Rock Formations (i.e., Crystalline Club);
- Expert Group on Operational Safety (EGOS);
- Thermodynamic/Sorption Database Development (TDB) Project; and
- Preservation of Records, Knowledge and Memory (RK&M) Project.

The NWMO also continued its participation in DECOVALEX and BIOPROTA. DECOVALEX is an international working group on Thermal-Hydraulic-Mechanical (THM) modelling. NWMO participated in the Task E on modelling a heater experiment in the clay rock at the Andra Bure underground facility. BIOPROTA is an international working group on biosphere modelling. The main projects in 2019 were the C-14 Project and the BIOMASS 2020 Update.

A significant project in 2019 was the preparation of RD2019 - NWMO's Program for Research and Development for Long Term Management of Used Nuclear Fuel (NWMO 2019). This report describes the major technical research and development activities of the NWMO. It is complementary to NWMO activities in site selection, site characterization, design and engineering proof testing, and considers the full lifecycle of the repository. A key point is that underlying science studies will continue throughout the repository phases in order to support future licence decisions. The report reviews the general status of understanding of used nuclear fuel properties, used fuel containers, sealing materials, geological processes, and safety assessment. It identifies directions for future research and development.

### 3. REPOSITORY ENGINEERING

Research and development progressed in the Repository Engineering program during 2019. Primary areas of work included: used fuel recovery and transport, used fuel container design, fabrication and corrosion tests, buffer and sealing systems and microbial studies of the sealing systems. Summaries of these activities are provided in the following sections.

#### 3.1 USED FUEL TRANSPORTATION

##### 3.1.1 Used Fuel Transportation System Development

Canada's used nuclear fuel is currently safely managed in facilities licensed for interim storage. These facilities are located at nuclear reactor sites in Ontario, Quebec and New Brunswick, as well as Atomic Energy of Canada's sites at Whiteshell Laboratories in Manitoba and Chalk River Laboratories in Ontario. Managing all of Canada's used nuclear fuel in a single repository location will require the transport of used nuclear fuel from these interim storage facilities to the central location of the DGR.

NWMO is currently in a site selection process for the repository and has narrowed its focus to three potential siting areas: the Township of Ignace in Northwestern Ontario; and the Municipalities of Huron-Kinloss and South Bruce in Southern Ontario. The map illustrates the locations of the interim storage facilities as well as identifies the potential siting areas (see Figure 3-1).



**Figure 3-1: Interim Storage Facilities and Potential Siting Areas**

As part of its responsibility for the long-term management of Canada's used nuclear fuel, the NWMO will be responsible for transporting used fuel to the selected repository site. Based on current projections and announced life plans for the reactor fleet, approximately 5.5 million bundles will need to be transported to the repository site from these interim storage facilities. Technical, operational and cost evaluations of options for used fuel transportation systems for these two potential siting areas are ongoing. Key components of the used fuel transportation system include:

- transportation modes;
- conveyances and fleets;
- routing;
- transportation infrastructure;
- interfacing facility infrastructure at interim storage facilities and at the DGR;
- transportation packages;
- nuclear security/escort requirements;
- emergency response and recovery requirements;
- logistics, i.e. cycle times including transit times and non-transit times for on- and off-loading of transport packages;
- operations, i.e. operations at facilities, operations during transport for modes of transport, escort operations, communication, tracking and monitoring.

Analysis of key components (listed above) are ongoing, and continued to be a focus of study from 2018 into 2019. The objective is to compare options for transportation systems including modes (i.e. all-road, and road-rail combination), package designs, and operational considerations taking into account the two potential siting areas. This work will support and provide a basis to the 2021 Life Cycle Cost Estimate.

### **3.2 USED FUEL CONTAINER (UFC)**

In 2019, the NWMO further advanced the Proof Test Program to validate the reference design of the Used Fuel Container (UFC), as illustrated in Figure 3-2, with a focus on its manufacturability. The UFC Serial Production campaign, launched in 2018 as part of this effort, progressed well and has started to drive changes to the existing design and the manufacturing processes. New developments in the UFC design, manufacturing and examination are summarized in the subsections below.

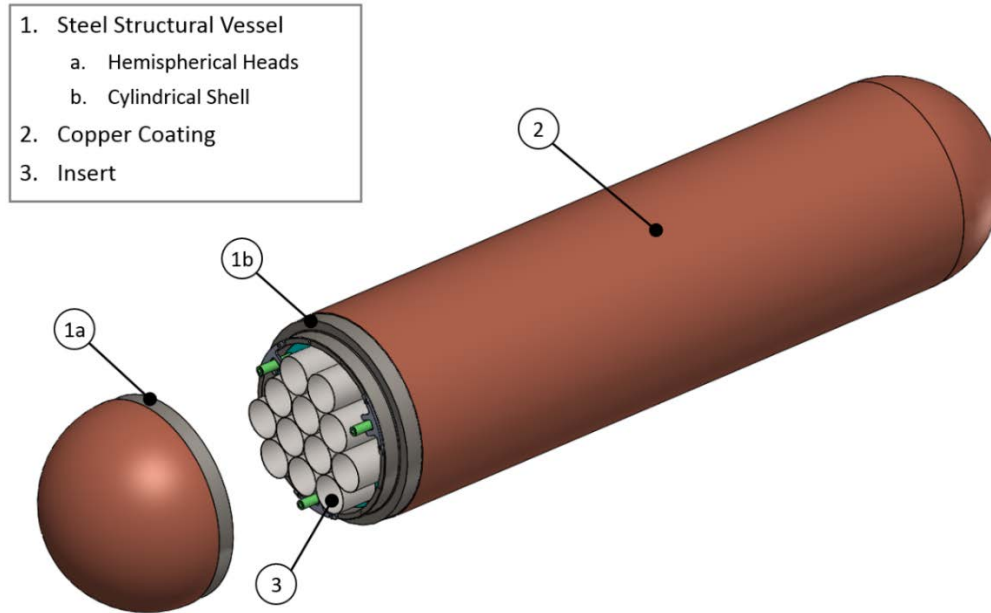


**Figure 3-2: Illustration of the Used Fuel Container Reference Design**

### 3.2.1 UFC Design

#### 3.2.1.1 Evolution of the UFC Design Methodology

The UFC design has reached the prototype demonstration stage and will remain at this stage until specific engineering details of the selected DGR site become known. Key documents detailing the reference UFC design have been completed, including the UFC design specification, material specifications and a set of design qualification documents, to use until the DGR site is selected and site-specific design inputs become available. The preliminary design was reviewed by technical experts from the Canadian Nuclear Safety Commission (CNSC) in a pre-licensing technical review in 2018. A number of gaps between the current UFC design and existing regulatory requirements were identified. This review was not for licensing purposes (i.e. certification) but helps the NWMO improve the design and documentation to achieve a licensable UFC product. The NWMO continues to refine its design approach to address these gaps.

A comprehensive review was undertaken in 2019 of the existing guidance on the detailed design of high-level nuclear waste disposal facilities, including relevant IAEA requirements and guidance documents, Canadian regulatory documents and relevant technical codes and standards. The results of the review were published in a conference paper addressing the new basis of the UFC design methodology and various key design requirements (Zhang et al., 2019).

The NWMO actively participates in the development of technical codes and standards related to the construction and management of nuclear waste disposal facilities. The NWMO is one of the founding members of the CSA Technical Subcommittee developing the new CSA N292.7 standard for disposal facilities. The NWMO is also contributing to the development of the ASME Boiler and Pressure Vessel Code Section III Division 3 regarding transportation and storage containments for high level nuclear waste.

### 3.2.1.2 Evolution of the UFC Design

With the UFC Serial Production campaign moving forward in 2019, a number of issues related to the UFC constructability were identified, and further efforts were invested in adjusting the manufacturing process and improving the fabrication technologies. The UFC design continued to be iterated in parallel with the manufacturing processes in order to achieve a high level of stability in the quality of the end product. For example, the UFC tolerance stack-up analysis revealed that the fit-up between the UFC lower assembly and its upper head might lead to issues in closure welding and the control of the copper coating thickness. The manufacturing processes, such as the intermediate machining steps and weld preparation, were revised to minimize the impact of the fit-up tolerance.

### 3.2.1.3 UFC Insert Design

The UFC Insert is the internal structure of the UFC which houses the used fuel bundles. A conceptual design was tested with prototypes made in 2018, as shown in Figure 3-3. An initiative of re-designing the UFC Insert was carried out in 2019 to improve its constructability and cost effectiveness while maintaining its functionality and performance. The starting point of this initiative was an update of the UFC Insert Design Requirements. The project continues with the development of multiple new conceptual designs, constructability review, cost estimates for mass production and prototype fabrication for one selected design.

## 3.2.2 UFC Serial Production Campaign

In 2019, the NWMO continued the UFC Serial Production campaign of the Proof Test Program. The objective is to fabricate up to 20 UFCs using reference materials, fabrication and inspection technologies and to verify the product against the reference design requirements and quality acceptance standards. Further design refinement and manufacturing optimizations will be applied as necessary based on feedback from testing, inspection, and validation programs.

In 2019, the machine shop services contract was set up, and machining work on UFC components started. Drawings, manufacturing, inspection and test plans, and related documentation (e.g., procedures, inspection report templates) were produced. The results achieved in 2019 are shown in Table 3-1.



**Figure 3-3: Prototype 2018 UFC Insert Design**

**Table 3-1: 2019 UFC Serial Production Results**

| UFC Component            | 2019 Quantity   |                    |                |                          |
|--------------------------|-----------------|--------------------|----------------|--------------------------|
|                          | Steel Machining | Welding & Weld NDE | Copper Coating | Copper Coating Machining |
| Upper Hemispherical Head | 5               | N/A                | 5              | 5                        |
| Lower Hemispherical Head | 5               | N/A                | N/A            | N/A                      |
| Shell                    | 5               | N/A                | N/A            | N/A                      |
| Lower Assembly           | N/A             | 5                  | 2              | 1                        |

Figure 3-4 shows a machined upper hemispherical head for UFC serial production. During manufacturing, the UFC structural vessel is referred to as two components; the upper hemispherical head and the lower assembly (lower hemispherical head welded to cylindrical shell).

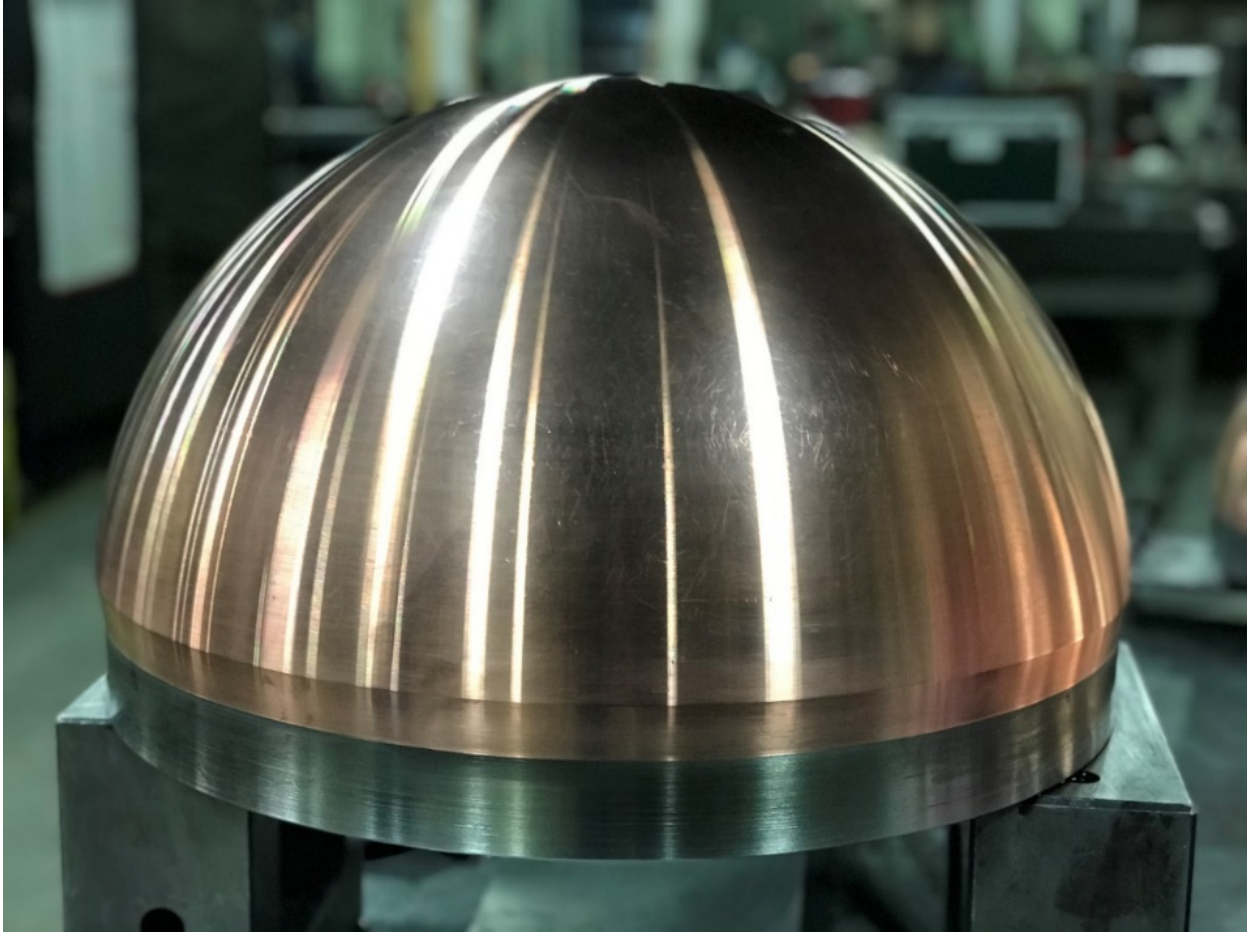


**Figure 3-4: Machined Copper Coated Upper Hemispherical Head for UFC Serial Production**

Moving forward into 2020 and beyond, the Serial Production campaign will continue to produce more components, and the first full UFC assembly. Development work is ongoing in all areas of manufacturing. Sections 3.2.3 and 3.2.4 describe the progress made on the welding, copper coating and NDE processes that support the Serial Production campaign.

### **3.2.3 UFC Manufacturing**

#### **3.2.3.1 Welding Technology Development**

The UFC structural vessel has two partial penetration welds that attach the lower and upper hemispherical heads to the shell. The design of the weld joint is such that the partial penetration weld need only be 8 mm minimum in thickness. This weld thickness permits the use of single pass welding technology. Single pass welding is particularly advantageous for the closure weld (upper head to lower assembly) which is to be performed in a radioactive environment under remote, automated application. In this regard, the NWMO selected Hybrid-Laser-Arc-Welding (HLAW) as a candidate technology for UFC welding. HLAW is a combination of Laser Welding and Gas Metal Arc Welding (GMAW). The NWMO has been working with Novika Solutions (La Pocatière, Canada) for several years to develop this technology through the execution of multiple R&D programs. In 2015, Novika Solutions prepared a reference Welding Procedure Specification (WPS) and Procedure Qualification Record (PQR) in accordance with ASME

Boiler and Pressure Vessel Code Sections IX and III (Division 3 Subsection WC) for use on prototype UFC lower assembly and closure welds.

In 2018, the NWMO contracted the Fraunhofer Institute (Berlin, Germany) to conduct thermomechanical modeling of NWMO's HLAW process as part of ongoing investigations into weld quality. This modeling was performed to determine the stress state of the partial penetration weld and surrounding areas of the weld joint. One recommendation from this modeling work was to reduce the molten volume of the weld by reducing the laser spot size (i.e. laser diameter) from 800  $\mu\text{m}$  to 400  $\mu\text{m}$ . This produced higher quality welds, but resulted in decreased process tolerance for weld head to weld joint alignment. This decreased process tolerance led to unfused regions at the weld root area (see Figure 3-5) decreasing effective weld penetration.

To increase process tolerance and ensure complete weld fusion with penetration  $> 8$  mm, a change to the weld process was initiated in 2019. The new process is called Laser-Preheated Gas Metal Arc Welding (LP-GMAW). This process does not use a laser for weld penetration, rather the laser is used to "pre-heat" the material close to the base metal melting point just prior to the weld filler metal being deposited in the weld joint. Preliminary work (see Figure 3-6) has shown that this process provides sufficient penetration and fewer defects (such as porosity) compared to HLAW. LP-GMAW has also proven to be a simpler process to implement than HLAW, due to less interaction between the laser and GMAW arc in the weld volume. This process change resulted in a change to the joint geometry to increase the weld filler metal volume. The prior weld joint (Figure 3-7 left) contained a small 1.5 mm chamfer while the new weld joint (Figure 3-7 right) contains a larger "double-J" or "U-groove" type design. Qualification of this weld for use in the Serial Production campaign is planned for 2020, with welding of Serial Production Components using the new process also planned for 2020.

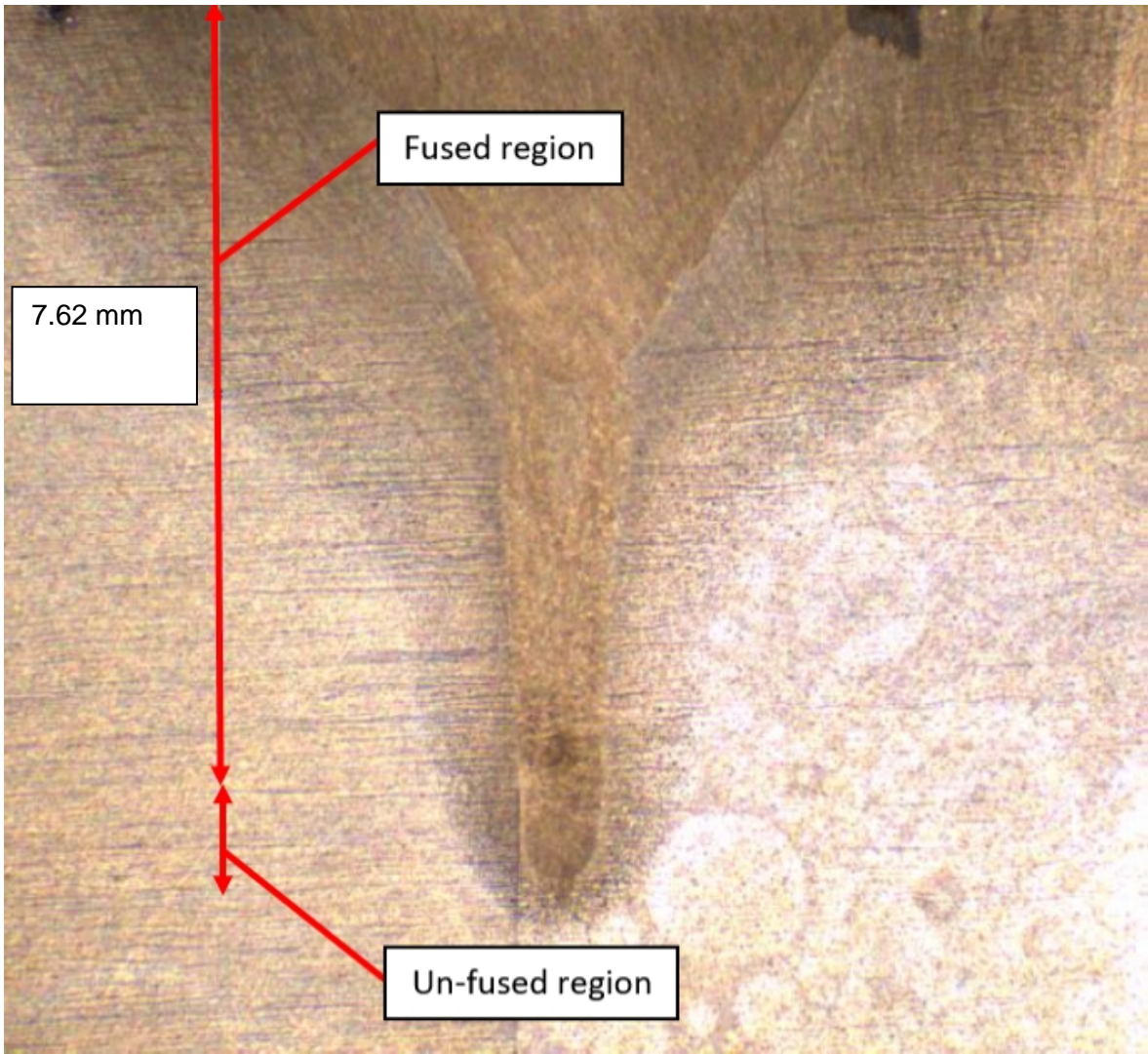


**Figure 3-5: UFC Weld Cross-Section Showing Unfused Region at Weld Root**

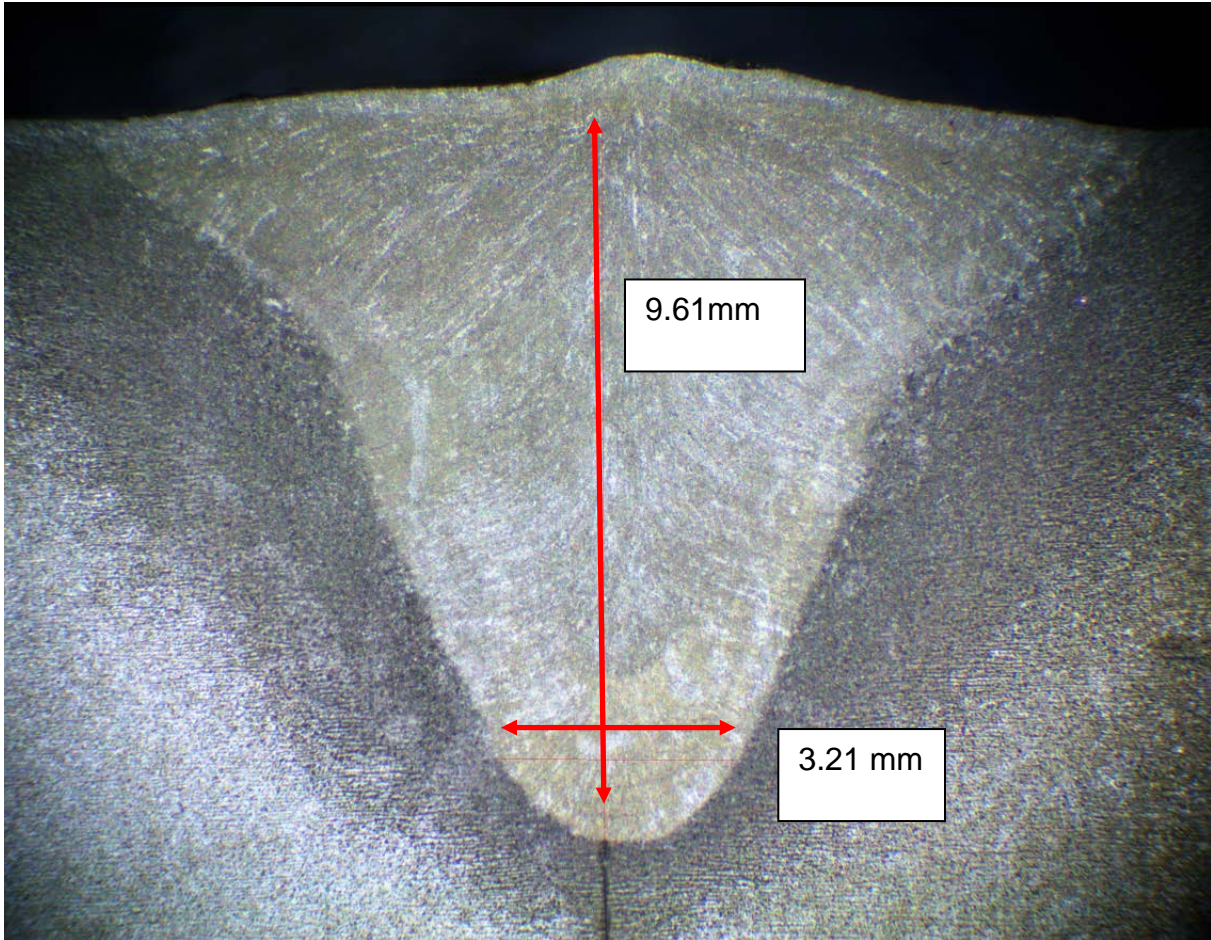


**Figure 3-6: Weld Cross-Section of LP-GMAW Sample Showing Wider Weld Root Region**

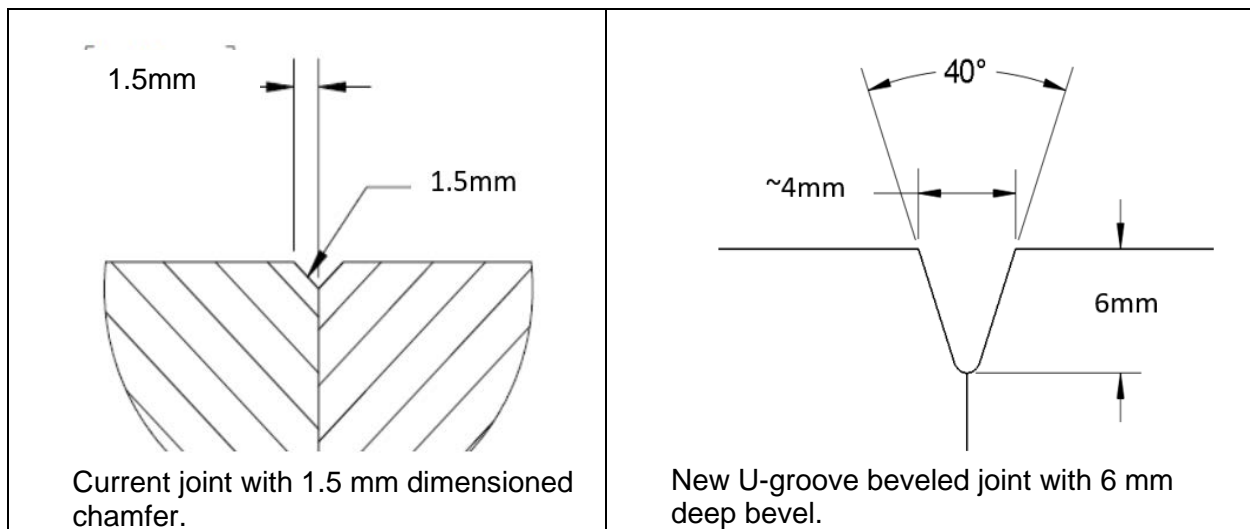


**Figure 3-7: Comparison of the Weld Joint in the Prior Design (Left) and the New Design (Right)**

### 3.2.3.2 Copper Coating Development

#### 3.2.3.2.1 *Electrodeposition Process Development*

Since 2012, the NWMO has engaged Integran Technologies, Inc. (“Integran”, Mississauga, Canada) for the development of a copper electrodeposition technology. To date, significant progress has been made whereby the process developed has been successfully scaled and deemed suitable to copper coat UFC components (i.e., hemispherical heads and lower assemblies) to the required bulk thicknesses. In 2019, the first five copper coated hemispherical heads were produced in a pilot production format as part of the Proof Test Program. In parallel, the installation of the Nanovate™ Tank System was completed and commissioned in mid-2019 to support the launch of process optimization and demonstration / validation for the production of copper coatings on lower assemblies.

#### Hemispherical Head Copper Coating Serial Production

Five hemispherical heads were produced with copper coatings having a thickness greater than 5 mm. Although the minimum requirement is 3 mm of thickness, extra material is conservatively required due to tolerance stack-up and joining the hemispherical head with the lower assembly. Figure 3-8 shows an example of one of the five hemispherical heads with the copper coating. The hemispherical heads were subjected to quality control inspections by visual and thickness measurements using a non-destructive (magnetic/eddy current) probe technique. The hemispherical heads were then shipped for machining and further non-destructive testing.



**Figure 3-8: Serial Production Hemi-Spherical Head**

Since non-destructive inspections are limited to visual and thickness, additional process performance measures were deemed necessary to indirectly assure the quality of the material. To achieve this, a representative “tube” employed as a quality assurance test coupon was subjected to the exact same process as the hemispherical head. This tube was then

destructively tested to determine copper purity, adhesion of the copper to the steel, hardness, ductility, and to produce a metallographic record. One test coupon was produced after the five hemispherical heads were completed for this purpose and found to be in compliance with the given specifications. Production of test coupons will occur at set intervals throughout the course of the Serial Production campaign.

### Lower Assembly Copper Coating Equipment Fabrication, Installation & Commissioning

In 2018, the design of an improved electrodeposition tank was completed, i.e., the Nanovate™ Tank System (NTS), for processing lower assemblies. Following this, fabrication was initiated by Empire Buff Ltée (Laval, Canada) and then completed with factory acceptance testing in mid-2019. Upon successful completion of this critical step, the NTS was shipped to Integran for installation and commissioning. Figure 3-9 shows the NTS installed at the NWMO pilot production line that is housed in a dedicated space within Integran's facility.



Note: Equipment shown installed at the NWMO Pilot Production Line at Integran Technologies, Inc. (Mississauga, Ontario, Canada).

**Figure 3-9: Nanovate™ Tank System (NTS)**

### Lower Assembly Optimization Trials

The process for coating the lower assemblies is required to be optimized considering various factors including primarily solution flow conditions and current density. It should also be noted that the use of the newly installed NTS also presents some challenges in that there are a number of controls needed to be investigated in relation to solution flow conditions, e.g., effects of pump speeds to achieve “overflow”, general flow for a surface finish that has no visual variations, etc. In 2019, three optimization runs were completed. Two additional runs are

planned in 2020, followed by another three demonstration/validation trials after process conditions have been fixed. One of the three lower assemblies from the demonstration / validation trials will be subjected to destructive testing to verify process performance (e.g., adhesion of copper to steel) and material characteristics (e.g., purity, microstructure, and ductility). When the process is deemed ready, serial production of lower assemblies will follow. Figure 3-10 shows the coated lower assembly in an optimization trial.



**Figure 3-10: Lower Assembly Optimization Trial**

#### 3.2.3.2.2 *Cold Spray Process Development*

Since 2012, the NWMO has engaged prime contractor National Research Council Canada (“NRC”, Boucherville, Canada) to develop a cold spray copper coating technology. Significant progress had been made to develop and optimize the process to meet NWMO requirements where coating application is confined to the closure weld zone of the UFC.

In 2019, further advancements were sought to eliminate the use of helium to achieve a “bond layer” in the copper cold spray process. The effort was set out in response to the fact that

helium is a non-renewable resource and therefore, a costly consumable. The need for helium in this process is primarily to achieve high copper particle velocities such that adhesion to the steel may be obtained. This first layer of copper using helium as the carrier gas provides the initial “bond layer”. The gas is then changed to nitrogen which accelerates the particles at a lower velocity but sufficient to achieve cohesion to the copper “bond layer” allowing for thickness build-up. In the work carried out to eliminate the use of helium, laser assistance was pursued along with only nitrogen as the carrier gas. The laser would be used to effectively heat the steel to a temperature where sufficient softening is obtained thereby lowering the required particle velocity for adhesion. After completing the “bond layer” using laser assistance, the laser would be turned off and cold spraying continue until the desired thickness is achieved.

At the end of 2019, a process using laser assistance was successfully demonstrated. To arrive at this point, a significant amount of trials were necessary to optimize processing parameters namely, laser/particle jet relative positions, laser power, spray gun traverse speeds, and step sizes. Initially, these trials were performed on flat test coupons and optimized accordingly. Figure 3-11 shows representative flat test coupons.



Note: The laser spot was positioned both to the right and to the top of the of the particle jet considering the dynamics of process.

### Figure 3-11: Example of Two Sets of Laser/Particle Jet Relative Positions

After developing a set of parameters deemed suitable, further development was carried out on pipe segments. This development consisted in adapting and optimizing the selected parameters to achieve a coating on a rotating surface with the same diameter as the UFC. Figure 3-12 shows the cold spray process using laser assistance to achieve the “bond layer”.

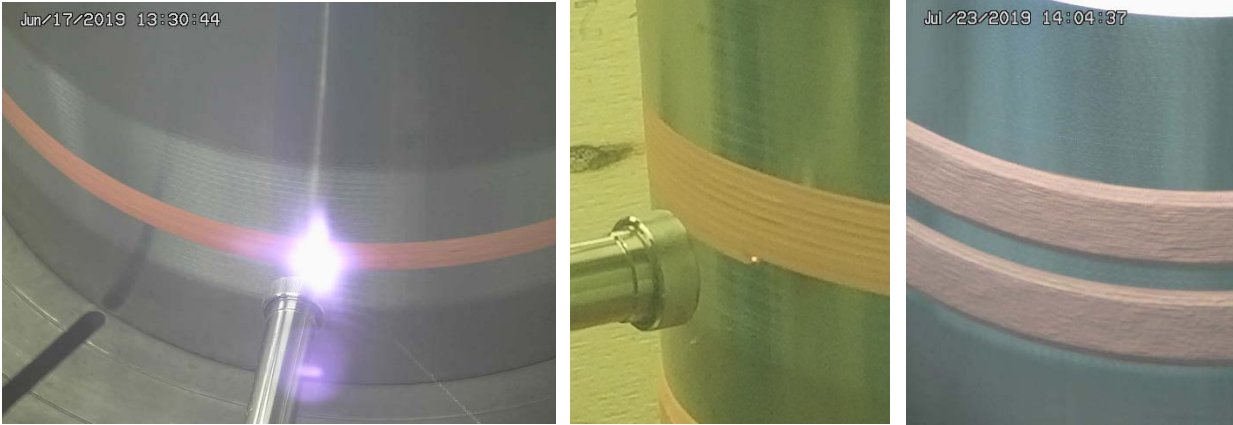


**Figure 3-12: Cold Spray Process Using Laser Assistance to Achieve the “Bond Layer”**

In order to assess the effectiveness of the selected parameters, “rings” of copper were cold sprayed onto the short pipe segment and adhesion test coupons extracted for evaluation. For the set of parameters deemed to be optimal, adhesion values in excess of 60 MPa were achievable, which is at least three times the minimum requirement.

To compliment this work, additional research and development was carried out at the University of Ottawa with the objective of ensuring that there is a fundamental understanding of the mechanisms for achieving adhesion to the steel. Some of the work performed included characterizing the particle impact behavior. Figure 3-13 shows a copper particle after impact on a steel surface having a temperature of 400°C.

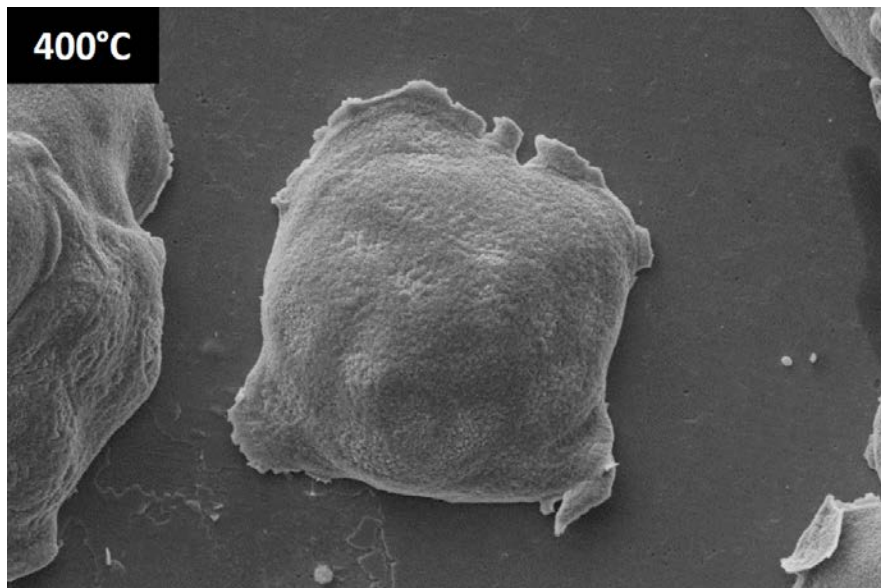


**Figure 3-13: Copper Particle after Impact on a Steel Surface Having a Temperature of 400°C**

The last part of this development is a demonstration of the technique on representative parts (e.g., a lower assembly) using the same rotational equipment to be employed in the Serial

Production campaign. In addition, other developments are planned using laser assistance include ablation to clean the steel surface prior to cold spraying and heat treatment. These efforts are planned to be pursued in 2020.

### Copper Material Characterization

In 2018, the NWMO sought the expertise of the University of Toronto to perform an in-depth characterization of the copper coating materials. The motivation for the work comes mainly from the notion that both the electrodeposited and cold spray materials in their processed form are non-standard. Therefore, a fundamental understanding of their microstructure and behavior is warranted. Since 2018, a significant amount of work has been performed to learn more about these materials leading to a publication entitled “*Microstructural and bulk properties evolution of cold-sprayed copper coatings after low temperature annealing*” (Yu et al. 2019). This study focuses on revealing the mechanisms behind the effect of heat treatment and imparting ductility in the cold sprayed material since it is well known that it is inherently brittle without a heat treatment. An example set of micrographs with analysis is provided in Figure 3-14.

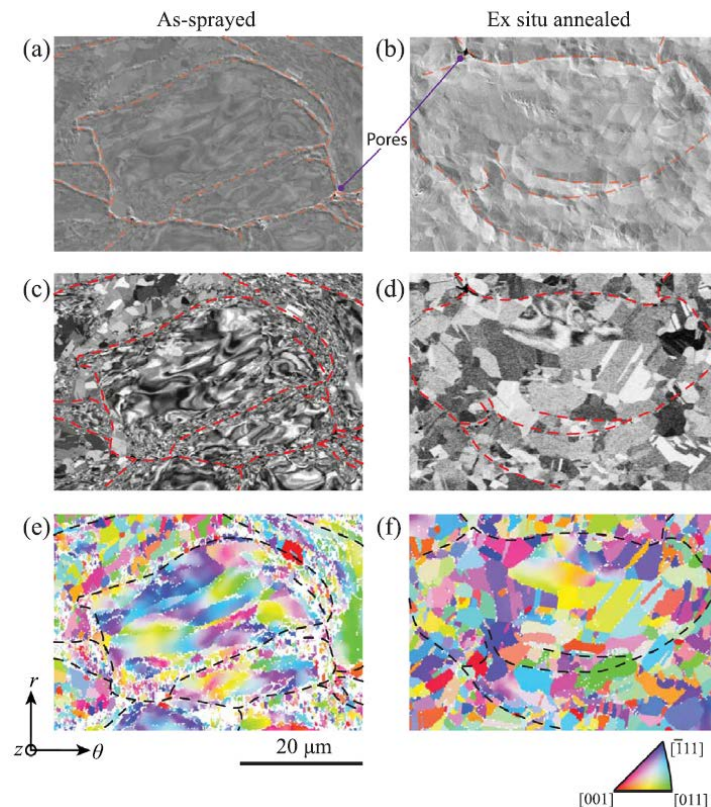


**Figure 3-14: Scanning Electron Micrographs of Cold-Sprayed Copper in the Axial Direction (Yu et al. 2019)**

A second journal submission was made at the end of 2019 with additional characterization studies considering both types of copper materials. This work focused on revealing the favorable microstructural characteristics of the materials for localized corrosion resistance. Of particular interest for the cold sprayed material is an in-depth characterization of copper particle-particle interfaces as this will help to provide insight into its expected corrosion behavior. These studies were initiated in 2019 and are expected to be completed in 2020.

### 3.2.4 UFC Non-Destructive Examination

In 2018, preliminary non-destructive examination (NDE) procedures were developed for the inspection of full-scale UFC components in the Serial Production campaign. The procedures use ultrasonic (UT) and Eddy current (EC) techniques to verify design criteria (component dimensions, weld penetration, coating thickness) and detect/size defects. These inspection procedures detail the techniques, equipment, and acceptance criteria used in non-destructive inspections. In 2019, the preliminary inspection procedures were tested on full-scale UFC components and revised prior to use in the Serial Production campaign. Using the finalized procedures, inspections were performed on 5 welds (welded lower assemblies) and 3 copper coatings (copper coated hemispherical heads). See Figure 3-15 for an example of copper coating inspection results from a zero degree ultrasonic inspection. The copper coating inspections showed a coating thickness of about 4 mm and no defects through the full volume of the coating.

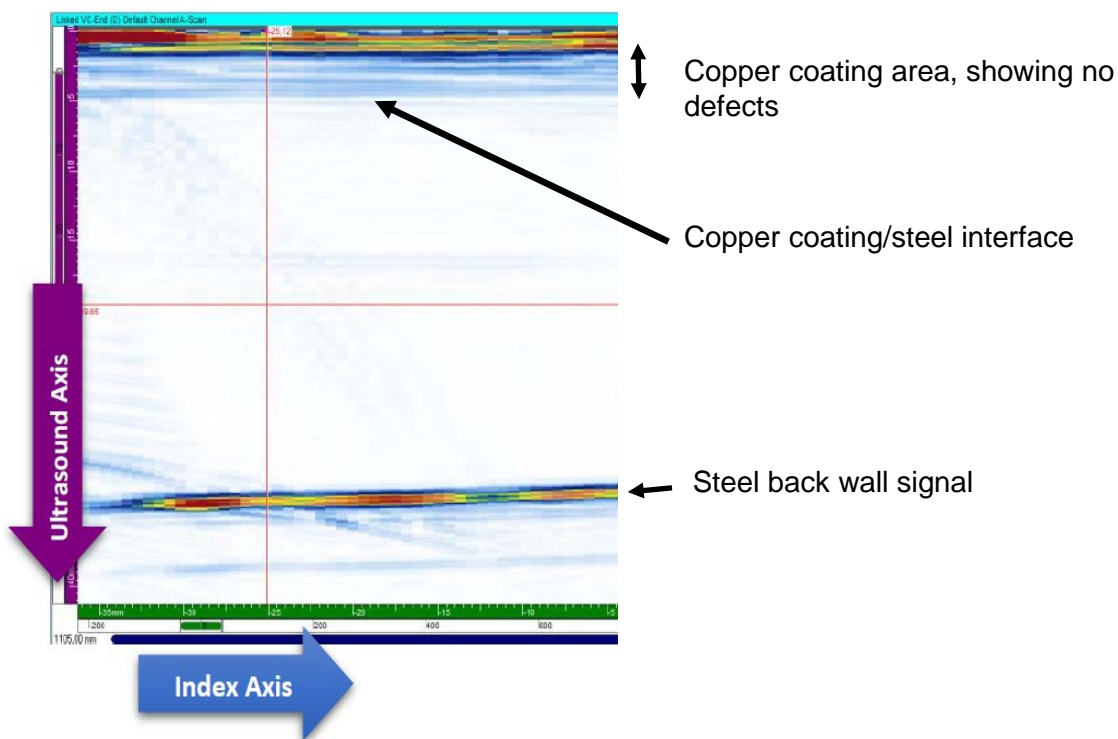


**Figure 3-15: Example of Hemispherical Head Copper Inspection Results from Zero Degree Ultrasonic Probe**

In addition, in 2019, the NWMO contracted Zetec Inc. (Snoqualmie, USA) to design and fabricate a custom-built NDE probe for shear wave inspection to be used in weld inspections. The purpose of the custom-built probe is to increase detection sensitivity and detect smaller defects. The probe will be tested on welds in the Serial Production campaign and the results will feed into the weld development program to improve weld quality.

### 3.2.5 UFC Testing

The NWMO has conducted mechanical testing of the UFC materials and established a material database. A new round of material property testing was launched in 2019 to further expand the database. The UFC carbon steel base materials were tested by the Cambridge Materials

Testing Limited (Cambridge, Canada) with a non-standard tensile test procedure (as shown in Figure 3-16). The goal is to obtain the strain hardening properties beyond the point of ultimate strength of the materials at room and elevated temperatures, which are needed to examine the materials' applicability to the strain-based design criteria newly included in ASME Boiler and Pressure Vessel Code Section III Division 3. Charpy V-notch impact tests were also conducted by the same vendor for the UFC carbon steel base materials to establish the ductile-to-brittle transition curve under impact loads (see Figure 3-17 for the test rig). The transition curve will be used to ensure that the UFC base materials will be free of the risk of brittle fracture at the lowest service temperature. The material testing work will continue in 2020 to include the welding material and the heat affected based materials near the weld.



**Figure 3-16: UFC Carbon Steel Material Tensile Test Rig With Heating Chamber And Video Extensometer**



**Figure 3-17: UFC Carbon Steel Material Charpy Impact Test Rig**

### **3.2.6 Fuel Integrity during Closure Welding of the UFC**

Following the loading of CANDU fuel in the UFC container, the copper coated steel lid is attached to the vessel by welding of the steel and, subsequently, the copper corrosion barrier is applied to the weld closure zone by the cold spray process. These operations will expose the closure zone to short term elevated temperatures (i.e. arc welding of the steel: pre-heat and welding and copper cold spraying: annealing). These manufacturing processes have been designed so that the temperatures inside the UFC during these operations will not exceed 400°C.

A study to address whether exposing used CANDU fuel to 400°C during UFC closure could affect its mechanical integrity was completed (Freire-Canosa, 2019). Several potential mechanisms may be postulated that could affect the fuel cladding: hydride re-orientation, Delayed Hydride Cracking (DHC), Stress Corrosion Cracking by iodine (SCC), Metal Vapour Embrittlement (MVE) by cesium and cadmium and degradation of the brazing zone of the bearing and spacer pads. Oxidation of the UO<sub>2</sub> fuel pellets in defected fuel was also considered.

The assessment of these mechanisms indicates that the integrity of non-defected fuel will be maintained to temperatures up to 400°C. In the unlikely event that defected fuel were present in the fuel load in the container, some oxidation of the fuel pellets may occur but it is not expected to breach the fuel or lead to the release of its radioactive content.

Further, as indicated by the USA NRC directive for the storage and transportation of used fuel (NRC ISG-11, Rev. 3, 2003), thermal cycling of the fuel at this high temperature should be less than 10 cycles to avoid re-precipitating hydrogen as hydrides in the radial direction of the fuel cladding. The UFC closure has only two cycles during the manufacturing process, and, therefore minimizes the risks of having radial hydrides in the fuel cladding.

### 3.3 SITE AND REPOSITORY

#### 3.3.1 Sealing for Decommissioning and Closure

During 2019, the design work focused in updating an earlier Technical Design Document (TDM) covering the decommissioning and closure of a conceptual DGR for CANDU fuel. In this updated TDM, conceptual design, information is thoroughly revised and updated for the sealing systems of two conceptual repositories sited in two different geological environments: crystalline and sedimentary rock. In particular, the seals and plugs for the following DGR components are developed in detail:

- Placement rooms as shown in Figure 3-18.
- DGR main shaft, primarily, for DGRs sited in sedimentary rock because they have more demanding requirements due to the complexity of their geology.
- Access tunnels (conceptual design as shown in (Figure 3-19) and ramps.
- Boreholes.

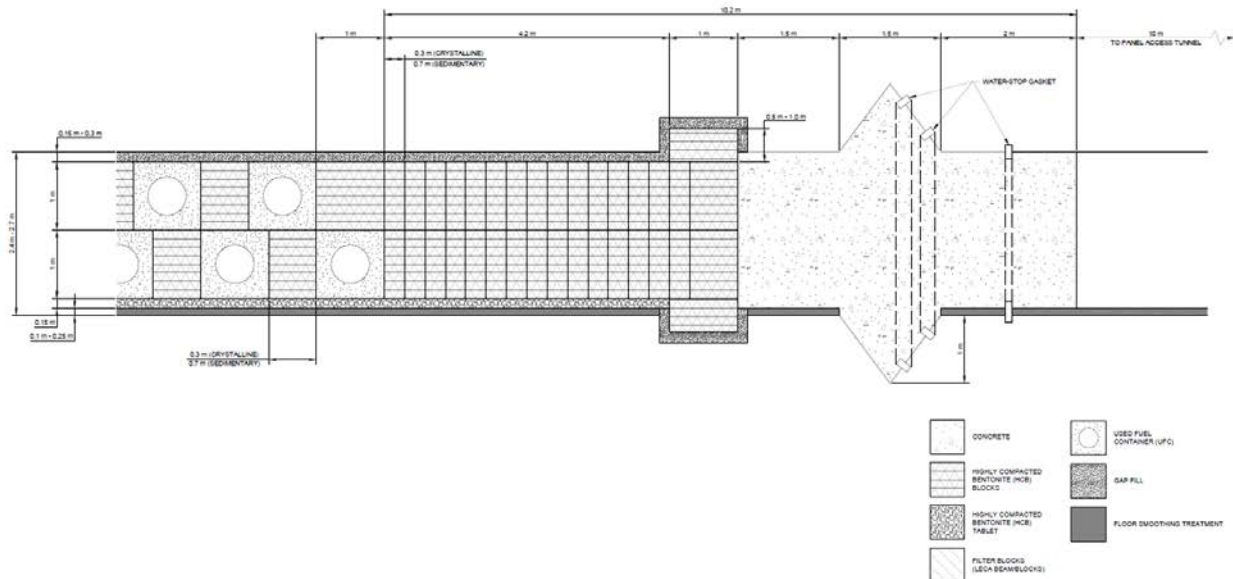


**Figure 3-18: Generic Reference Placement Room Seal for Use in Sedimentary or Crystalline Host Rocks Where Water Control or Gas Venting Is Not Required**

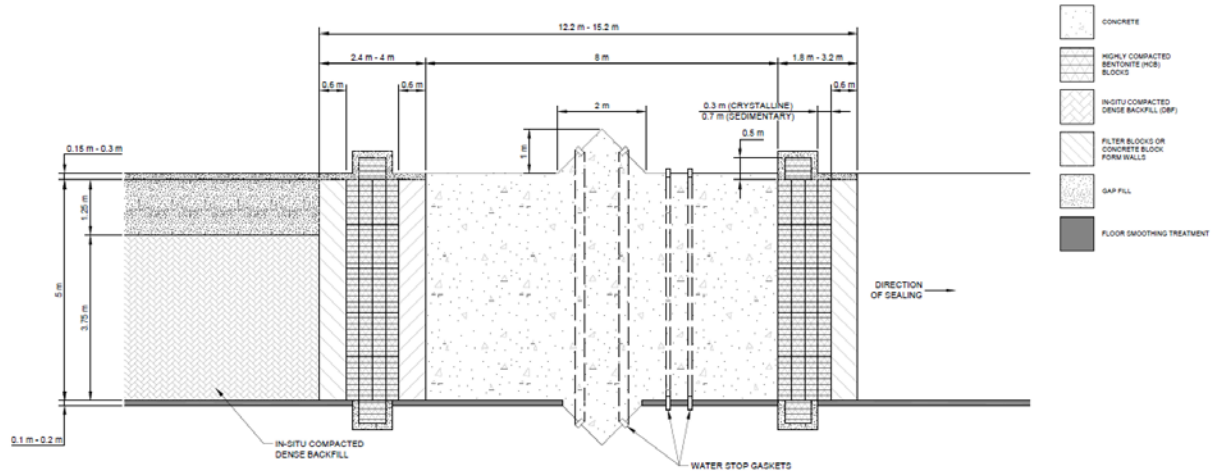


**Figure 3-19: Access Tunnel and Ramp Sealing System Concept for Use in Sedimentary or Crystalline Rock**

Current DGR layout geometries as well as recent developments in materials and technologies since the preparation of previous concepts were also considered, including pertinent requirements and site specific details of the current layout geometries under consideration. Information available from the design, construction and operation of various repository development programs in Europe and elsewhere was used to advantage where applicable. For example, full scale experimental data/results from the following programs were used: Canada's Tunnel Sealing Experiment (TSX), Canada's Enhanced Sealing Project (ESP), Finland's Posiva's full scale demonstration Plug (POPLU) and the SKB/Posiva DOME PLUG (DOMPLU) for deposition tunnels.

Additionally, the following activities are on-going:

- Localized sealing for fractured zones (grouting, Posiva/SKB micro grout mixes).
- Effects of highly saline environment on seal performance.
- State-of-the-art in borehole sealing and proposed application to DGRs with schematic representations of concepts based on information in the public domain (SKB, Posiva, RWM, Clay Technology, VTT, PNC, DOPAS 2016 Proceedings, etc.).

Finally, the conceptual decommissioning and closure concepts are described for a four-phased approach (see Figure 3-20) for the DGR facility (i.e., how the seal designs would be implemented). In particular, the following activities are detailed at a conceptual level:

- Transportation of the sealing materials to the DGR site.
- Installation of seals with emphasis on potential issues such as EDZ cut-off.

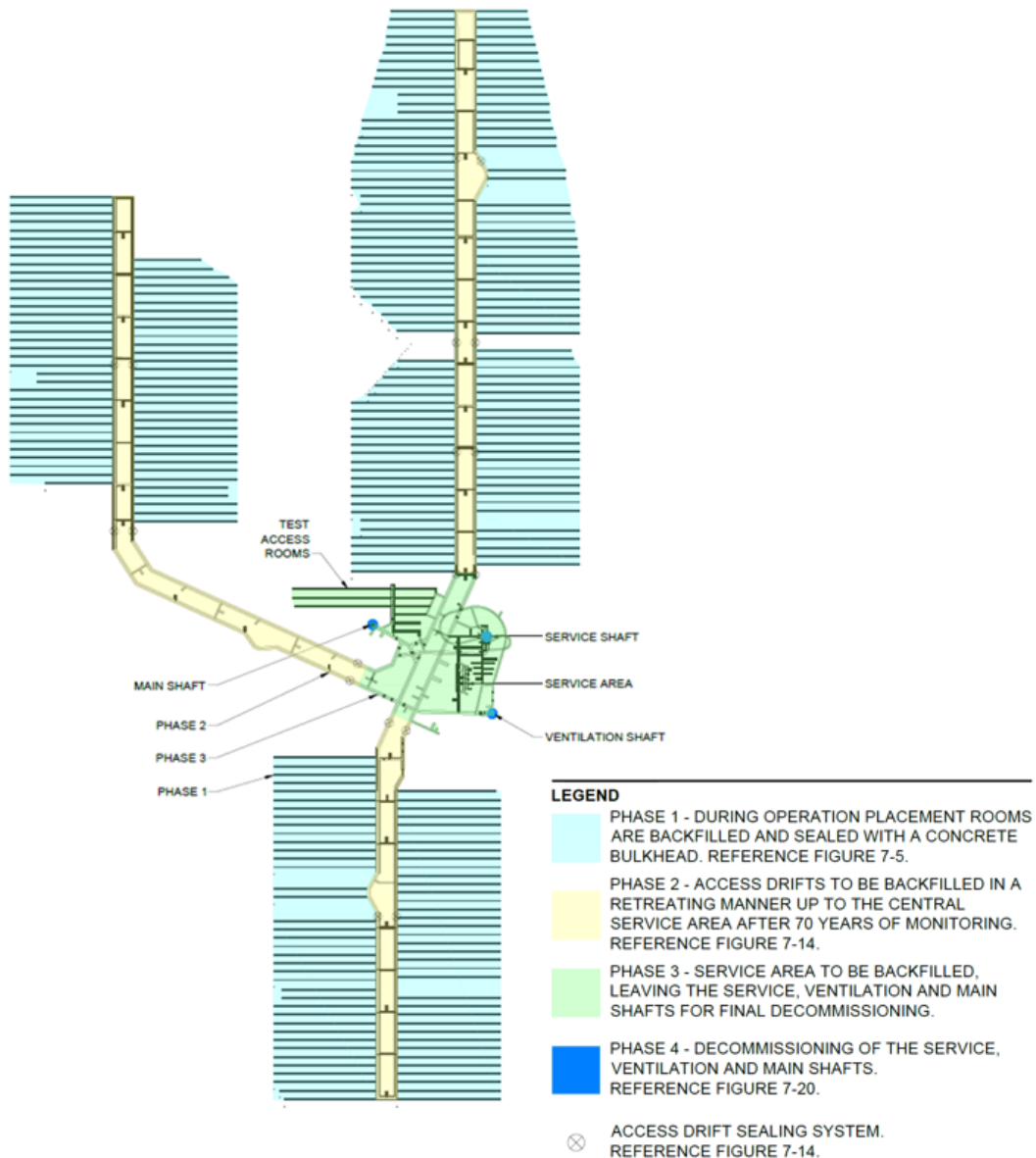


**Figure 3-20: Phased Approach to Closure**

### 3.3.2 Underground Ventilation System

The Ventilation system requirements for the DGR layout were also addressed in a TDM for both crystalline and sedimentary bedrock. The findings of this work have been documented as part of the APM Phase 2 Engineering Support. Key components of those findings included:

- Network modelling techniques (as shown in Figure 3-21 using Ventsim Software to create a three-dimensional model of the ventilation systems).
- Engineering design procedures to size and select the primary ventilation fans.
- Draft sketches (as shown in Figure 3-22 for primary infrastructure installations (i.e. fixed location fans, HEPA filters, etc.).
- Estimating AACE Class Four capital costs at - 30% to + 50% level of accuracy and operating costs for comparison with the 2016 Lifecycle Cost Estimate.

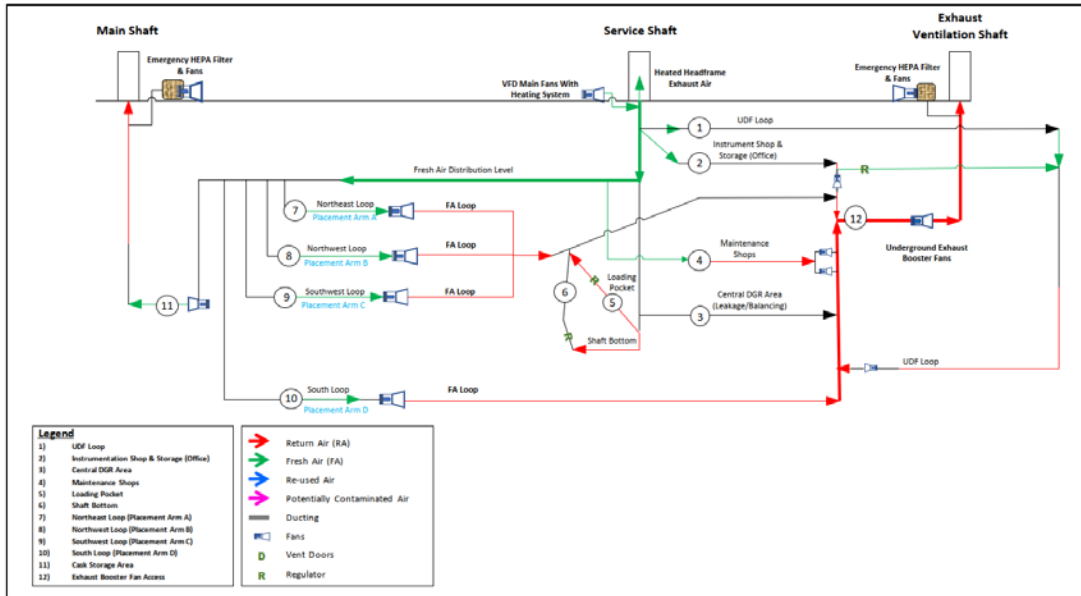


Figure 3-21: Ventilation Infrastructure locations for the Crystalline Repository Layout

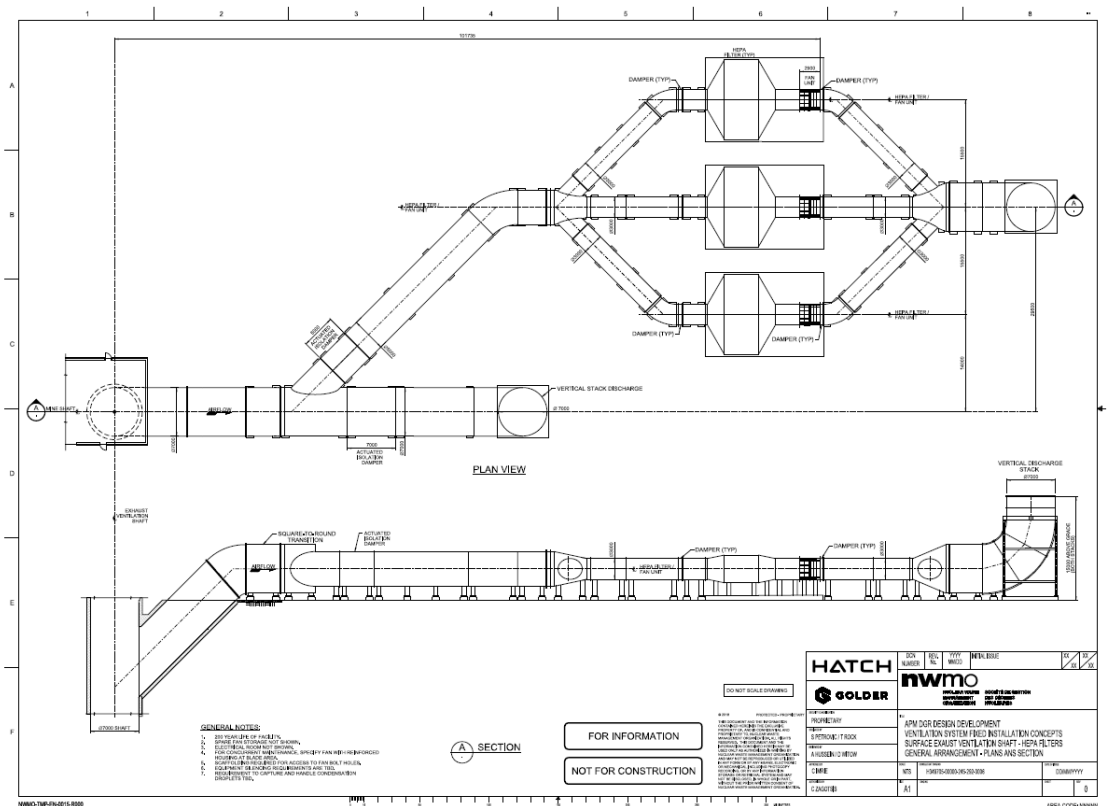


Figure 3-22: APM DGR Design Development Ventilation System Fixed Installation Concepts Surface Exhaust Ventilation Shaft - HEPA Filters General Arrangement - Plans ANS Section

### 3.3.3 Excavated Rock Management Area

The Excavated Rock Management Area for the DGR was also conceptualized and a preliminary design was completed and documented. Waste rock volumes to be generated during DGR construction were estimated. Two siting locations for the DGR were considered at Ignace Revell, Northern Ontario, in crystalline rock and in a Southern Ontario location in sedimentary rock. The developed conceptual designs will assist the NWMO in discussions with communities during siting and engagement activities, as well as support further technical development and cost updates.

Several design options of the Waste Management Area were considered viable for the Ignace Revell site. The difference between these options was the maximum height of the rockpile. They were narrowed down to the one shown in Figure 3-23 (plan view). Note that the difference between NAG (non-acid generating rock) and PAG (potentially acid generating rock) is the liner and runoff containment system.

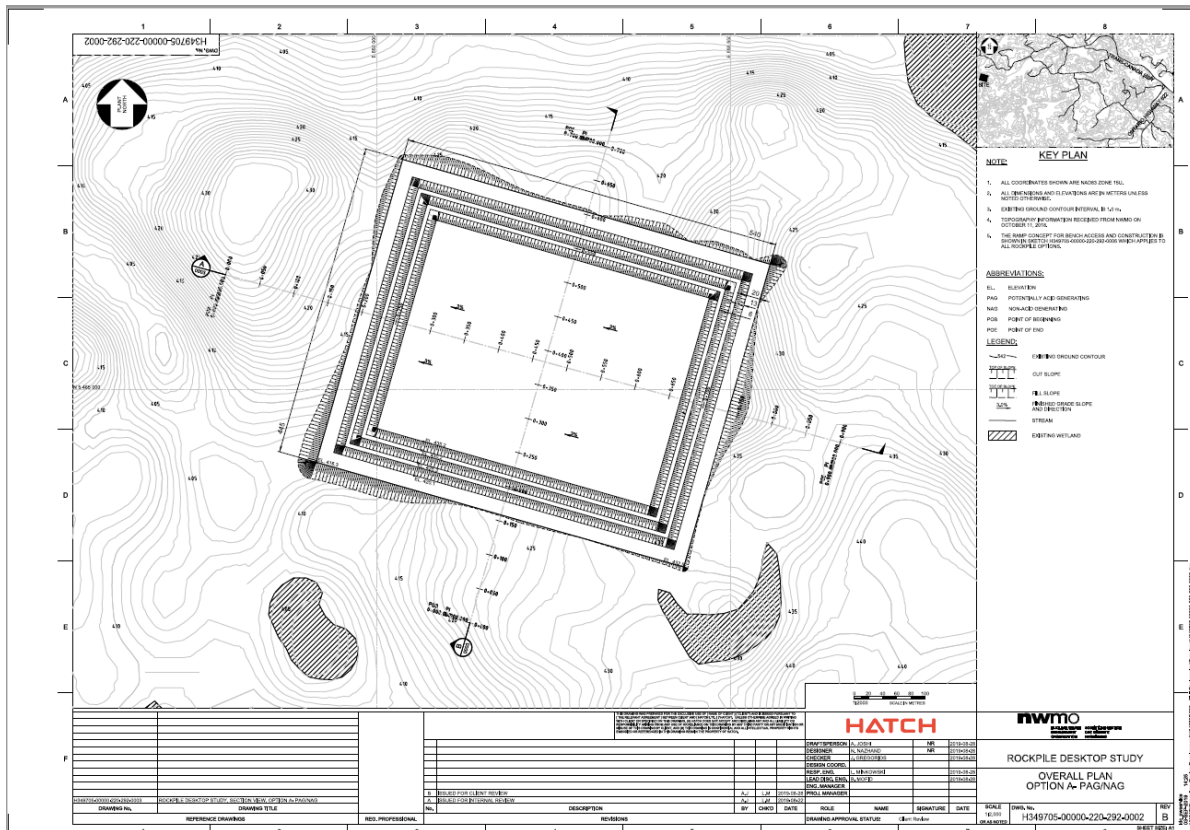


Figure 3-23: Excavated Rock Management Area Plan

### 3.3.4 Life Cycle Cost Estimation

A significant level of effort was expended on the Life Cycle Cost Estimating scope of work. The estimating deliverable is based on Hatch Ltd. estimating guidelines and NWMO estimate requirements. The cost estimate was prepared in accordance with ACEC Recommended Practices as a Class 4 estimate with an overall accuracy range of:

- Low: -15% to -30%
- High: +30% to +50%

## 4. BUFFER AND SEALING SYSTEMS

The NWMO continued to support the development of the buffer and sealing systems including optimized manufacturing, storage, and emplacement technology for the Highly Compacted Bentonite (HCB) blocks that are placed directly around the UFCs.

### 4.1 EMPLACEMENT EQUIPMENT

An enhanced emplacement technology was developed in 2018 and tested in 2019. The finalized prototype emplacement equipment was designed and built by Medatech Engineering Services (Collingwood, Canada) to NWMO requirements, and tested at the NWMO Oakville Facility.

### 4.2 EMPLACEMENT EQUIPMENT TESTING

The purpose of this work was to perform a preliminary set of movements to verify that the new buffer box delivery tooling is capable of lifting and placing buffer boxes of different configurations in the opening of the mock emplacement room without damage to the assembled buffer box (specifically the HCB blocks), emplacement equipment or the mock emplacement room. Additionally, this work was carried out to verify the strength the HCB blocks when stacked and loaded with weighted containers.

#### 4.2.1 Background

##### 4.2.1.1 Bentonite

The bentonite buffer serves multiple roles in the engineered barrier system. Its swelling characteristic fills voids to block pathways for radionuclide migration and provides support to the surrounding rock and container. Its low permeability inhibits porewater flow to and from the container and its sorption properties inhibit radionuclide movement in the event of container breach. The bentonite also transfers heat from the container to the surrounding rock. At the right dry density, it reduces water activity to  $<0.96$  (Stroes-Gascoyne, 2010). This is required to suppress microbiologically influenced corrosion of the used fuel container. Given the geometry of the placement room and the requirement to be suitable in both sedimentary and crystalline rock geospheres, the NWMO requires a minimum HCB block dry density of  $1.7 \text{ g/cm}^3$ .

##### 4.2.1.2 HCB Blocks

HCB blocks are pressed from raw MX-80 sodium bentonite. The raw bentonite is sourced from the United States at a moisture content of 10-12% ( $m_{\text{water}}/m_{\text{dry solid}}$ ). It is then up-blended with water to bring the moisture content up to 20%. This blending work is performed by a local food blending company in a large industrial blender. The blended bentonite returns to the NWMO proof test facility in tote bags where it is loaded into an isostatic pressing bag and form assembly. Once the bag is filled, air withdrawn and the bag sealed, it is sent to Pennsylvania State University to be cold isostatically pressed at their High Pressure Test Facility. The bentonite is pressed at 100 MPa in their 60 inch diameter pressure vessel which results in a HCB block with a dry density  $\geq 1.74 \text{ g/cm}^3$  (Figure 4-1).



**Figure 4-1: HCB Block**

The isostatic pressing results in a block that is “near net shaped”, meaning it is close to the final desired shape. The blocks are machined to final dimensions for the Buffer Box assembly in the robotic milling cell at the NWMO Oakville test facility (Figure 4-2).



**Figure 4-2: Shaped HCB Block**

#### 4.2.1.3 Used Fuel Container

The engineered barrier closest to the fuel is the Used Fuel Container (UFC), illustrated in Figure 3-2. The used fuel container is a mid-sized capacity (12 bundle/layer x 4 layers= 48 bundle) vessel which incorporates a steel core for structural strength and a 3 mm exterior copper coating for corrosion resistance. The weight of the container loaded with fuel is approximately 2,865 kg.

#### 4.2.1.4 Buffer Box and Assembly

The buffer box assembly (Figure 4-3) is two HCB blocks containing a Used Fuel Container.



**Figure 4-3: Buffer Box Assembly**

The HCB blocks and the UFCs have no lifting features and generally cannot be handled with conventional equipment without damage. The Buffer Box is therefore assembled with vacuum lifting equipment. The vacuum lift is capable of lifting the HCB block (Figure 4-4) on either the bottom flat surface or on the top cavity surface, and with a vacuum pad change, it can pick up the UFC (Figure 4-5). The unit is a purpose built, battery powered Vacuum Lifting Company SF4KB unit with a safe working load rating of 4,200 kg with the HCB vacuum pad.



**Figure 4-4: Vacuum Lift HCB**



**Figure 4-5: Vacuum Lift UFC**

#### 4.2.1.5 HCB Block Storage

The HCB blocks are sensitive to humidity. Once the HCB blocks are removed from the pressing bag, they need to be stored in a location where the vapour pressure of water in air is in equilibrium with the vapour pressure of the water in the block. This is accomplished by storing the HCB blocks in a humidity controlled room and maintaining the relative humidity above 70% at 20°C.

#### 4.2.1.6 Mock Emplacement Room

The NWMO has fabricated a mock emplacement room in Oakville for testing (Figure 4-6). The mock emplacement room simulates the anticipated dimensions, as well as, the drill and blast profile of underground excavation. The resulting rock surface is rough with near 90 degree angles at the “look outs” (i.e. sharp profile changes due to the drill and blast process).



**Figure 4-6: Simulated Emplacement Room with Faux Rock Walls Simulated Drill And Blast Profile. (A) Exterior Steel Frame Approximately 3m X 3m X 15m in Size; (B) Interior With Faux Rock Walls and (C) Actual Blast Profile from Underground Research Laboratory**

#### 4.2.1.7 Buffer Box Delivery Tooling

The buffer box delivery tooling, or buffer box attachment, is a custom engineered forklift attachment that is used with the electric Versa Lift 25/35 lift truck at the NWMO Oakville test facility (Figure 4-7). It was designed specifically to lift and place Buffer Box assemblies. It features:

- Three wide, adjustable/removable tines with independent hydraulic load levelling;

- Inflatable air bags to apply a compressive load to the ends of the buffer box assembly; and
- Five cameras and three alignment lasers to allow remote placement of the buffer box assembly using the Versa Lift's remote control pendant.

The attachment was designed and built as a research tool; as such, it has many features that can be changed including, adjustable/removal of tines to allow test flexibility, adjustable bag pressure, different tine configurations, etc. Buffer boxes with 2 or 3 pockets can be used and the tines can be repositioned along the width of the buffer box. This feature allows testing of several different configurations before settling on a 'reference' design. The inflatable airbags apply a compressive load of up to 1000 kg to the ends of the buffer box assembly. This load helps with sagging of the buffer box, depending on the position of the tines, but more importantly, prevents the HCB from separating should there be a crack or a break. Since in the future this equipment will have to be remotely operated due to the high radiation fields, it is important to demonstrate that the buffer boxes can be placed remotely. The cameras and lasers help the operator drive the vehicle and correctly position it to place the buffer box.



**Figure 4-7: Buffer Box Attachment installed on Versa Lift 25/35**

#### **4.2.2 Buffer Box Stacking Trial**

In order to prepare for the stacking trial, buffer box attachment trials with the Medatech test box were performed to regain familiarity with the placement procedure. Once rehearsals were completed, trials at the entrance to the emplacement room began. To simulate the floor tablets, four concrete spacers were placed on the floor of the Mock Emplacement Room.



**Figure 4-8: Stacked Buffer Box Placement**



**Figure 4-9: Stacked Buffer Boxes**

The lower buffer box assembly was picked up with the buffer box attachment and placed on the concrete spacers at the entrance to the emplacement room per the placement procedure. Once the lower buffer box was placed, the upper buffer box assembly was picked up and stacked on top of concrete spacers placed on top of the lower Buffer Box assembly (Figure 4-8 and Figure 4-9). The stacking trial was completed successfully without incident.

#### 4.2.3 Stacking Trial #2

The second stacking trial was a repeat of the first stacking trial, with the following exceptions:

1. No containers were used in buffer boxes.
2. No steel plates were used to provide additional support to the buffer boxes.
3. The buffer box that was stacked, had a lower block with pockets machined to accommodate the three tines of the attachment.
4. The rock ceiling panels of the emplacement room were re-installed.

The intent of this trial was to test the HCB block with fork pockets. By incorporating the pockets into the blocks, spacers like in the first trial are not needed (Figure 4-9).

The first buffer box was placed without issue, as expected. The second box, with the fork pockets was successfully picked up and stacked at the entrance to the room without incident. Figure 4-10 shows the final result at the entrance to the emplacement room. To illustrate how the pockets would be filled, plugs were made from polystyrene to fill the holes.



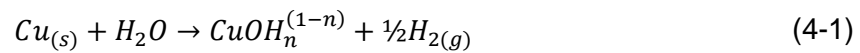
**Figure 4-10: Stacked Buffer Boxes with Fork Pockets (Top assembly)**

### 4.3 MATERIAL STUDIES

#### 4.3.1 Used Fuel Container Corrosion Studies

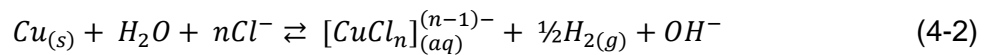
##### 4.3.1.1 Anoxic Corrosion of Copper

Although oxygen will be present in the DGR for a brief period following closure and decommissioning, anoxic conditions will persist for the majority of the repository's lifetime. Using thermodynamics, it is possible to predict very long lifetimes of copper in these conditions, an assertion supported by natural analogues such as "native" copper, which can be excavated as a metallic species that is millions or even billions of years old. Despite this, in some experiments where copper is placed in oxygen-free water, trace amounts of hydrogen have been detected, and some researchers have claimed the hydrogen is a corrosion product of Equation (4-1).

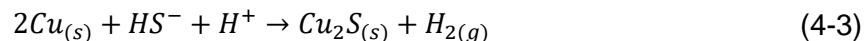


Despite being forbidden by classical thermodynamics and the inability of independent researchers to reproduce experimental results or unequivocally identify the copper corrosion product, "CuOH<sub>n</sub><sup>(1-n)</sup>", the existence of such a mechanism must be validated or invalidated by the NWMO. In fact, compelling evidence now exists from SKB (Hedin et al. 2018) that the process represented by Equation (4-1) does not occur, but that exposures of copper to water allow for the release of hydrogen trapped during the copper manufacturing process, and this effect can be eliminated by careful pretreatment of copper before exposure to water.

Equation (4-1) is related to a second, anoxic corrosion of copper that occurs in acidic, highly saline solutions according to Equation (4-2). As per the above example, some observations of hydrogen have been made during immersion of copper in brine; however in this case trace hydrogen is expected as the system comes to equilibrium. In a DGR, the forward (corrosion) reaction will be suppressed owing to the neutral (i.e. not acidic) pH, the low diffusivity of the copper-chloride reaction products through bentonite clay, and the dissolved hydrogen in the groundwater that is present in the anoxic condition. At extremely high brine concentrations (i.e. 5 to 10 X seawater), there is some question regarding the precise equilibrium conditions, which require characterization and quantification.



The third process of interest, anoxic copper corrosion in the presence of sulphide, Equation (4-3), is afforded the largest UFC copper corrosion allowance. Although Canadian groundwater contains virtually no sulphide, it is possible that microorganisms existing far away from the UFC could produce sulphide from their metabolic processes, which would enter the groundwater. Due to the presence of the bentonite buffer, diffusion of sulphide inward to the UFC will be slow. However, once the sulphide reaches the container corrosion proceeds quickly; thus more information is required with respect to the mechanism of this process, as well as the affect other groundwater species may have on the process or the products of the process.



Work being conducted by NWMO at CanmetMATERIALS (Hamilton, Canada) in collaboration with the University of Toronto investigates the individual and combined effects of Equation 4-3

along with pH effects. This work utilizes a specialized corrosion cell, depicted in Figure 4-11 (a) and (b), which maintains an anoxic environment at 75 °C while allowing for the introduction of chemical species (gas or liquid) into the cell. Hydrogen is measured by purging the headspace of the cell and the amount is correlated to a rate of corrosion by assuming the reactions shown in Equation 4-3 take place. Notably, the release of trapped hydrogen from within the copper, or the production of hydrogen from other corrosion reactions within the cell (i.e. through the interaction of steels and water) will be assumed to be copper corrosion using this calculation method, and this will overestimate copper corrosion (Senior et al. 2019). Similarly, hydrogen produced via corrosion that is absorbed by the metal will be missed in a corrosion calculation; although this process is not expected. Nonetheless, a representative graph of the results is shown in Figure 4-11 (c) which plots the presumed corrosion rate versus time for deionised water cells and a strong brine cell over the course of approximately four years.

The corrosion experiments are ongoing but some consistent trends are exhibited by the data following the approximately four year duration of the program. In pure water, hydrogen was evolved, and initial corrosion rates were calculated to be less than 0.5 nm/year before falling below the detection limit of the experiment. Similar results were seen for dilute and strong chloride solutions; that is, an initial small release of hydrogen followed by a gradual decline with time to near or below the detection limit as shown in Figure 4-11 (c). It is also important to note that each cell underwent integrity and leak testing at the end of 2019 to ensure that hydrogen was not escaping the cells. These tests will continue with the introduction of various other oxidants (e.g. gaseous hydrogen sulfide) to investigate the behaviour of the copper. When complete, test cells will be disassembled and the copper interrogated for the presence of absorbed hydrogen and the makeup of corrosion products. Preliminary but more detailed results from this program have been published by Senior et al. (2019).

As expected, the introduction of sulphide to either saline or pure water environments did result in hydrogen evolution, producing initial low corrosion rates equivalent to 0.1 and 0.2 nm/year, respectively. As with the cells described above, the rates dropped over time. However, even if for a damage assessment, it were assumed these rates were sustained, the largest of these miniscule rates would produce less than 0.25 mm of damage in 1,000,000 years, and are consistent with the NWMO total corrosion allowance of 1.27 mm over that period of time.

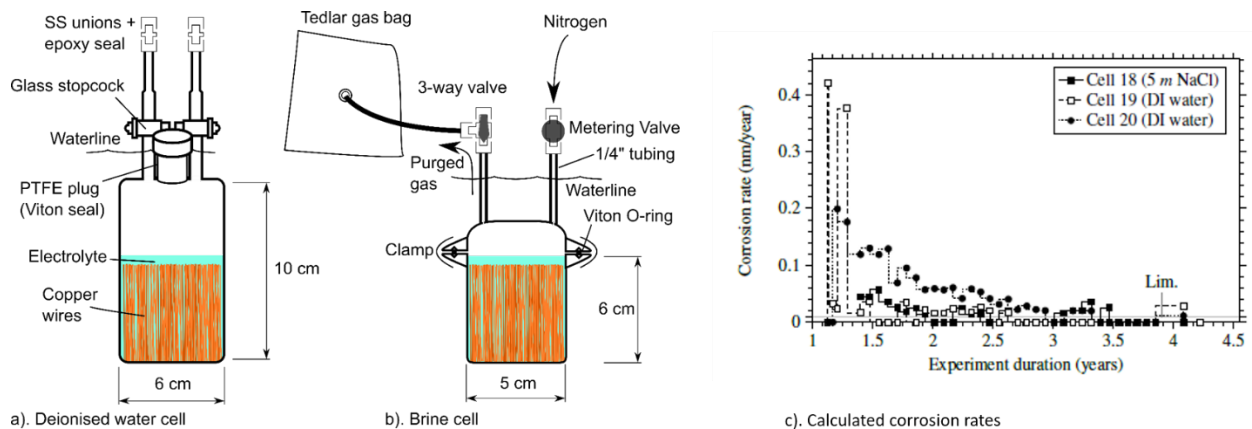


**Figure 4-11: (a) and (b) Schematics of Test Cells for Anoxic Copper Corrosion Investigations in Deionised and Brine Cells Respectively at CanmetMATERIALS; (c) Calculated Copper Corrosion Rates Based On Hydrogen Measurements for Two Deionised Cells and One Concentrated Brine Cell Over Approximately Four Years**

#### 4.3.1.2 Corrosion of Copper Coatings

With the development of copper coatings, it has become necessary to investigate different copper forms to ensure that corrosion does not occur preferentially via mechanisms that do not occur for wrought coppers. Because thermodynamic arguments are used (as opposed to kinetic arguments) to describe the ability of copper to have a very long life in the repository, there is little risk of this occurring in a general sense, but there is a possibility that localized effects may differ among copper species. NWMO has done extensive work in this area with its research partner, Western University, including:

1. Long-term exposures of copper samples;
2. Electrochemical polarizations to simulate corrosion;
3. Comprehensive surface analysis to assess samples before and after the exposures noted above.

Despite more than five years of effort, little difference can be found among the samples, regardless of test method. Only very slight differences can be seen only where extensive cycles of electrical currents to initiate copper oxidation (i.e., to artificially simulate corrosion) are used. In these experiments, there is some minor evidence that the copper coatings made by electrodeposition or cold spray undergo a very minor preferential grain etching, such that corrosion depth may be very slightly greater near grain boundaries. Studies are ongoing to quantify this depth, which at present appears to be a few micrometres (and thus, insignificant to the safety of copper coatings on the order of 3 mm thick). Future detailed reporting will provide a comprehensive description of the current understanding of copper coating corrosion.

#### 4.3.1.3 Corrosion of Copper in Radiolytic Environments

Immediately after emplacement, the UFC will be exposed to a diminishing dose of low strength gamma radiation emitted from within the used nuclear fuel. During the first few decades when this field is highest, there is the possibility that trapped air and/or water near the UFC may absorb low doses of radiation. Through radiolysis, trace amounts of redox active species may be produced, and this may impact the corrosion behaviour of the copper coating.

A series of experiments on copper samples have been initiated to determine the influence of gamma radiation during the different stages of DGR conditions:

- Copper coating samples in aqueous solutions including a range of possible groundwater anions such as  $\text{SO}_4^{2-}$ ,  $\text{HCO}_3^-$ ,  $\text{Cl}^-$ , exposed to high gamma radiation fields to artificially accelerate corrosion processes, and identify possible reaction mechanisms.
- Copper coating samples undergoing atmospheric corrosion experiments in low strength gamma radiation fields, similar to those expected for the repository to directly observe samples for potential damage.
- Copper coating samples exposures to small volumes of aqueous nitric or nitrous acids, to simulate the most aggressive humid air radiolysis products that could be in condensed water droplets on the container surface.

In addition, experiments have been extensively supplemented with modelling, including assessments for:

- Production of radiolytically formed species, including to determine oxidant concentrations that may affect the copper corrosion;

- Total corrosion of radiolytic copper corrosion in solutions containing groundwater anions such as  $\text{SO}_4^{2-}$ ,  $\text{HCO}_3^-$ ,  $\text{Cl}^-$  as a projection from direct measurements.

Experimental results confirmed that low strength gamma radiation fields do not influence corrosion, producing no measurable corrosion damage beyond that observed in the absence of radiation (i.e. in humidified air). The corrosion products were patchy; although the depth of damage below these patches is only a few micrometers (i.e.  $< 10 \mu\text{m}$  after a year of exposure), with or without radiation.

As nitric acid is a possible species produced from radiation reacting with air and water, a conservative calculation that presumed a mass-balance limited accumulation of nitric acid-containing droplets was performed. The result indicated that the maximum damage from radiolytically produced nitric acid is perhaps a few micrometres (i.e.  $< 10 \mu\text{m}$ ) of corrosion. Experimental tests were performed on the copper system using water droplets containing nitric acid, and confirmed that damage will be small (i.e.  $< 10 \mu\text{m}$ ). Results also revealed a poor ability of nitric acid to oxidize copper in the absence of oxygen, and minimal damage, except where oxygen was allowed to enter.

#### 4.3.1.4 Oxidic Corrosion of Copper

Following closure of a DGR, the conditions will evolve from an initial warm oxidic period to a long-term cool, anoxic period (Guo 2016). As a result, the maximum depth of copper corrosion during the early oxidic stage has been evaluated based on the quantity of  $\text{O}_2$  trapped when the DGR is sealed (Hall et al. 2018).

The inventory of trapped oxygen was determined to be 13 mol per UFC (Hall et al. 2018), which corresponds to a maximum corrosion depth of  $81 \mu\text{m}$ . Ongoing work on oxidic corrosion focusses on validating the corrosion mechanism, which is presumed to be via uniform, and not non-uniform, corrosion.

### 4.3.2 Internal Corrosion of UFC

When the UFC is welded closed, it is possible that there will be some air and moisture in the internal atmosphere. Its proximity to the used nuclear fuel has the potential to produce a very small amount of corrosive species. NWMO published a technical report (Wu 2019) that outlined conservative corrosion calculations carried out based on NWMO's reference design. These calculations defined the scale of certain corrosion scenarios, and validated assumptions that uniform corrosion would be negligible, i.e. less than  $10 \mu\text{m}$  on even the most conservative scenario, for components that are more than 30 mm thick. Previously, it was confirmed that the weld region is not susceptible to localized attack, thus current research is investigating low probability localized corrosion elsewhere in the UFC (Wu et al. 2017).

The evolution of carbon steel corrosion is being studied by performing coupon exposure tests in a small water volume under stagnant conditions as a function of time. Conditions include systems with added oxygen,  $\text{H}_2\text{O}_2$ , and/or the presence of high dose gamma radiation. While these conditions are much more extreme than would be seen for the inside of a container in a DGR, mechanistic information derived from these experiments will be informative in gaining a more thorough understanding of the reactivity of steel in milder conditions. The results from these studies will be compiled and published in graduate theses and peer-reviewed journals.

### 4.3.3 Microbial Studies

The design of the repository emplacement room utilizes HCB to suppress microbiological activity near the UFC. However, as microbiological activity may occur within bentonite that is improperly placed, as well as elsewhere underground, considerable efforts are being made to study it. Recent work has focused specifically on extraction and characterization of the DNA held within the bentonite clay, as this material is present in extremely low quantities (Engel et al 2019a). Much of this work is conducted in concert with corrosion and bentonite programs, as well as within work that is performed at the underground research laboratories (Mont Terri and Grimsel) in Switzerland (Engel et al 2019b). To supplement the *in situ* work being performed in underground labs, a set of 18 pressure vessels (Figure 4-13 (a)) have also been designed, fabricated and commissioned to perform a large number of *ex situ* experiments at Western University. In 2019, an initial set of scoping experiments were started with the goal of comparing the results of similar experiments conducted by Stroes-Gascoyne et al. (2010).

The upcoming experimental conditions of interest will be exposure to pure water for up to 1 year in an anaerobic environment. Should these results be comparable to the work by Stroes-Gascoyne et al. in aerobic conditions, follow up experiments are considered to investigate saline waters in an anoxic environment for up to two years duration. Such an experimental campaign which has simulated a range of possible DGR environments has not been conducted in a laboratory setting before.

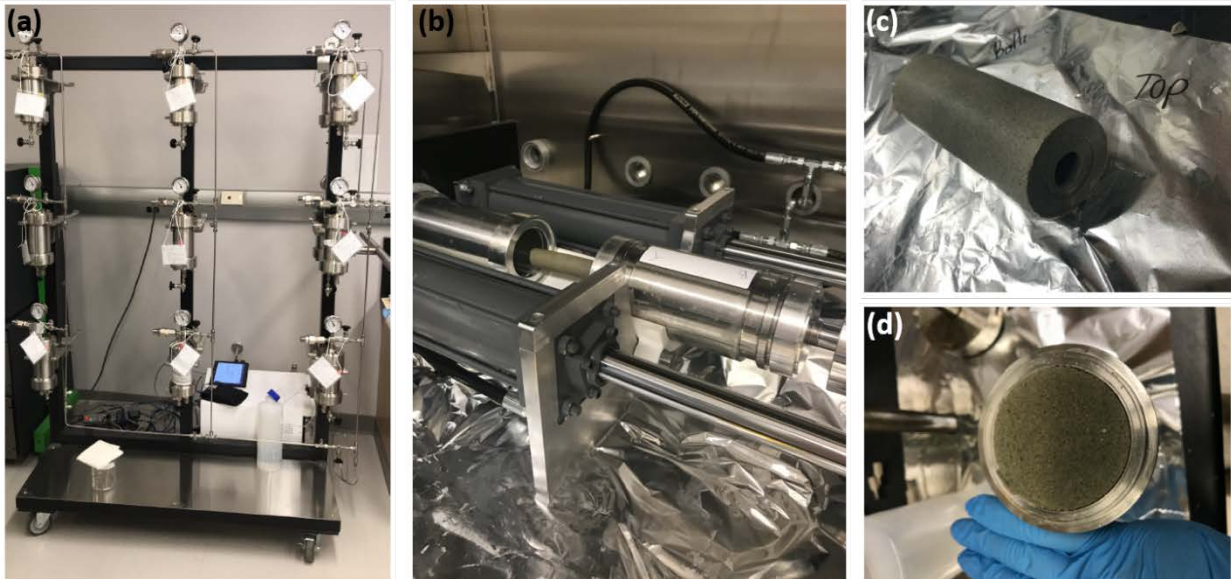


**Figure 4-12: (a) Experimental Setup for all 18 Pressure Cells Connected to the HPLC Pump. (b) Custom Press Housed Inside an Anoxic Chamber Used to Compress Bentonite to the Desired Density and to Core Bentonite Plugs for Analysis. (c) Sectioned Bentonite Plug Following Removal from Pressure Cell. (d) Dismantled Pressure Cell Following and Experiment Prior to Sectioning**

#### 4.3.4 Bentonite

Based on the favourable results of previous work analyzing trace amounts of carbon in bentonite (Michaela et al. 2014a, b), new work was initiated to further the understanding of what percentage of natural organic carbon is available as “food” for microbial processes. The goals of this program are to compare various bentonite clays from additional sources such as that from Japanese and Swedish formations with current NWMO’s reference material MX-80, as well as to assess if there is any change to bioavailability of carbon when bentonite undergoes exposure to radiation and/or high temperature and salinity, as will occur in the DGR. Through this research project, the natural organic carbon in the bentonite samples employed in the pressure cells experiment will be also evaluated to assess its molecular structure and potential for use as a microbial substrate. Demonstrating that the natural organic carbon composition at the molecular-level does not change over time, is an additional line of evidence to support that microbial growth and activity does not occur in highly compacted bentonite clay.

In 2018, the NWMO initiated a series of experiments to place bentonite and container materials into test modules that will be deployed in the deep Pacific Ocean. Test modules were designed and fabricated based on modules initially developed by Nagra for the underground research described above. In October of 2018, two test modules were shipped to Ocean Networks Canada at the University of Victoria, British Columbia and deployed in the Pacific Ocean at a depth of 95 m, with the goal of developing methods and protocols for future operations a greater depth, and pressure. Modules were then retrieved in March 2019 and sent to Western University for corrosion, bentonite, and microbiological analysis over the course of the next several months. The results of the preliminary analysis will be available in 2020. Photos of the deployment and retrieval of the test modules are shown in Figure 4-13. Informed by this trial at a shallow depth, a second set of two test modules was deployed at a depth of ~1000 m where they will stay immersed for up to two years before being retrieved and analyzed.

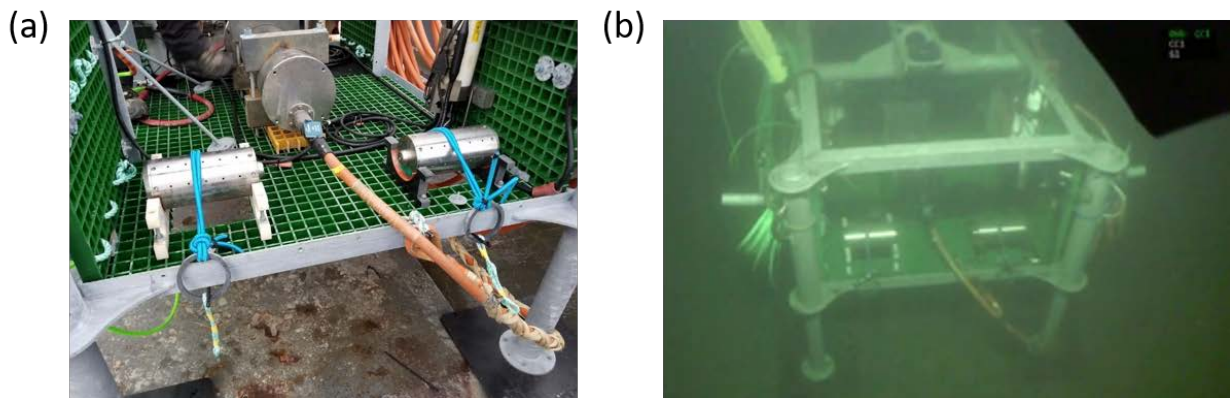


**Figure 4-13: Photos of the Test Modules Containing Copper Embedded in Bentonite Clay on the Immersion Platform (a) Prior to Immersion in the Pacific Ocean and (b) During Immersion at 95 m**

#### 4.3.5 Corrosion Modelling

##### 4.3.5.1 Localised Corrosion Modelling

The development of a probabilistic model to predict the extent of localised (pitting) corrosion of copper canisters was on-going in 2019. The model accounts for not only the stochastic nature of pitting corrosion but also the variability and uncertainty in the repository environment and in how

it evolves with time. Because of the availability of mechanistic information and of suitable input data, the model was developed on the assumption of aerobic, saturated conditions in the near field. This work was presented at 7<sup>th</sup> International Workshop on Long-term Prediction of Corrosion Damage in Nuclear Waste Systems (LTC 2019) with expected publication of the proceedings in 2020.

#### 4.3.5.2 FE-G Oxygen Modelling

Gas monitoring in FE-G was on-going in 2019 and included gas composition studies, numerical modelling and complementary table-top experiments. The gas composition in the FE-G, similar to a potential DGR, is controlled by different relevant bio-, geo, chemical and transport processes. Continued in 2019 was analysis of aerobic conditions after backfilling, gas advection through the tunnel EDZ and plug, gas exchange with the clay host rock and other bio-chemical processes. Composition of the bentonite porespace has been monitored since construction in 2014 to capture long term behaviour of, for example, unsaturated transport of corrosive species (ex. O<sub>2</sub> and H<sub>2</sub>S) and gas generation (eg. H<sub>2</sub>) (Tomonaga et al. 2019).

### 4.4 OTHERS

#### 4.4.1 Reactive Transport Modelling of Concrete-Bentonite Interactions

The multi-component reactive transport code MIN3P-THCm (Mayer et al. 2002; Mayer and MacQuarrie 2010) has been developed at the University of British Columbia for simulation of geochemical processes during groundwater transport. Prior reactive transport modelling work related to engineered barriers (e.g. bentonite) included the Äspö EBS TF-C benchmark work program (Xie et al. 2014), and the geochemical evolution at the interface between clay and concrete (Marty et al. 2015).

Reactive transport simulations have been performed with MIN3P-THCm to investigate long-term geochemical interactions driven by diffusion-dominated transport across interfaces between bentonite, concrete and host rock in the near field of a repository. The impact of altered interfaces on the migration of radionuclides (i.e. I-129) has also been numerically investigated. Simulation results indicate that porosity reduction and pore clogging at the interfaces can significantly inhibit radionuclide migration. A technical report documenting the reactive transport simulation across interfaces is expected in 2020.

#### 4.4.2 Gas-Permeable Seal Test (GAST)

Potential high gas pressure within the emplacement room due primarily to corrosion of metals and microbial degradation of organic materials is a significant safety concern for long term repository performance. To address this potential problem, Nagra initiated the GAST project at Grimsel Test Site, Switzerland in late 2010. The main objective of GAST is to demonstrate the feasibility of the Engineered Gas Transport System which enables a preferable flow path for gas at over-pressures below 20 bars where the transport capacity for water remains very limited. NWMO has been part of the GAST project since its inception.

Presently the experimental facility is still in the saturation phase. The delay is due to a major leak event occurring in 2014 and due to the significantly underestimated speed of the saturation process in the sand bentonite mixture.

In 2019, a smaller scale, well instrumented laboratory experiment - mini-GAST was initiated at UPC (Polytechnic University of Catalonia), Barcelona, Spain. The mini-GAST project aims to mimic the GAST experiment in a much better controlled fashion in the lab within a much shorter testing time frame. The mini-GAST experiment comprises of two semi-cylindrical shape mock-up tests, MU-A (50 cm in length and 30 cm in diameter) and MU-B (1/3 size of MU-A). The reduced size test MU-B will be carried out first to gain more understanding and experience for MU-A.

#### **4.4.3 DECOVALEX**

DECOVALEX (DEvelopment of COupled models and their VALidation against EXperiments) is an international research and model comparison collaboration program, initiated in 1992, for advancing the understanding and modeling of coupled thermo-hydro-mechanical-chemical (THMC) processes in geological systems. Prediction of these coupled effects is an essential part of the performance and safety assessment of geologic disposal systems for radioactive waste and spent nuclear fuel, and also for a range of sub-surface engineering activities.

The NWMO participated in the Task E on modelling a heater experiment in the clay rock at the Andra Bure underground facility.

##### **4.4.3.1 DECOVALEX-2019 Task E: Step 1, Step 2 and Step 3 – Coupled Thermal-hydraulic-mechanical Modelling of the Multi-Scale Heating Experiments**

Andra performed a wide range of in-situ experiments at its Meuse/Haute-Marne Underground Research Laboratory (MHM URL). The purpose of these experiments is to study the feasibility of a radioactive waste repository in the Callovo-Oxfordian claystone formation (COx). An important research program has been conducted by Andra since 2005 to investigate THM response of the COx to a thermal load through laboratory and in situ experimentations (Armand et al. 2017). A step-by-step approach is followed, which starts with small scale heating boreholes (TED experiment as shown in Figure 4-14) and extends to full-scale (ALC experiment as shown in Figure 4-15). Modeling and interpretation of the TED and ALC experiments were conducted in the context of the Task E within the DECOVALEX-2019 framework (Birkholzer et al. 2019).

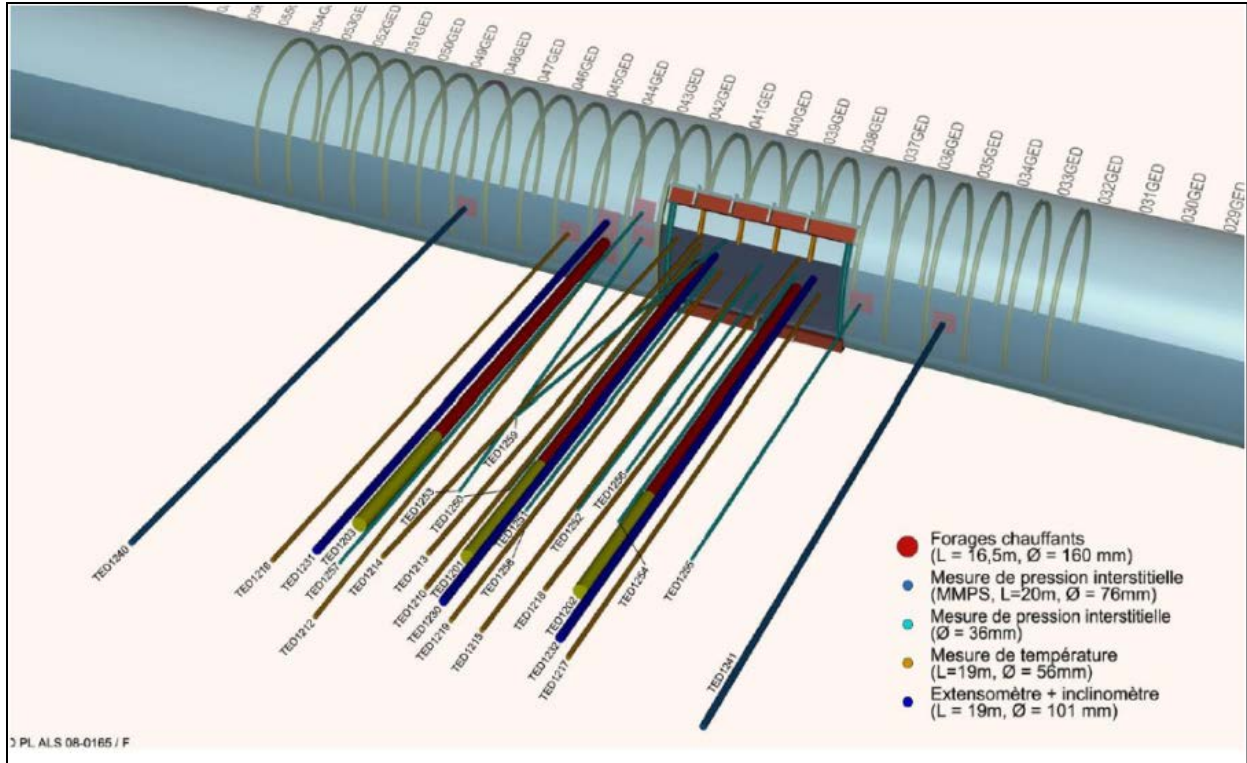


Figure 4-14: Three-dimensional Layout of the TED Experiment Indicating Heaters and Instrument Boreholes (Armand et al. 2017)

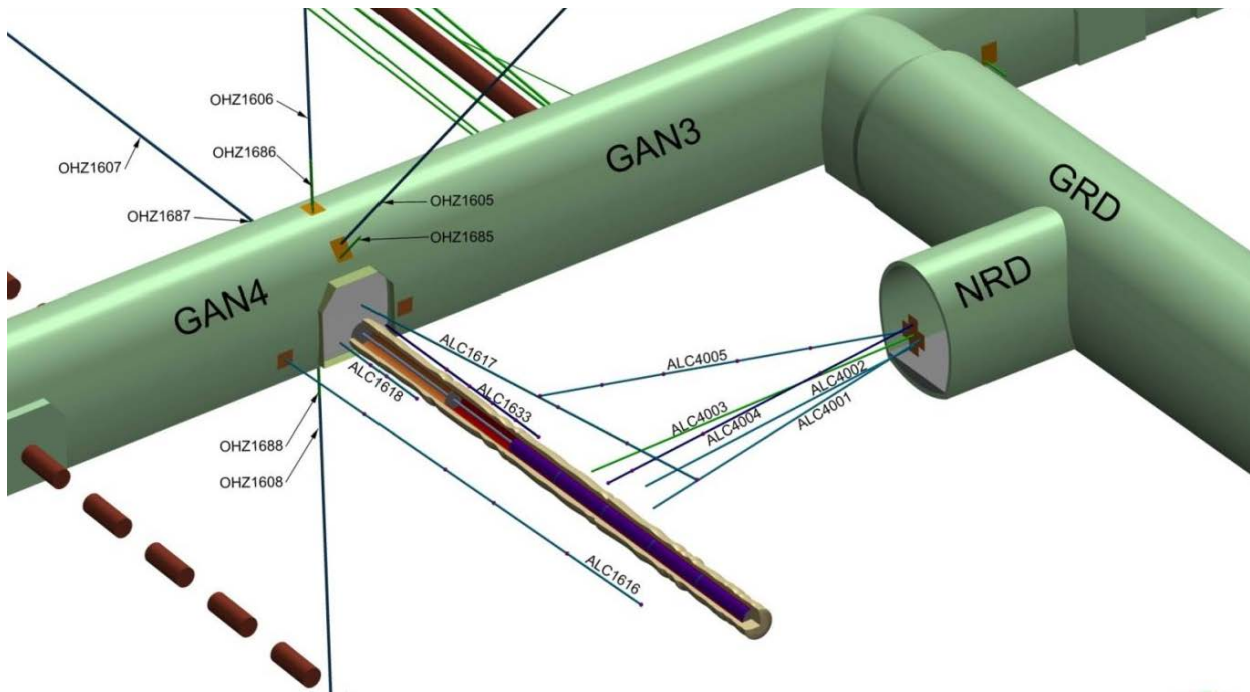
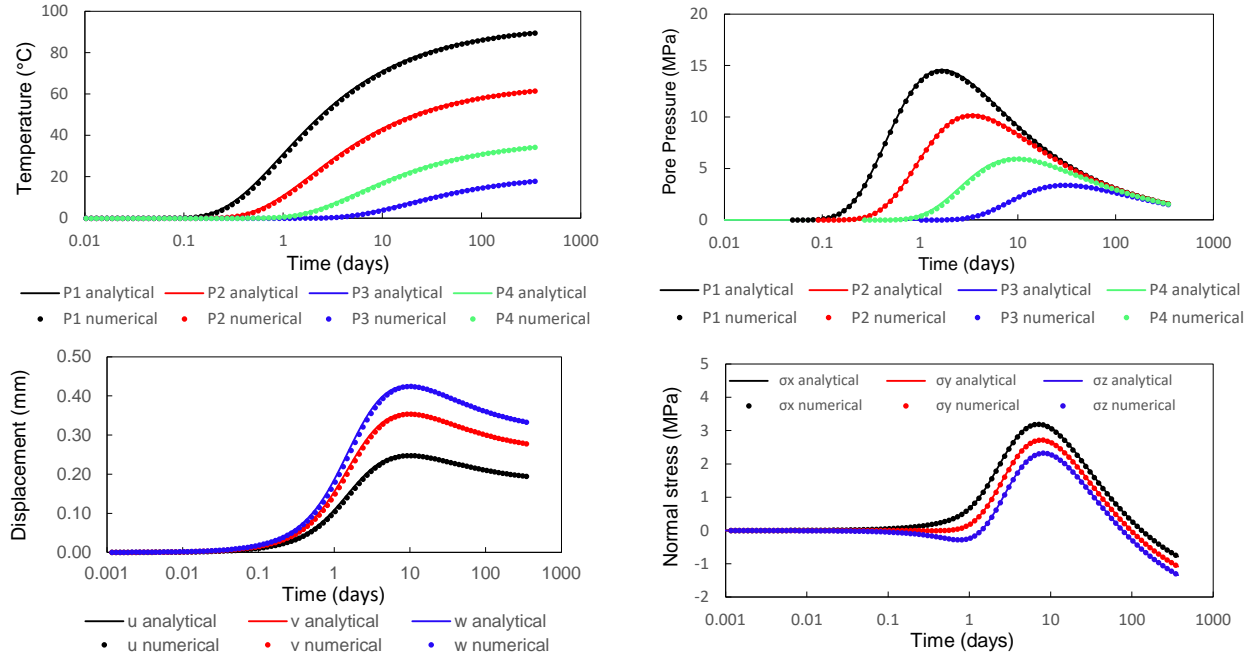


Figure 4-15: Three-dimensional Layout of the ALC Experiment Indicating Heaters and Instrument Boreholes (Armand et al. 2017)

To perform the modelling of the TED and ALC experiments, a fully coupled thermal-hydraulic-mechanical (THM) model was developed in COMSOL for fully saturated geotechnical materials (Guo 2019a, b). This model was initially validated by comparing the model results against the analytical solution for the consolidation of an infinite homogeneous saturated porous medium around a constant point heat source (Booker and Savvidou 1985) (Figure 4-16).



**Figure 4-16: Comparison of Temperatures, Pore Pressures, Displacements and Normal Stresses Calculated using the COMSOL Model and the Analytical Solution with a Biot Coefficient of 1.0**

The model was then used to calibrate the THM properties of the Callovo-Oxfordian claystone (COx) based on measurements of thermal and hydraulic results in the TED Experiment (Figure 4-17). A set of calibrated THM parameters of the COx was obtained.

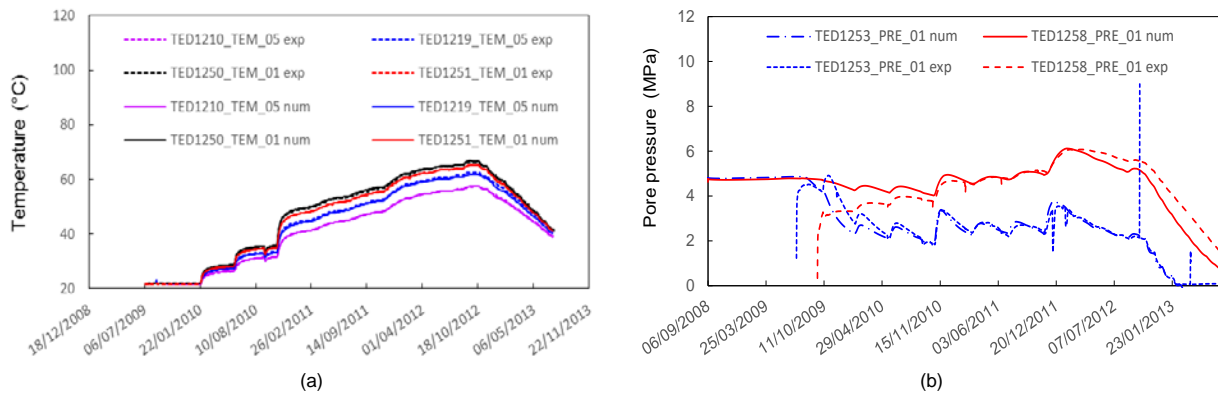


**Figure 4-17: Comparison of Calibration COMSOL Model Temperatures (a) and Pore Pressures (b) with Measurement at Different Locations**

The proposed model and the calibrated THM parameters were then used to predict the initial THM response of the COx in the larger-scale ALC experiment (Figure 4-18).

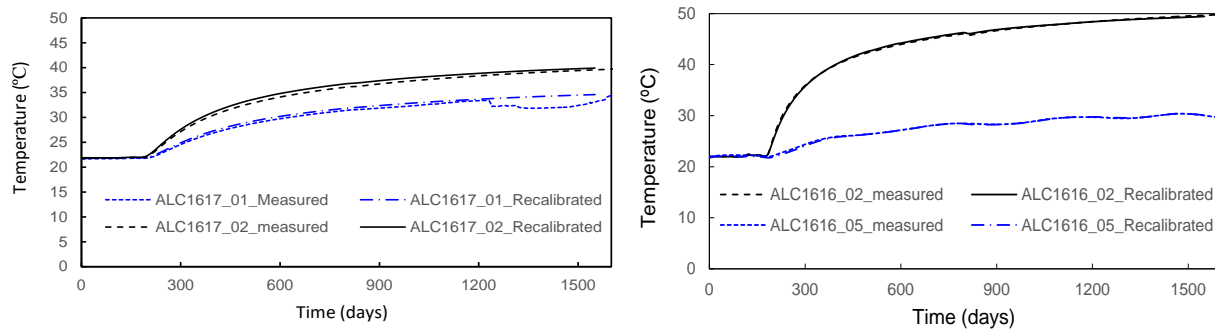


**Figure 4-18: Interpretative Temperatures at Different Locations in the ALC Experiment using Parameters Determined from Calibration Modelling of the TED Experiment with Measurements**

Excellent match between the COMSOL model and the ALC experiment measurements validated the effectiveness of proposed coupled THM COMSOL model, and also confirmed the success of the calibration of the THM parameters through modelling of the TED experiment. Excellent match also indicates that thermal radiation and thermal advection in the open length inside the casing and in the gap between the casing and the heater in the ALC experiment can be simplified by using equivalent thermal conduction.

#### 4.4.3.2 DECOVALEX-2019 Task E: Step 4 – Prediction of the Thermal-Hydraulic-Mechanical Response of a Geological Repository at large Scale and Sensitivity Analysis

In the current French concept, the High-Level Waste (HLW) will be placed in a set of parallel micro-tunnels 0.75 m to 0.80 m in diameter and 80 m to 150 m length (Figure 4-19) (Armand et al. 2017). The HLW zone covers an area of around 8 km<sup>2</sup> in which the rock shows vertical and horizontal mineralogical variation and therefore, the thermal-hydraulic-mechanical (THM) properties are variable. A case study based on Cigéo data to better assess modelling of deep geological repositories was conducted in the context of the Task E within the DECOVALEX-2019 framework.

## Bloc diagramme 3D Cigéo

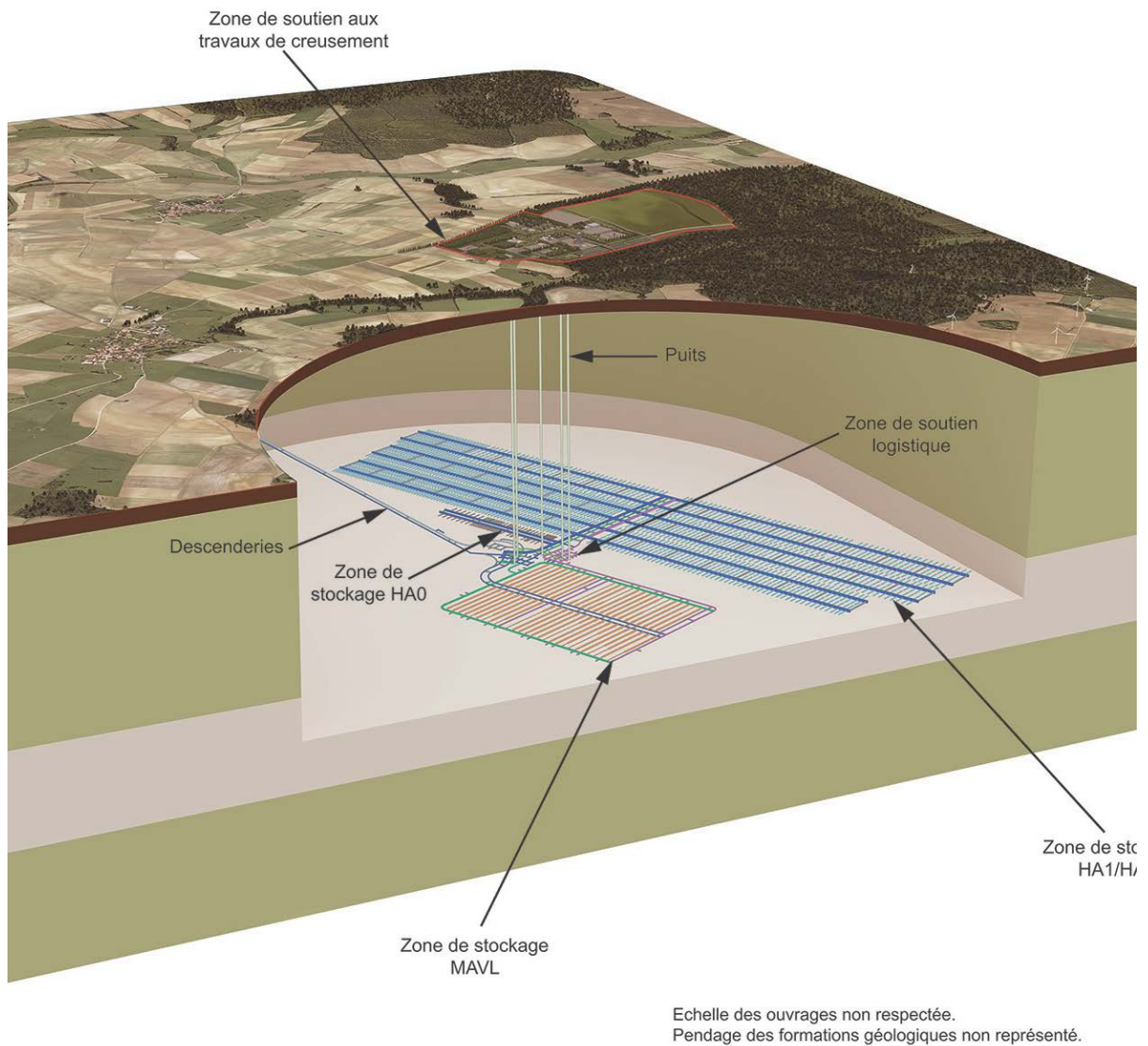


**Figure 4-19: Diagram of the Facilities of the Cigéo Project**

To gain a better understanding of the THM response caused by the high-level radioactive waste released heat in the Callovo-Oxfordian formation (COx) for the near field and far-field areas, a series of 3D coupled THM modelling has been performed (Figure 4-20). To shorten the calculation time, the DGR was represented by using six cuboid blocks with only six centered cells of interest modelled in detail and this simplification is validated. This model can be used to model not only the near-field THM response of the rock but also the far-field THM response.

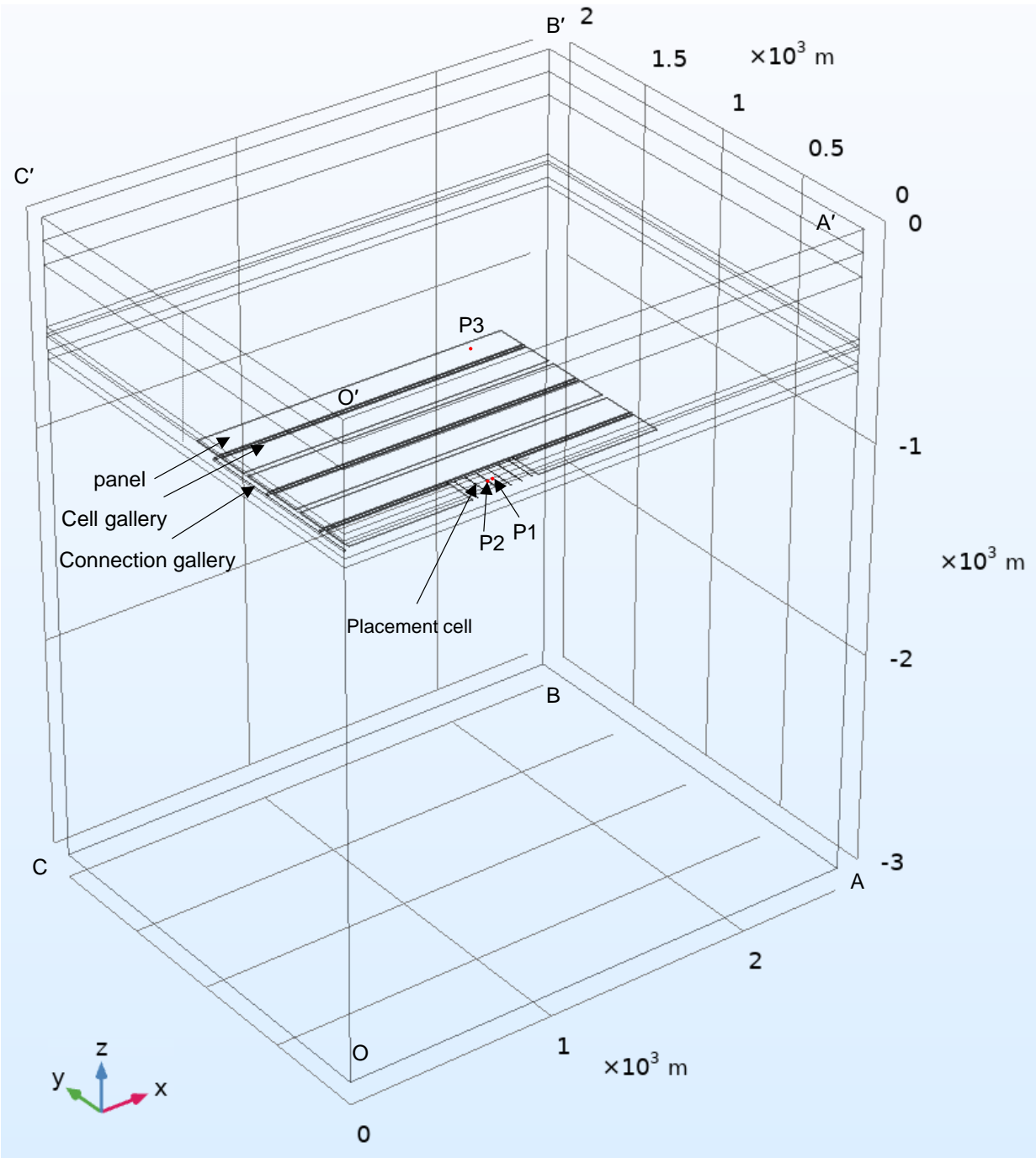


**Figure 4-20: Model Geometry of the Base Case with 6 Placement Cells Presented in Detail**

In this study, the theory used to perform the coupled THM modelling is validated by comparing the modelled THM results for a point heat source in an infinite rock mass with an analytical solution (Smith and Booker 1993). The coupled COMSOL model for the case study is also validated by comparing its thermal component for the Base Case with accurate results calculated using other methods (Figure 4-21) (Guo 2017).

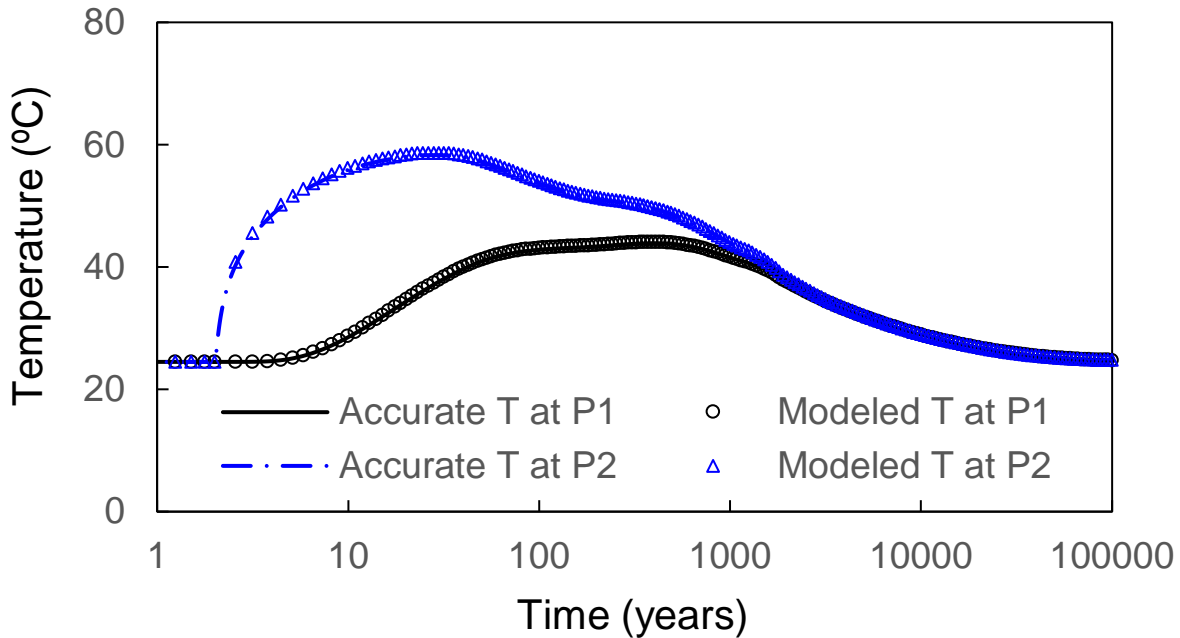


**Figure 4-21: Comparison of Temperature between Coupled THM COMSOL Model and the Accurate Results at Point P1 and Point P2**

The sensitivity analyses of the THM parameters of CO<sub>x</sub> on the THM response at different location were performed. The most important factor influencing temperature development is thermal conductivity. The most important factor influencing pore pressure is rock permeability. The most important factors influencing the ground surface uplift are rock thermal expansion and rock permeability. Results of the modelling have been submitted for journal publication.

#### 4.4.4 Shaft Seal Properties

In 2019, the NWMO continued with its program to identify an optimized bentonite/seal mixture by evaluating the seal behavior of bentonite/sand mixtures having composition ratios other than 70:30. In this study, the use of a crushed limestone based sand material is studied in addition to granitic sand. Composition ratios of bentonite/sand mixture of 50:50, 60:40, 70:30, 80:20 and 90:10 (by weight) are assessed.

The tests evaluate the following:

1. Compaction/fabrication properties of the materials (to Modified and Standard Proctor density);
2. Consistency limits (Atterberg Limits) and free swell tests;
3. Density of as-fabricated material;
4. Moisture content of as-fabricated material;
5. Mineralogical/chemical composition, including measurements of montmorillonite content;
6. Swelling pressure;
7. Saturated hydraulic conductivity;
8. Two-phase gas/water properties, specifically the capillary pressure function (or soilwater characteristic curve, (SWCC)) and relative permeability function, measured over a range of saturations that include the as-fabricated and fully-saturated condition;
9. Mineralogical/chemical composition of the materials exposed to brine for an extended period of time;

To date the test results shown that the performance for a bentonite- granitic sand and a bentonite - crushed limestone sand are similar, and that the performance of the various blends are in general agreement with the predicted results based on the amount of bentonite.

#### 4.4.5 Thermo-hydro-mechanical Modelling of NWMO Placement Room

Using the program CODE\_BRIGHT for the NWMO placement concept, fully coupled THM models were developed to understand the saturation evolution in the buffer, and the degree of homogenization in buffer density at full water saturation (Malmberg and Birch 2019).

The modelling process includes constructing the modelled geometry, determining suitable initial and boundary conditions, as well as defining the parameter sets used to describe the modelled constituents. The geometry was generated to represent the placement room setup as close as possible. To represent the partial offset between the upper and lower rows correctly, two NWMO geometries were constructed to assess the models:

- No offset: with lower and upper rows of buffer boxes aligned, and
- Maximum offset: with lower and upper rows of buffer boxes fully misaligned.

An example of the modelling results is shown in Figure 4-22, for a flux limited model. In this case the final dry density upon full saturation in the both the maximum offset model and fully aligned model are shown. For both alignments the final GFM dry density ( $\rho_d$ ) has increased from the as placed minimum allowable ( $\rho_d = 1410 \text{ kg/m}^3$ ) to more than  $1500 \text{ kg/m}^3$ , and the HCB dry density has decreased from its as-placed value ( $\rho_d = 1700 \text{ kg/m}^3$ ). The results showed that the final UFCs movement was less than 25 mm in all cases. The modelling also showed the offset between the upper and lower rows of containers does not seem to have an impact on the vertical movement of the upper containers.

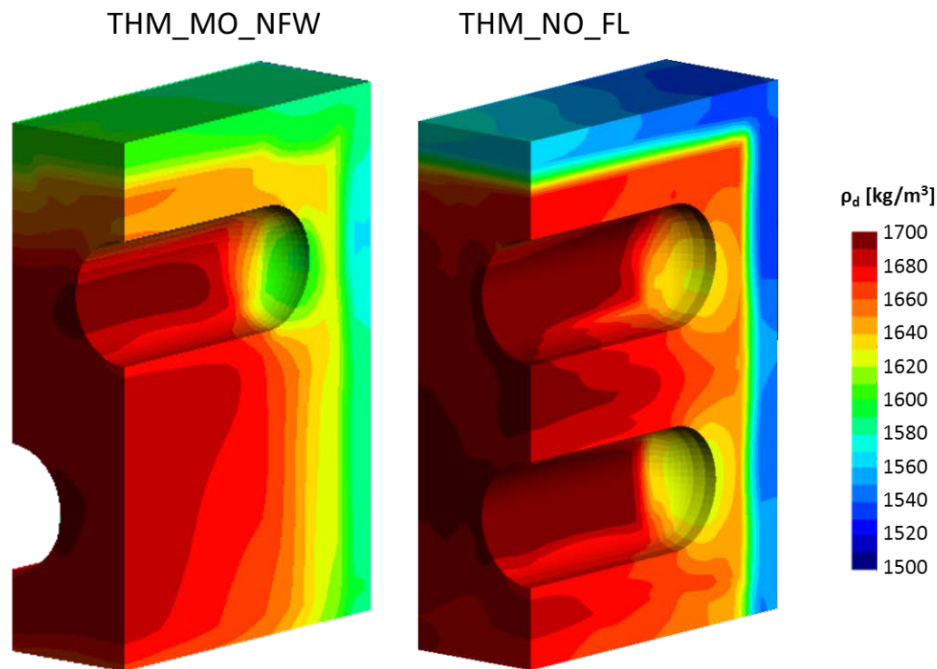


**Figure 4-22: Dry Densities at Full Water Saturation in the THM Model with Maximum Offset Geometry (Left) and THM Model with a Flux-Limited Water Inflow**

## 5. GEOSCIENCE

### 5.1 GEOSPHERE PROPERTIES

#### 5.1.1 Geological Setting and Structure - Bedrock Geology of Southern Ontario

A regional 3-D lithostratigraphic model of the Paleozoic bedrock of southern Ontario was recently released (Carter et al., 2019). In 2019, NWMO launched a new research project in collaboration with the Geological Survey of Canada (GSC) to support further development and refinements to this 3D geological model. Two important objectives of this work are to: i) reduce uncertainty in the thickness and occurrence of formations in the 3D geological model of southern Ontario by improvements to formation top records; and ii) incorporate regional faults in the 3D lithostratigraphic model to more accurately represent continuity / discontinuity of bedrock layers, relationships to hydrocarbon traps and potential locations for cross-formational flow of groundwater, and hydrothermal dolomite features. As part of this program, the 3D geological model will be provided to NWMO for use as the framework for the geosphere model at a sedimentary site, which will be further developed and refined with site-specific data.

The regional model encompasses an area of 110,000 km<sup>2</sup> and up to 1600 m of sedimentary strata underlying southern Ontario, with 54 bedrock layers representing 70 Paleozoic bedrock formations, plus unconsolidated sediment, with Precambrian basement forming the model base. Modelled volume is over 75,000 km<sup>3</sup> with a practical (data support) limit on horizontal spatial resolution of 400 m. Issues and challenges identified in the published model are to be addressed, with a focus on variable data density and data gaps in the Lockport Group, and with thin formations, which create anomalies and discontinuities in model layers. Extrapolation issues with some formations will be addressed, in particular for the Cambrian bedrock formations. Additional measured sections and control points may be required.

QA/QC edits for version 2 of the lithostratigraphic model are in progress with re-evaluation of formation tops completed for: the Early Silurian Lockport Group, the Collingwood Member of the Cobourg Formation, the Rouge River Member of the Blue Mountain Formation, and formation tops for all 412 wells in Bruce and Huron counties encompassing the NWMO area of interest for the APM project. A hydrostratigraphic chart has been developed for assignment of hydrostratigraphic units, and regional faults and domain boundaries for Precambrian lithostratigraphic domains have been added to the model. A further component of the study is an analysis of geologic controls on porosity and permeability variations in the Lockport Group. Three-dimensional models of 150 solution-mined caverns in salt beds created using sonar survey data were completed and are being tested for inclusion into the lithostratigraphic model. Early trial designs for a 3-D printed model have been completed. Methodology to enable virtual reality tours of the model is in development. Other additions will include oil/gas and gas storage reservoirs, as well as salt mines.

The model published by Carter et al. (2019) was constructed using Leapfrog® Works (Seequent Limited) implicit modelling software (Figure 5-1). Model construction for version 2 will utilize both Leapfrog Works and SKUA-GOCAD software. Export of revised data for the first iteration of version 2.0 has been completed and will be followed by an iterative cycle of interim model construction, expert geological appraisal to identify errors/issues, followed by QA/QC re-evaluation of formation top depths and re-modelling.

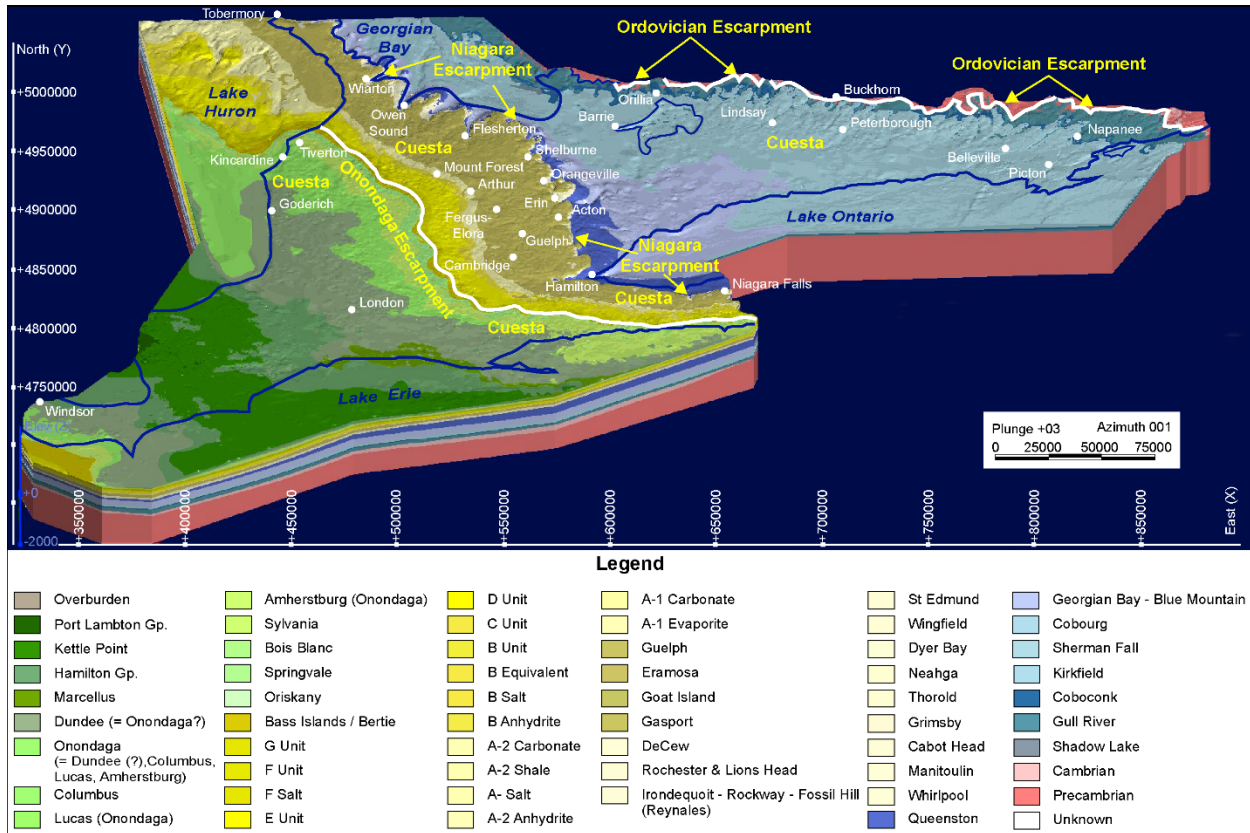


**Figure 5-1: Published 3-D Model of the Paleozoic Bedrock of Southwestern and Southcentral Ontario, Surficial Sediment Cover Removed (from Carter et al., 2019)**

### 5.1.1.1 Fractures and Fracture Zones, Faults and Joints

#### 5.1.1.1.1 Numerical Methods – Discrete Fracture Networks

Fracture network modelling involves using 3-dimensional (3D) geostatistical tools for creating realistic, structurally possible models of fracture zone networks within a geosphere that are based on field data. The ability to represent and manage the uncertainty in the geometry of fracture networks in numerical flow and transport models is a necessary element in the development of credible geosphere models. Fracture network modelling will also be used in 3D integrated geosphere models. The creation of fracture network models in MoFrac (software that generates 3D fracture network models for rock mass characterization) is a multistep process that involves integrating interpretations of lineament data and other available field data to define fracture orientations and size distributions.

MoFrac is capable of creating DFN models at the tunnel-, site- and regional scale (e.g. Bastola et al. 2015; Junkin et al. 2017, 2018, 2019a, 2019b). Version 3.0 of MoFrac is currently being used within the site investigations program. In parallel to MoFrac use in site characterization activities, further development and refinements to MoFrac are conducted through the research program. This enables model development and validation to occur in an iterative manner to support site characterization activities.

In 2019, work commenced to develop version 4.0 of the code. Two examples of key development tasks were chosen to further advance the code for application to additional site-specific information as it becomes available are:

- Fracture branching and clustering: Fracture branching will permit MoFrac to simulate either branching or coalescing fractures. Fracture clustering will allow for control of the spatial distribution of fractures.
- Time slicing: Time slicing will be used to propagate multiple fractures simultaneously. Propagation will no longer be a whole-fracture process, but instead will operate on extending a partially-complete-fracture mesh.

### 5.1.1.2 Metamorphic, Hydrothermal and Diagenetic Alteration

#### 5.1.1.2.1 Hydrothermal Alteration in Crystalline Rocks

An understanding of regional metamorphic processes, such as hydrothermal fluid alteration and its associated water-fluid-rock interactions is required to determine the past evolution of waters at a potential repository site. Lakehead University initiated new research in 2018 to understand the deformation of the rocks in the Wabigoon Subprovince through characterization of hydrothermal fluid compositions and different reaction mechanisms that have taken place over geological time.

The research is unique in that uses granitoid rocks of Wabigoon Subprovince—instead of greenstone belts—as proxies of metamorphism in the region. This research combines structural studies with an examination of the mineralogy and petrology of the hydrothermal alteration assemblages. In addition to reconnaissance mapping and structural studies, the study includes petrographic analysis and mineral chemistry characterization, applying different techniques such as XRF, ICP-MS, Chlorite Geothermometry, and  $\delta^{18}\text{O}/\delta^2\text{H}$  isotopic analysis. Figure 5-2 shows the localities for sample collection and structural mapping as part of ongoing research.

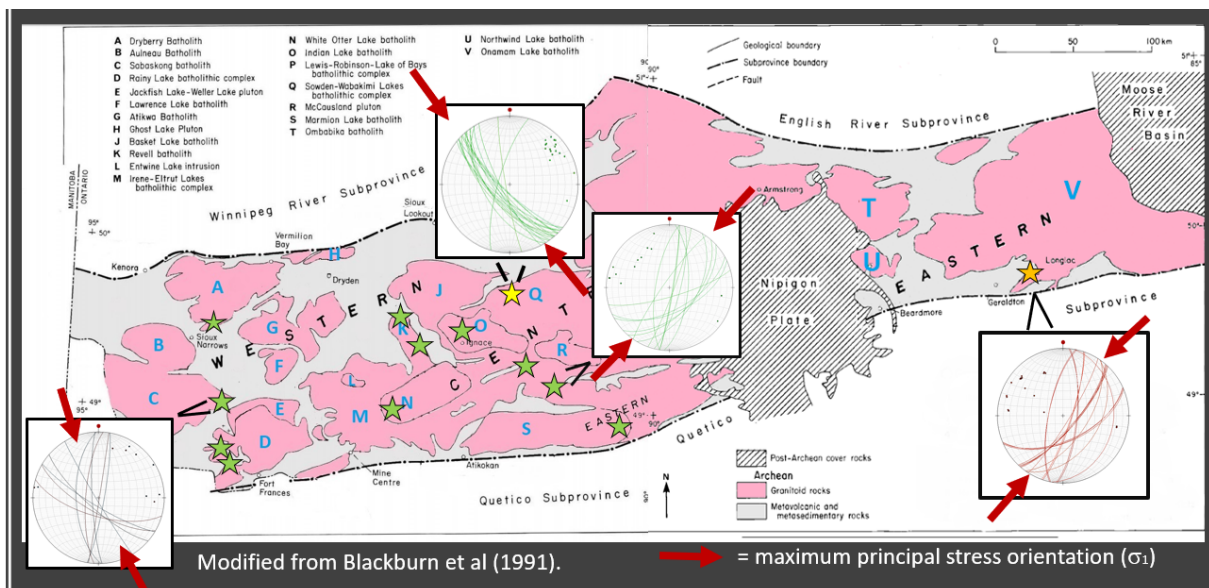


**Figure 5-2: Target Locations for Sample Collection and Structural Mapping**

Preliminary results of the structural mapping campaigns and the petrography analyses indicate that the nine plutons examined to date display the following features:

- Hydrothermal chlorite and/or epidote which precipitated along oblique strike-slip faults.
- Alteration of wall-rock (replacement of feldspars by epidote, chlorite, white mica, biotite, sphene).
- Ductile deformation temperatures in the amphibolite facies of metamorphism.
- Faulting/hydrothermal alteration occurred during regional-scale Archean deformation (brittle-ductile deformation) in at least 2 plutons.

In the second phase of the study, the focus will be placed on mineral chemistry. In particular:

- SEM analysis will be carried out to better determine the chemistry of fracture infill.
- $\delta^{18}\text{O}/\delta^2\text{H}$  stable isotope analysis on chlorite and epidote coated faults will be used to constrain the source of hydrothermal fluids.

Additionally, three drill cores will be studied to understand the regional granitoid metamorphism of the Wabigoon Subprovince in three dimensions (Figure 5-3).

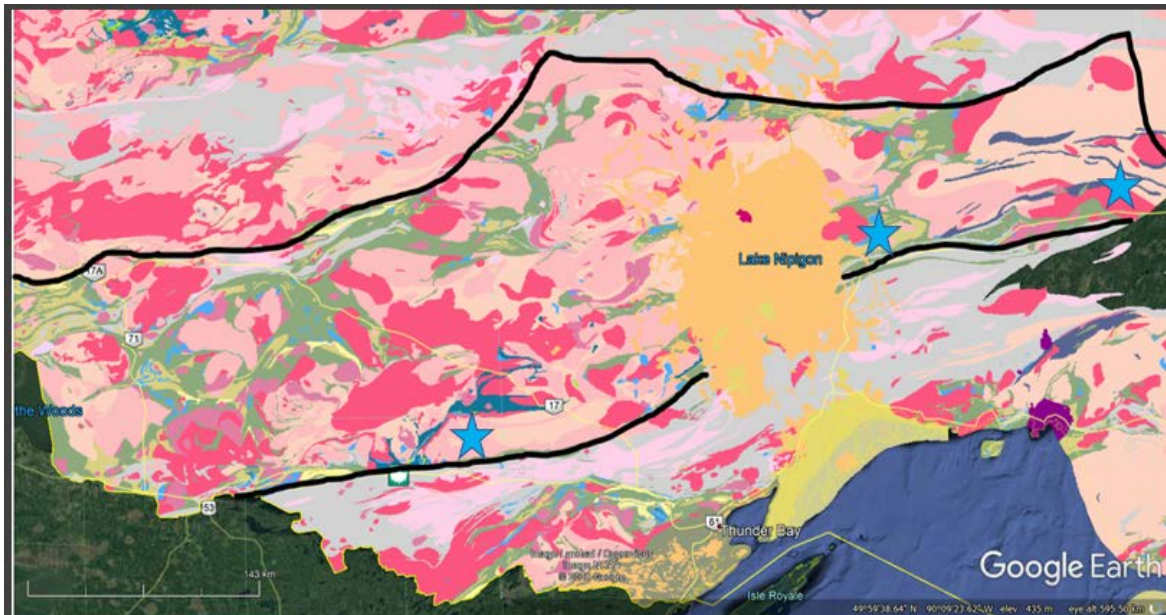


**Figure 5-3: Target Locations for Sample Collection and Structural Mapping**

#### 5.1.1.2.2 *Diagenetic Alteration of Sedimentary Formations*

Starting in 2015, research has been underway to investigate the nature and origin of strata-bound near-horizontally layered dolomitized beds occurring within the bedrock formations of the Black River Group in the Huron Domain of southern Ontario. During 2018, research continued to look for evidence of fault-related dolomitization at a regional scale, to determine if the non-fault-controlled dolomitizing conditions observed at the Bruce nuclear site are consistent across the Huron Domain. To date, no evidence from sampled wells in the Huron Domain have shown

the presence of fault-controlled dolomites. A summary of the research conducted between 2015 and 2017 is available in Al-Aasm and Crowe (2018).

In 2019, the research scope shifted to focus on the determination of Rare Earth Elements (REE) in both previously examined samples and new samples collected during 2018. The purpose of this next phase of the research is to better understand the provenance of the source material for the formations. Research proceeded in three main areas:

- Additional geochemistry and micro sampling (fluid inclusions) of samples from Bruce / Huron Domain including new samples from Silurian and Devonian formations to further expand understanding of the entire stratigraphic column and to produce a more complete picture of the local environment surrounding the formerly proposed L&ILW DGR at the Bruce nuclear site;
- Continued research to increase knowledge of fluid inclusion history by differentiating between basinal (regional) and hydrothermal (local) sources of diagenesis. Recent work suggest that the Silurian/Devonian systems have a separate and more recent fluid history; and
- Determination of Rare Earth Elements (REE) in both previously examined samples and new samples. REE's are applied in an attempt to distinguish between a meteoric or hydrothermal source fluid for the dolomitized carbonates and silicates at the Bruce nuclear site and Huron Domain.

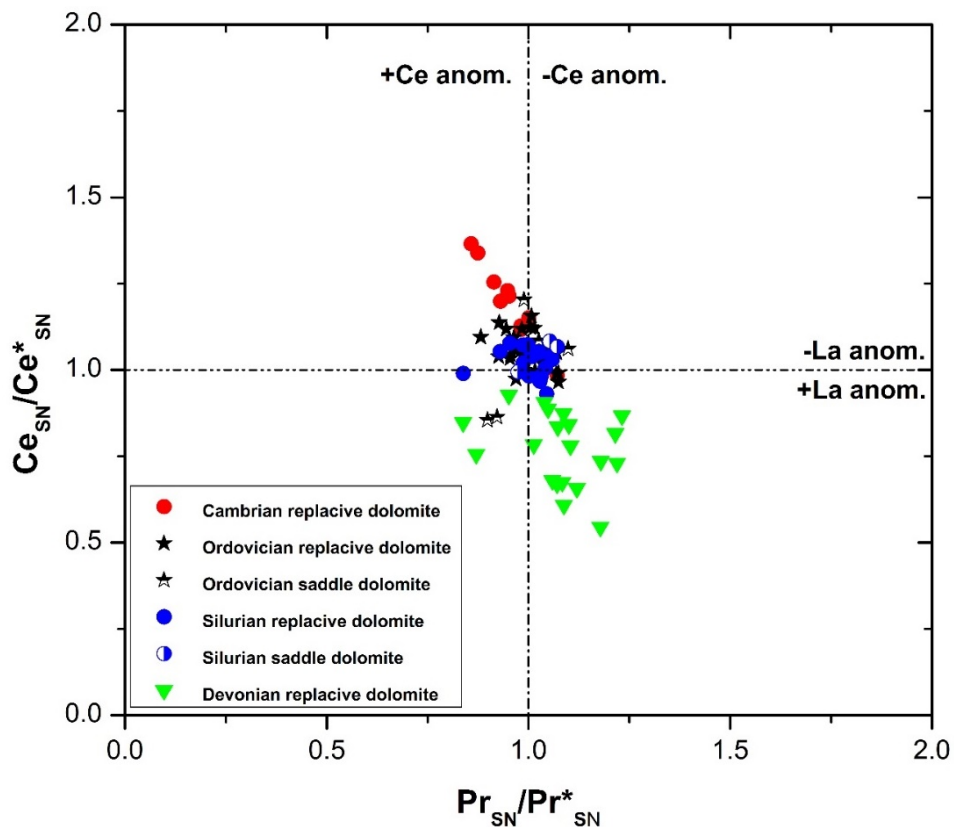


Figure 5-4: Ce Anomaly Cross Plot for Different Types of Dolomite

As shown in Figure 5-4, Silurian dolomite trends are characterized by a mainly negative La anomaly and positive Ce anomalies, possibly implying formation from evolved seawater. Devonian dolomites have maintained an original seawater REE characteristic showing a negative Ce anomaly and slightly positive La. In contrast, Cambrian and Ordovician dolomites show negative La anomaly reflecting a hydrothermal fluid source.

During 2019, recent research results were documented in a Master's thesis (Tortola 2019) and in a journal article submitted in December 2019.

#### 5.1.1.3 Fracture Mineralogy in Sedimentary Rocks

Research undertaken with the Jack Satterly Geochronology Laboratory at the University of Toronto, which began in 2014, culminated in 2019 with the publication of two journal articles summarizing results from the work (Davis et al., 2019; Sutcliffe et al., 2019). The aim of the research program run by Dr. Don Davis was to assess the geologic stability and fluid migration events of the sedimentary rocks underlying southern Ontario by applying radiometric Uranium-Lead (U-Pb) age analysis techniques to vein calcite, dolomite and silica cements. The analytical approach used a comparative analysis of Laser Ablation-Inductively Coupled Mass Spectrometry (LA-ICPMS) and Isotope Dilution-Thermal Ionization Mass Spectrometry (ID-TIMS) techniques.

Secondary calcite from >650 m deep Ordovician carbonate rocks yields a Silurian age of  $434 \pm 5$  Ma, possibly related to infiltration of seawater from overlying evaporitic basins as well as hydrothermal solutions that infiltrated from below. Calcite cement in sub-horizontal fractures near the base of the Silurian sequence record U-Pb ages of  $318 \pm 10$  Ma by laser ablation inductively coupled plasma mass spectrometry and  $313 \pm 1$  Ma by isotope dilution thermal ionization mass spectrometry. In contrast, near-surface Devonian rocks mostly give vein infill ages over the range of 80–100 Ma with evidence for younger infill down to 50 Ma. Vein calcite samples previously dated from surface outcrops of Ordovician carbonate exposed up to 500 km to the east yielded similar U-Pb ages. Coincidence of near-surface vein calcite ages indicates widespread vein emplacement synchronous with a change in direction of motion of the North American plate as well as possible erosional unroofing following passage of the region over the Great Meteor hotspot approximately 125 Myr ago.

Secondary dolomite and silica cements in Cambrian sandstone at the base of the sedimentary sequence beneath the Bruce nuclear show an average U-Pb age of  $320 \pm 10$  Ma, which is consistent with the calcite cement in the Silurian rocks noted above. The initial common Pb end member is slightly, but distinctly, enriched in  $^{206}\text{Pb}$  compared with that in older and younger calcite cements elsewhere within the sedimentary section. This age is interpreted to record episodic migration of a saturated hydrothermal brine.

Overall, the results of this research program suggest that despite more recent perturbations to sedimentary rocks in the near-surface environment, deeper formations have remained apparently impermeable to post-Paleozoic disturbances.

### 5.1.2 Hydrogeological Properties

#### 5.1.2.1 Hydraulic properties of Fractured Crystalline Rock

Research at the University of Waterloo is being undertaken to characterize the hydraulic behaviour and evolution of groundwater systems in Canadian Shield settings. Research

activities in 2019 investigated how variations in horizontal spatial scales in numerical groundwater models impact net exchange fluxes between surface-water and groundwater systems. Snowdon et al. 2019 found that for increasing horizontal spatial discretizations, the net exchange flux between the surface and groundwater will decrease compared to the point recharge estimate. The study compared 10 m, 50 m, and 250 m horizontal grid discretizations, and found that although the 50 m grid resolution was able to provide similar predictions for exchange fluxes, the 250 m grid resolution showed significant deviations.

During 2019, an extensive review of the literature was undertaken to define hydraulic and geochemical properties of crystalline rock. This database will permit the creation of depth dependent EPM rock mass and fracture zone properties for Canadian Shield settings. The data are drawn from technical documents developed by Atomic Energy of Canada Ltd between 1975 and 1996, and include 620 permeability estimates from sites across the Canadian Shield. The data, once collected and verified, are used to define depth dependent variations in EPM rock mass and fracture zone permeability. A journal publication on this work is in preparation with submission expected during 2020.

#### 5.1.2.2 Numerical Methods – Groundwater

HydroGeoSphere (HGS) is a 3D integrated surface-subsurface flow and transport simulator developed by Aquanty Inc (Aquanty 2018). Currently, HGS is the reference NWMO computer code) for groundwater flow and radionuclide transport simulations. In 2019, NWMO requested that Aquanty develop a few new HGS features to better adapt the code to the unique modelling requirements of NWMO projects. These new features will improve modelling capability and computational efficiency of future HGS simulations in general, especially for NWMO projects.

One of the main new features is the ability to identify fracture faces based on discrete fracture network data output from MoFrac in VTK format. MoFrac is a computer code that generates realistic, structurally possible models of fracture networks based on field data (see Section 5.1.1.1.1 for more detailed information). In addition, this new feature will also allow users to assign unique property values (such as hydraulic conductivity, porosity and thickness) to each individual fracture face. Other new features are the ability to directly import 3D geology data (voxel) and 2D elevation data (tsurf) from a GOCAD (a popular 3D geology modelling tool) model into HGS. It is expected that code development of these new features will be completed early 2021.

### 5.1.3 Hydrogeochemical Conditions

#### 5.1.3.1 Microbial Characterization – Waters & Rocks

The microbiological organisms and their activity in DGR level groundwater is an important parameter with respect to the long-term behavior of engineered barriers. In particular, should sulfate-reducing bacteria be present and active in either the groundwater or rock, there is the potential for these microbes to produce the corrosive species sulfide via sulfate reduction. While the highly compacted bentonite in the emplacement rooms is expected to prevent any microbiological activity, if sulfide is produced at the bentonite-rock boundary or further out in the far-field there is the potential for sulfide to diffuse towards the UFCs causing corrosion. Such corrosion is currently accounted for in the NWMO's copper corrosion allowance, but it is important to include site-specific data to ensure that the corrosion allowance is acceptable.

As part of site characterization activities, samples of rock and groundwater will be collected at various depths from NWMO boreholes and analyzed using methods developed through applied research at multiple Canadian universities (Waterloo, Toronto and McMaster). These methods utilize DNA, RNA, PLFA and NMR techniques to determine the type of organisms, the activity of organisms, and the potential of organisms to grow in rock and groundwater.

#### 5.1.4 Groundwater and Porewater Compositions

Knowledge of the geochemical and isotopic composition of groundwater and porewater at proposed DGR sites is required to determine potential flow pathways, origins and evolution of fluids, as well as estimates of residence time.

#### 5.1.5 Measuring pH in Highly Saline Groundwaters

Hydrogeochemical research, whether it is lab- or field-based, commonly requires knowledge of the master variable, pH. pH measurements are commonly done potentiometrically, with electrodes, which is very challenging in high ionic strength ( $I$ ) systems, such as the brines that make up the porewater and deep groundwaters in the Michigan Basin (up to  $I = 8\text{M}$ ). Spectroscopic methods offer an alternative approach for pH measurement in brines. This approach involves calibration of the spectroscopic properties of colorimetric indicators using specially-prepared buffer solutions, with the pH of the buffers determined by geochemical modelling. Initial work was completed using a single indicator (phenol red) in the measurement range of  $\text{pH} \approx 7 - 9$ . More recently, work is nearly complete to extend this technique over a wider range of  $\text{pH}$  ( $\sim 3 - 9$ ) using a multi-indicator solution. The technique is applicable up to  $I = 8\text{M}$ .

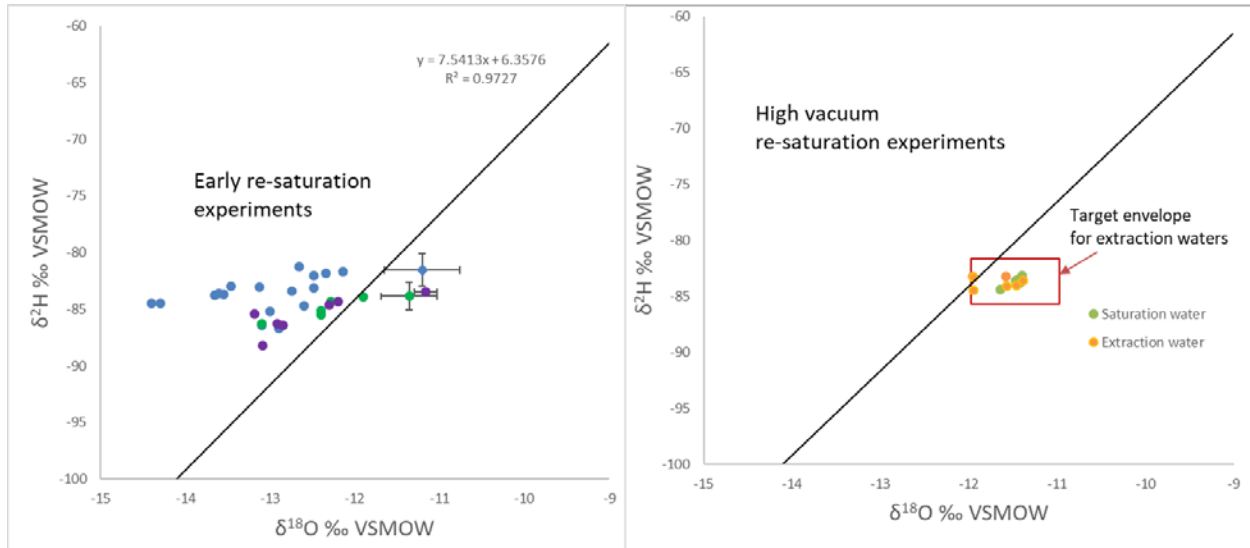
##### 5.1.5.1.1 Porewater Extraction Method Development

Vacuum distillation is a well-established method to extract porewater from low-permeability sedimentary rocks (Clark et al. 2013; Al et al. 2015). During vacuum distillation, water is evaporated from a substrate under vacuum and cryogenically trapped (using liquid nitrogen) in a sample vessel. Vacuum distillation can be coupled with aqueous leaching of solutes from post-dehydrated samples to reconstruct the geochemistry of the porewaters.

The objectives of research currently underway at the University of Ottawa are to 1) develop and optimize a vacuum distillation method to fully extract porewater from intact crystalline core samples; and 2) benchmark the approach (using crystalline rock saturated with water of known isotopic composition). The primary challenge of this work to-date was development of a method to fully re-saturate the cores with a water of known isotopic composition for use in benchmarking experiments, while avoiding fractionation of the porewater isotopes from the original re-saturating water. To resolve this, the testing criteria for achievement have been established as: (i) complete extraction of porewater (better than 95%) to avoid Rayleigh-type isotope fractionation and (ii) measured isotope contents of the extracted porewater that are within an acceptable margin of those of the saturating water reservoir.

During 2019, experiments were conducted to test several different methods for core re-saturation. The results demonstrate that some of the re-saturation methods tested resulted in a relatively low degree of porewater uptake into the core sample, which is also accompanied by a diffusive fractionation of isotopes in the porewater, as shown in the left-hand plot in Figure 5-5.

Through these experiments, it was determined that re-saturation experiments using a combination of high vacuum (45 mTorr), followed by heating (121°C) at elevated pressure (15 PSI) for long durations of time produced high levels of saturation with no significant isotope fractionation. Representative results from such high vacuum re-saturation/extraction experiments are shown in the right-hand plot in Figure 5-5.



Note: Left chart: Showing a Depletion Trend from Early Data, Attributed to the Resaturation Process. Right chart: Final Resaturation Protocols Produce Porewaters Essentially Free of Resaturation Artifacts. Extraction Method Reproduces the Isotope Signature of the Porewater.

### Figure 5-5: Isotope Diagram of Porewaters Extracted from Crystalline Rock

It was determined that extended porewater extractions can be undertaken in two stages, assuring 100% yields for fully-saturated cores, without inducing isotope artifacts. The isotope results indicate that this extraction procedure is quantitative and without isotope exchange or fractionation, providing an accurate measurement of the in-situ porewater isotope content in crystalline core samples. A technical report documenting the successful benchmarking of this new extraction protocol is currently in preparation. The next step will be to apply this method to extract porewaters from fresh, fully-saturated crystalline cores collected during site investigations, and compare the porewater compositions with those determined on a second, adjacent core samples using established extraction methods.

Also at the University of Ottawa, a novel method has been under development for several years to extract porewater from sedimentary cores into cellulosic papers for subsequent analysis of the porewater composition. Recent work (2018-2020) focuses on i) extracting porewater for stable isotope ( $\delta^2\text{H}$  and  $\delta^{18}\text{O}$ ) measurements, and ii) verification of the major-ion data using core samples that have been equilibrated with a known synthetic porewater composition. For the stable isotope measurements, the main challenges are the avoidance of artifacts from evaporative fractionation and minimizing the blank signal from atmospheric water that adsorbs on the highly-hygroscopic cellulosic paper. Extensive testing was completed, and unfortunately, it was concluded that these challenges cannot be overcome and the paper absorption method cannot be applied for measurement of porewater stable isotopes. The experiments designed for verification of the porewater chemistry are on-going.

### 5.1.5.2 Profiles of Li, Mg and Ca Isotopic Compositions of Porewater

Site characterization activities at a formerly proposed DGR for L&ILW at the Bruce site show that the low-permeability Ordovician sediments of the Michigan Basin contain Na-Ca-Mg-Cl brines (>5M) considered to originate as evaporated, post-dolomitic Silurian seawater, with residence times exceeding 400 Ma. To further constrain solute migration, a study is underway at the University of Ottawa to generate  $\delta^7\text{Li}$  and  $\delta^{26}\text{Mg}$  profiles of porewaters in these strata. During 2019, the main task was the preparation of porewater leachates for isotopic analysis, based on extensive pretreatment using ion-specific column chromatography to remove interfering geochemical matrices. Current efforts are focused on completing sample preparation and ICP-MS analysis.

Interpretation of the isotope profiles for  $\delta^6\text{Mg}$  focuses on shifts related to porewater-matrix exchange in association with dolomitization ( $\uparrow\delta^{26}\text{Mg}_{\text{pw}}$ ), possible secondary silicate formation ( $\downarrow\delta^{26}\text{Mg}_{\text{pw}}$ ) and possible shield-derived fluid mixing in the deep Ordovician. In addition to expanding the  $\delta^{26}\text{Mg}_{\text{pw}}$  porewater dataset, measuring  $\delta^{44}\text{Ca}$  in porewater will help to constrain the nature of fluid-rock interactions and potential mixing with a deep brine source in the Ordovician limestones. All samples for  $\delta^{26}\text{Mg}$  and  $\delta^{44}\text{Ca}$  in the porewaters have been analysed by ICP-MS for QA/QC purposes, before analysis using the Neptune MC-ICP-MS at the Queen's Facility for Isotopic Research (QFIR).

Lithium is a highly soluble cation that is enriched in evaporative brines, but the isotope composition may be altered through sorption onto clays and organics ( $\uparrow\delta^7\text{Li}_{\text{PW}}$ ) as well as mixing with crustal fluids in the deep Ordovician sediments. In 2019, the  $\delta^7\text{Li}_{\text{PW}}$  profile was expanded and several replicates were added for improved quality assurance and control. Measurement of  $^7\text{Li}$  in the Ordovician shales will provide further insight into the fluid-rock interactions in these formations and will be the final step in this work program. Given the large difference between the  $\delta^7\text{Li}$  of interlayer and structural Li in clays, and that interlayer  $\delta^7\text{Li}$  may be influenced by later changes in porewater composition, bulk analysis of the shales will not provide the most representative picture of the conditions under which these clays formed. A method for leaching the Ordovician shales to remove exchangeable Li, including interlayer Li in clays, was developed to isolate the structural Li in the silicates. The leached rocks and sequential leach fluids will be analyzed at QFIR.

### 5.1.5.3 Porewater Residence Times: Noble Gases and Strontium

The isotopic analysis of heavy noble gases in porewaters within preserved cores was initiated to complement helium isotope studies performed as part of geosphere model development for the Bruce nuclear site. In 2019, the functionality of the Helix multi-collector noble gas mass spectrometer has been improved through upgrades to the noble gas purification and separation line. The noble gas laboratory at the Advanced Research Complex is the only one in Canada with instrumentation for analysis of the isotopes of helium and the higher-mass noble gases, and the ingrowth of geogenic noble gases, including  $^4\text{He}$ ,  $^{21}\text{Ne}$ ,  $^{40}\text{Ar}$  and  $^{136}\text{Xe}$ , which can be used as measures of groundwater and porewater age.

Observations from archive core samples from the Bruce nuclear site, after 10 years of preservation, suggest that many of the samples have degassed into the vacuum-sealed aluminum foil packaging over time. For many, this gas contains the same isotopic ratios of methane as those originally measured for adjacent core samples during site characterization activities for the formerly proposed L&ILW DGR at the Bruce site.

Gas samples have been taken from several of these long-preserved cores, and core crushing conducted for porewater content and water isotopic analysis. From these archived samples, a  $^{136}\text{Xe}$  excess has been discovered from select samples, with an average  $^{136}\text{Xe}/^{130}\text{Xe}$  value of 2.24. This finding is a demonstration of the enrichment that should be observed if the porewaters are as old (>260 Ma) as suggested by the helium isotope work (Clark et al. 2013).

In addition to the noble gas analysis, a refined method for heavier noble gas separation has been advanced over 2019 to improve the selective trapping of Kr and Xe, and to avoid the loss of Kr when sequentially trapped on the stainless steel in-line with a more aggressive activated charcoal trap. A polished stainless steel wool trap was found to improve the Kr signal 35-fold.

It is anticipated that determination of the ingrowth of the higher-mass noble gas isotopes above their atmospheric ratios will provide robust chronologies of the porewaters in this system, which will be complementary to the He,  $\text{CH}_4$ , and  $^{87}\text{Sr}$  chronometers that have already been developed during characterization activities. A manuscript documenting the noble gas compositions and isotopic signatures will be prepared in 2020.

#### 5.1.5.4 Stable Water Isotopes in Clay-bound Water

Reliable measurement of water stable isotope compositions for porewaters entrapped in Paleozoic shales and related rocks of the Michigan Basin in southern Ontario presents a challenge because of their very low water content and, potentially, because of porewater interaction with clay minerals. A concern being examined in the current research is the potential for bias in porewater hydrogen (H) and oxygen (O) isotope compositions arising from isotopic fractionation between connected-porosity water and clay hydration water, depending on the method of porewater analysis.

The first stage of this project examined the mineralogy, and O and H isotope geochemistry, of clay minerals from southern Ontario Ordovician shales, including samples from the site formerly proposed for a L&ILW DGR. This work is largely complete. Key findings are that: (1) illite > kaolinite > chlorite comprise the <2 $\mu\text{m}$  fraction of these shales; (2) the clay mineral O and H isotope compositions plot to the left of terrestrial clay weathering lines in H and O isotope space; (3) calculated water O and H isotope compositions in equilibrium with these clay minerals at maximum burial temperatures (60-90°C) match porewater O and H isotope compositions measured by various techniques; and (4) H isotope clay mineral-water exchangeability was demonstrated in short-term experiments at 68°C using isotopically-labelled water. Results suggest that isotopic exchange with structural O and H in clay minerals can play a role in determining porewater O and H isotope compositions at low temperatures in silicate-dominated, low water content shales. The technical report summarizing these findings will be prepared during 2020.

Next steps in the research are to achieve the goal of measuring the H and O isotope compositions of bound water associated with non-swelling clay minerals and smectite-group clay minerals; the latter also contain bound water within their interlayer space. Progress has been made in two main areas:

1. A method to reproducibly analyze the H isotope composition of structural hydrogen in small samples of smectite minerals has been developed. The sensitivity to smectite exchangeable cation and associated retention of residual sorbed water has been established both isotopically and through thermogravimetric measurements. The next

step in this research is to implement a successful approach for measuring bound water – mobile water isotopic fractionations for smectite group minerals.

2. A major challenge is isolation of sufficient quantities of water bound to clay mineral surfaces for isotopic analysis. This difficulty arises in part from (i) the nature of the clay minerals being studied, and (ii) available instrumentation. Item (i) is being addressed by the move to examining swelling clay minerals, for which the content of bound water is typically much higher. A prerequisite, however, is methods for accurate and reproducible measurement of structural H isotope compositions of smectite, which is in place (as reported above).

In 2020, additional experiments on non-swelling clay minerals and clay mineral assemblages will be conducted, testing both for H and O isotope exchange with water over longer time periods and at higher temperatures (150°C). The diagenesis of clay minerals in the Ordovician shales of southern Ontario, and the implications of diagenesis for porewater isotopic compositions in low water content shales, will also be investigated.

#### 5.1.5.5 Binding State of Porewaters - NEA CLAYWAT Project

The Magnetic Resonance Imaging (MRI) Research Centre in the Department of Physics at the University of New Brunswick (UNB) has unique facilities and capabilities for the measurement of fluids in porous materials. The instrumentation available ranges from a low field 0.2 Tesla MRI instrument to a higher field 2.4 Tesla instrument. These instruments feature a range of magnetic resonance (MR) and MRI methodologies, developed at UNB, which are well suited to measurement of the short lifetime MR signals characteristic of fluids in confined environments (e.g., petroleum reservoir core plugs).

As part of the NEA CLAYWAT project, which has the objective of defining the binding state of porewater within argillaceous media, the MR and MRI methods available at UNB were applied attempt to elucidate information about water content and the water environment in a range of clay samples from several international nuclear waste management organizations. Despite the low water content and very short-lived MR signal lifetimes, it was possible to image water content in the full range of clay samples studied. The most successful measurements were undertaken at low static magnetic field (0.2 Tesla). The low magnetic field strength results in a lesser MR signal but reduced magnetic susceptibility effects result in a longer-lived signal and higher quality images. All clay samples could be imaged at 0.2 Tesla (a minority of samples could be imaged at 2.4 Tesla due to ultra-short signal lifetimes). The images revealed that some of the clay samples are heterogenous, however most are homogeneous in structure and water content.

In parallel to MRI studies, bulk whole-sample signal lifetime measurements of various types were undertaken. The goal was to distinguish interlayer water and porewater to determine the relative amount of each in the samples under study. Measurements at 2.4 Tesla were not successful, due to increased magnetic susceptibility mismatch effects (which distort the field homogeneity in the pore space). Measurements were more successful at 0.2 Tesla. Water exchange between interlayer and porewater environments was judged to be rapid on the MR time scale, with the result that a weighted average signal amplitude and signal lifetime was measured. The lifetime measurements also revealed the presence of a short-lived signal assigned to hydroxyl species inherent to the clay matrix. While it is not possible to resolve the signal from interlayer water and porewater directly, it may be possible to probe the population ratio by changing hydration through relative humidity change. This would be anticipated to shift

the population balance between the two environments, changing the weighted average signal lifetimes. During 2020, a written contribution documenting the findings from this study will be prepared for inclusion in the CLAYWat project report.

#### 5.1.5.6 Mont Terri Geochemical Data (GD) Experiment

The NWMO is a partner in the Geochemical Data (GD) Experiment at the Mont Terri Underground Research Laboratory (URL) in Switzerland. The GD Experiment aims to collect and evaluate data from various activities in the URL, in terms of assessing coherence / agreement with the established porewater conceptual model for system evolution. Open questions that are identified in the model(s) or in the understanding of behaviour often become targeted research projects within GD (e.g., lab investigations, in-situ measurements and/or modelling activities). In 2019, the GD Experiment was focused on three main subjects: 1) sulphate content, source and composition in Opalinus Clay porewater, 2) trace element presence, concentrations and behaviour in porewater, and 3) carbonate composition in clay rocks (e.g., temperature diagenesis, reactivity, content). In 2020, work as a part of GD will continue to focus on trace elements in porewater, carbonates in clay rocks, as well as redox and the role of Fe-containing minerals in controlling system Eh.

### 5.1.6 Transport Properties of the Rock Matrix

#### 5.1.6.1 Permeability

The primary motivation for this research at McGill University is to assess the permeability characteristics of a low-porosity crystalline rocks from the Canadian Shield and similar in origin to those being considered as potential host rock for a DGR. The conventional steady state or transient permeability testing of rock cores is usually limited to samples that are less than 100 mm in diameter. When heterogeneities are not dominant (e.g., granitic rocks), the testing of cores at this scale may still provide representative values of the permeability of the rock matrix. This research involved estimation of the effective permeability of a large cuboid sample of the Lac du Bonnet granite from Manitoba which was 280 mm in dimension.

The method used for estimating the permeability characteristics of cuboidal samples of rocks by performing surface permeability tests was developed by Selvadurai and Selvadurai (2010, 2014). The method involves either establishing a steady flow rate through an annular sealing region that is placed on the surface of the sample, or subjecting the central region of the annulus to a constant pressure and allowing the development of a steady flow rate. In the current research, the basic concepts put forward in Selvadurai and Selvadurai (2010, 2014) were adopted to estimate the surface permeability of a cuboid of the Lac du Bonnet granite measuring 280 mm x 280 mm x 280 mm. To ensure that there was no interface leakage between the annular sealing region and the granitic rock, the sealing efficiency was confirmed through the application of a constant pressure to the permeameter in contact with a stainless steel plate. Based on these tests, the normal sealing stress that needs to be applied to the annular region was established at approximately 1.5 MPa. This would imply that the maximum water pressure that can be applied will be around 500 kPa. From previous experimentation involving permeability testing of granitic rocks, it is observed that the steady state tests are best conducted by applying a constant pressure to the region in contact with the fluid and by estimating the flow rate from the volume of fluid permeating into the granitic rock over a given time. The general view of the experimental facilities, a detailed view of the permeameter, and a schematic view of experimental facility are shown below.



Figure 5-6: Cuboidal Sample of the Lac Du Bonnet Granite from the Canadian Shield

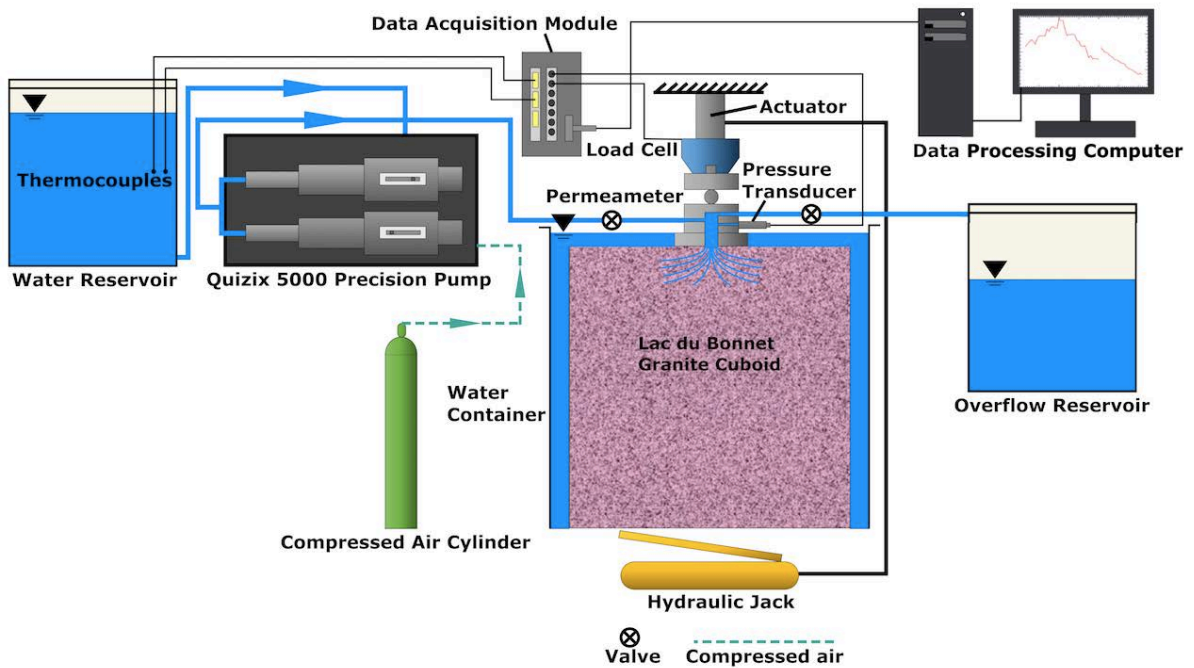


Figure 5-7: Schematic View of the Experimental Facility

### 5.1.6.2 Diffusion Properties

Near-field performance, safety assessment and groundwater transport/evolution models require knowledge of groundwater and porewater geochemical compositions, as well as petrophysical and solute transport properties, in order to provide representative estimations of long-term system behaviour. The following research programs contribute to the NWMO's technical capabilities in the context of assessing long-term solute mobility and retention.

#### 5.1.6.2.1 *Method Development – X-ray CT Imaging*

The University of Ottawa acquired an X-ray CT system in 2016 and have conducted extensive testing to assess its capabilities to improve imaging capabilities in low-porosity rock and to optimize measurement parameters for tracer experiments. Experiments on low-porosity limestone (porosity 1 - 2%) have demonstrated that the instrument is capable of detecting tracer signals with acceptable signal-to-noise ratios. Initial experiments with archived samples of the Lac Du Bonnet granite from Pinawa, Manitoba were not successful and demonstrated the need for methodological improvement for crystalline rock samples (porosity < 0.5%). Recently, this challenge has been overcome by rotating the sample during image acquisition, which minimizes registration artifacts and dramatically improves the signal-to-noise ratio. The method is now capable of resolving diffusion signals for iodide and cesium tracers in crystalline rocks. Refinements of the method, to conduct calibrations and complete the data analysis with numerical modelling, are ongoing. The results for crystalline samples will be presented at the 2020 Goldschmidt Conference.

The X-ray CT instrument was custom-built to allow for modifications to the source, detector and sample stage, allowing experiments with a variety of configurations. The goal is to use spectrometric measurements to minimize the effects of beam hardening and increase signal-to-noise ratios for improved tracer detection. The principal modifications are the addition of a highly collimated beam (~1 mm diameter) and an energy-dispersive spectrometric detector. The system has been designed and constructed and is now successfully operating to conduct diffusion measurements. During the first phase of testing, it has been confirmed that beam hardening effects are virtually eliminated, but a rigorous comparison of the signal-to-noise ratios achieved with radiography versus spectrometry has not yet been completed. Using samples of Queenston Formation shale, experiments with both conservative (iodide) and reactive (cesium) tracers were conducted. Both experiments yielded coherent diffusion profiles, indicating that the method is working as expected. Calibration and modelling are still underway to complete the analysis of the data. Advancements in this novel method will be presented at the 2020 Goldschmidt Conference.

#### 5.1.6.3 Mont Terri DR-B Experiment

The NWMO is a partner in the Long-term Diffusion Experiment (DR-B) at the Mont Terri URL. The objectives of the experiment are i) to develop a means for the long-term monitoring (>10 years) of in-situ iodide diffusion process at a large scale in a clay formation; and ii) to validate the diffusion process understanding developed and transport parameters determined through previous experiments. The experimental setup consists of a central borehole and 3 surrounding observation boreholes. Sodium iodide (NaI) solution was injected in the central borehole in April 2017 and is expected to diffuse over time toward the observation boreholes. Starting in November 2018, a breakthrough of iodide in the observation borehole located closest to the injection borehole was observed. Regular measurement of iodide concentration in the observation boreholes continued during 2019.

#### 5.1.6.4 Sorption

Sorption is a mechanism for retarding sub-surface radionuclide transport from a DGR to the environment. The NWMO has initiated the development of a sorption distribution coefficient ( $K_d$ ) database for elements of importance to the safety assessment of a DGR (Vilks 2011). This initial database was further developed to include sorption measurements for Canadian sedimentary rocks and bentonite in saline solutions (with ionic strength  $I = 0.23\text{--}7.2\text{ M}$ ) including a reference porewater SR-270-PW brine solution (Na-Ca-Cl type with  $I = 6.0\text{ M}$ ).

Researchers at McMaster University continued to systematically study the sorption properties of Se and Tc on limestone, shale, illite and bentonite (MX-80) in SR-270-PW brine solution, as well as on crystalline rocks and bentonite in a reference groundwater CR-10 (Ca-Na-Cl type with  $I = 0.24\text{ M}$ ) under reducing conditions. Most recently the effects of ionic strength and pH on Se and Tc sorption on shale, illite, limestone, bentonite and crystalline rocks have been investigated (e.g. Racette et al. 2019, Walker et al. 2018). It was found that there was a general decrease in the sorption of Se(-II) on illite, MX-80, limestone and granite with increasing pH, which is consistent with anion sorption. Sorption of Se(-II) on shale did not decrease with increasing pH. The 2-site protolysis non-electrostatic surface complexation and cation exchange model (2 SPNE SC/CE model, Bradbury and Baeyens 2005) was applied to simulate the pH dependence of  $K_d$  values of Se(-II) on MX-80 and illite at  $I = 0.1, 1.0$  and  $3\text{ M}$  as well as the pH dependence of  $K_d$  values of Se(-II) on MX-80 at  $I = 0.05, 0.1, 0.24$  and  $1\text{ M}$ . It was found that the sorption model predicted the observed pH dependence of  $K_d$  (Figure 5-8). Sorption of Se(-II) on granite showed a slight ionic strength dependency with sorption decreasing as ionic strength increased, while there was no clear ionic strength dependency for MX-80.

A new three-year new research program will be initiated in 2020, in collaboration with McMaster University, to study the sorption properties of (1) U on limestone, shale, illite and bentonite (MX-80) in SR-270-PW reference water, as well as on crystalline rocks and bentonite in CR-10 reference water under both oxidizing and reducing conditions; and (2) Eu on limestone, shale, illite and bentonite (MX-80) in SR-270-PW, as well as onto crystalline rocks and bentonite in CR-10 under reducing conditions. The measured sorption  $K_d$  values will be used to update the NWMO sorption database.

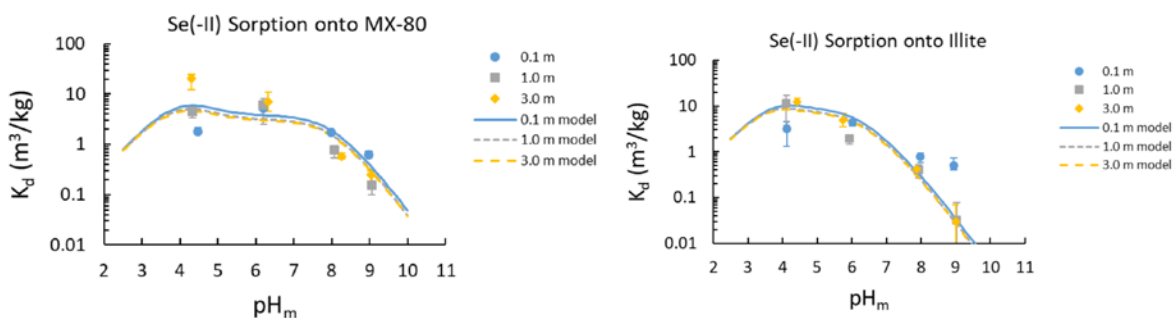


**Figure 5-8: 2 SPNE SC/CE Model Simulation of Sorption of Se(-II) on MX-80 (Left) and Illite (Right)**

#### 5.1.6.5 Surface Area & Cation Exchange Capacity

In 2018, the University of Bern completed research to characterize external surface area (BET) and cation exchange capacity (CEC) in sedimentary rock cores from the Bruce nuclear site. Samples from the Queenston, Georgian Bay, Blue Mountain and Collingwood Member

formations were evaluated (rock types included claystone, marl and limestone). The research focused to address the question of mineralogical fractionation induced by sieving to different grain sizes (i.e., can a specific fraction for geochemical experiments be used and the results considered representative of the whole rock?), as well as the effect of crushing on determined CEC values (e.g., does crushing create new mineral surfaces, and is it permissible to extrapolate geochemical data obtained on disintegrated or crushed material to the intact rock?).

The main findings are summarized below.

- 1) Chemical and mineralogical compositions do not vary systematically between grain-size fractions, indicating that size reduction and sieving do not lead to a resolvable fractionation (with the exception of the limestone sample).
- 2) BET surface area increases with decreasing grain-size fraction by 50 – 100% (claystone and marl) and 300% (limestone). Crushing to smaller particle sizes, thus, provides access to surfaces that are inaccessible or not present in the intact rock.
- 3) CEC of claystone and marl samples increase by 7–31% between fractions 1–4 mm and <0.063 mm. While crushing to smaller grain size creates new surfaces, these are predominantly related to minerals with a small or negligible CEC, such as carbonates or quartz. It is concluded that the effect of grain size plays a relatively limited role for CEC.
- 4) CEC of the limestone sample between fractions 1–4 mm and <0.063 mm increases by 110%. Care needs to be taken when extrapolating data produced on crushed limestone samples to the intact rock.
- 5) Good linear correlations can be found between clay content, BET surface area and CEC. BET surface measurement can be used as a proxy of the cation-exchange capacity of the sample, which is a feature known for other sedimentary rocks.

The results of this work were compiled in a Technical Report for the NWMO in 2019, and it is anticipated that the report will be published during 2020.

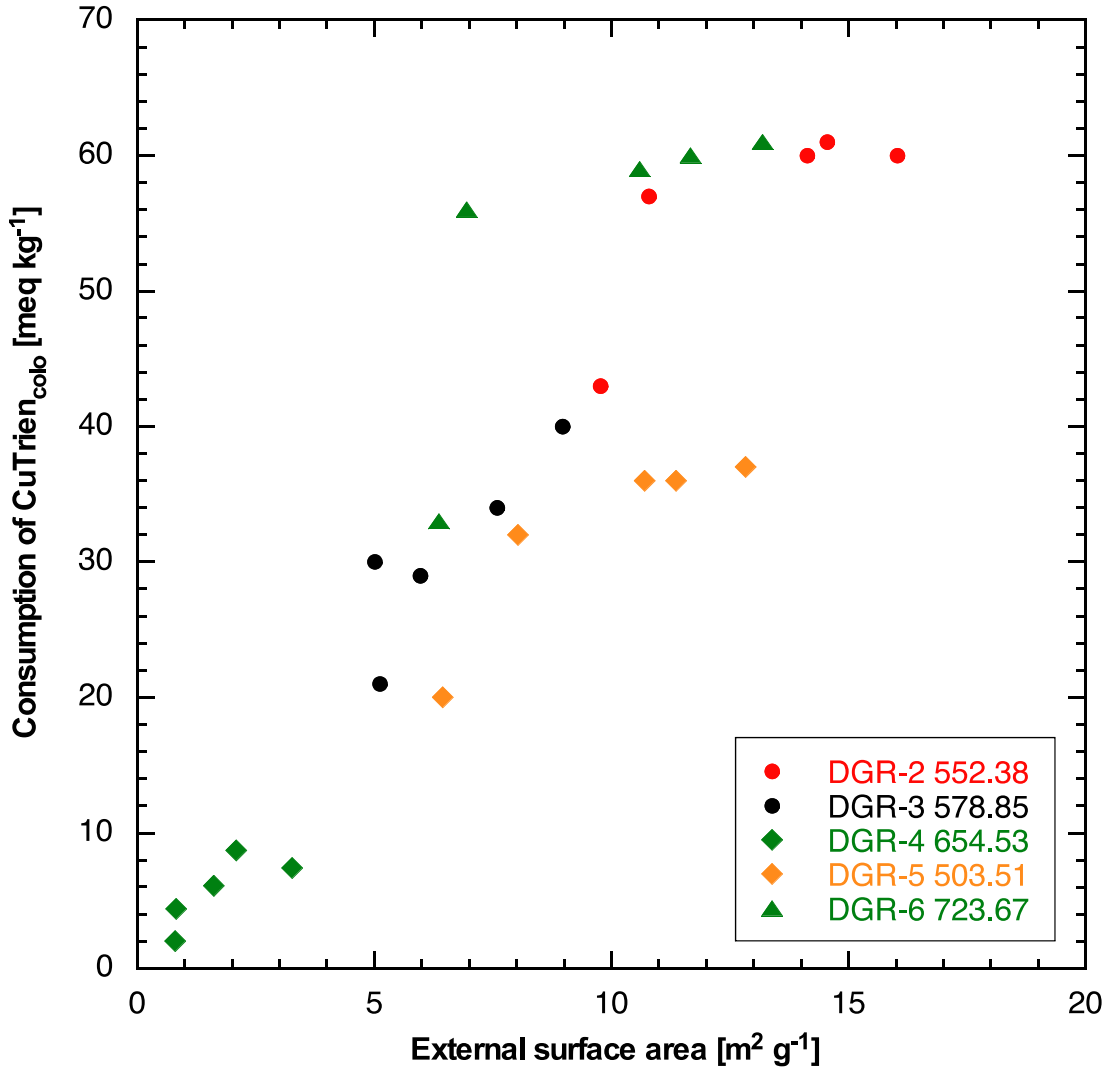


**Figure 5-9: Correlation Between BET Surface Area and CEC (Expressed by Brobe Consumption)**

## 5.1.7 Geomechanical and Thermal Properties

### 5.1.7.1 In-Situ Stress

The in-situ stress state is a fundamental parameter for the engineering design and safety assessment of a DGR. Obtaining reliable estimates of in situ stress is of significant importance, however, this is often hindered by small numbers of field stress measurements as well as by variability arising from the geological environment. Bayesian data analysis applied to a multivariate model of in situ stress can potentially overcome these problems and generate a multivariate stress tensor for a site.

Together with SKB (Sweden), NWMO will establish a new research program during 2020 at the University of Toronto to investigate the use of Bayesian data analysis in the statistical quantification of in situ stress at a test site and to develop protocols suitable for application at other sites.

### 5.1.7.2 Rock Properties from Laboratory Experiments

#### 5.1.7.2.1 *Thermal Properties*

Thermal conductivity is a fundamental parameter for thermal modelling of a DGR. Thermal conductivity of the Cobourg limestone and the Lac du Bonnet granite are studied as two reference rocks for sedimentary and crystalline settings, respectively.

In 2019, the focus of research on the Cobourg limestone at McGill University shifted to determining its thermal conductivity. This latest research is a continuation and completion of the work on the intact Cobourg limestone, which included the estimation of the Biot Coefficient (Selvadurai, 2019a) and the effective permeability (Selvadurai, 2019b).

Estimation of the effective thermal conductivity of the Cobourg limestone employed a cuboidal region of the Cobourg limestone measuring 80 mm x 120 mm x 300 mm which was dissected into ten slabs measuring 80 mm x 120 mm x 8 mm. The surface features of the sections were digitally imaged, and the interior distribution was estimated. The assembled ten slabs were used to estimate the volume fractions of the lighter and darker facies, and their mineralogical compositions were determined using XRD techniques. This data, along with theoretical estimates for determining the effective thermal conductivity values were used to estimate the effective thermal conductivities of the lighter and darker facies. Theoretical studies based on multiphase theories that employ (i) the volume fractions of the lighter and darker facies and (ii) the effective thermal conductivities of the lighter and darker facies determined using the thermal conductivity values for the separate minerals reported in the literature, were adapted to estimate the thermal conductivity of the Cobourg limestone at 273 K and 373 K. The details of these studies are given by Selvadurai and Rezaei Niya (2019c).

During 2020, McGill University will be studying thermal conductivity of the Lac du Bonnet granite.

#### 5.1.7.2.2 *Poroelastic Properties*

This phase of research at McGill University involved the estimation of Biot coefficient which is one of the poroelastic properties used in coupled thermal-hydro-mechanical (THM) modelling of DGR.

The Biot coefficient indicates how the applied total stresses are partitioned between the skeletal effective stress and the pore fluid pressure. The pore fluid pressure is modified by the Biot coefficient ( $\alpha$ ), which depends on the bulk modulus of the porous skeleton ( $K_D$ ) and the bulk modulus of the solid material ( $K_S$ ) composing the porous skeleton.

The skeletal bulk modulus was measured by performing uniaxial compression tests on samples with a diameter of 150 mm and length of 300 mm. Samples were tested after oven drying the cylinder at 60 °C and periodic monitoring of to sample weight to ensure complete drying was achieved. Uniaxial compression tests were conducted on strain gauged samples loaded from 20 MPa to 30 MPa, which represented a stress level well below the lower estimate of a failure stress of 125 MPa. Higher estimates for the UCS in the range 200 MPa have been given in Martin and Chandler (1994) and the applied stress is well below the crack initiation stress level of 90 MPa. The test conducted is therefore adequate for the purposes of estimating the skeletal bulk modulus, ( $K_D$ ) provided isotropy holds. The uniaxial test with measurement of Poisson's

ratio is the simplest procedure for estimating  $K_D$ . It is possible to measure volume changes in dry samples subjected to isotropic compression and measuring the axial strain to estimate  $K_D$ .

The experimental evaluation of the bulk modulus of the solid material is a complicated exercise if the permeability of the rock is very small (less than  $10^{-19} \text{ m}^2$ ), as the saturation of the 150 mm diameter 300 mm long sample can take an inordinate amount of time. Also, when the fluid in the pore space is subjected to a pressure equal to the cell pressure, there is a time delay for the pore fluid pressure in the sample to reach equilibrium within the entire sample. The procedure adopted in this research was to estimate the bulk modulus of the solid material by considering the mineralogical composition of the Lac du Bonnet granite, and to use multiphase elasticity theories to determine the value of ( $K_S$ ). Using these methods, the Biot coefficient for the Lac du Bonnet granite was estimated to be within the range  $0.30 \leq \alpha \leq 0.31$ . The fundamental constitutive law governing the Biot coefficient is linear Hookean elasticity. If the theory is to accommodate non-linear elastic estimates for  $K_D$  and  $K_S$ , then Biot's theory needs to be revised to accommodate non-linear and elasto-plastic phenomena (Suvorov and Selvadurai, 2019).

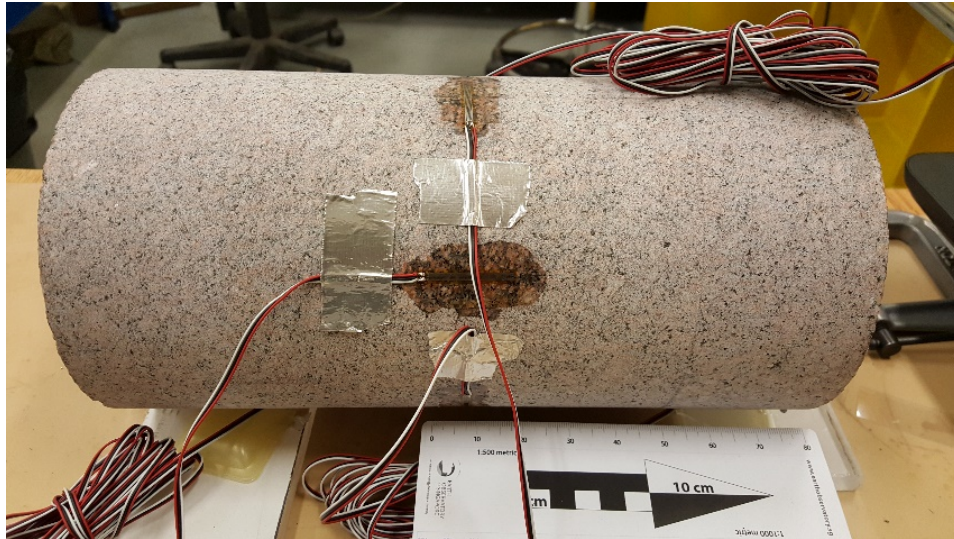


**Figure 5-10: Sample of the Dry Lac du Bonnet Granite Prepared for Uniaxial Testing**

### 5.1.7.3 Rock Properties from In-Situ and/or Large-Scale Experiments

#### 5.1.7.3.1 *POST Project*

The POST project aims to develop an understanding of the mechanics of rock joints during shearing under loads that are representative for depths of approximately 300-500 m. This is an area of research which is important for assessing the long-term safety of a DGR.

During the first phase of the project, the need for well-controlled laboratory experiments on rock joints at a larger scale than exists today and under full stress that is equal to the in-situ stress at the underground repositories was identified (Siren et al. 2017). The second phase of the project (POST2) began in 2017. In parallel, there are two on-going PhD-projects in Sweden in collaboration with KTH (Royal Institute of Technology) which use data from the project. One project investigates rock and replica joints in direct shear loading including an examination of

scale effects. The second project is focused on the improvement of tools - laboratory, analytical and numerical - for estimation of rock fracture peak shear strength, including scale effects.

POST2 initially contained four major components:

1. Design and manufacture of new shear test equipment for large specimens
2. Develop methods for conducting well-controlled direct shear tests experiments with thorough documentation of specimen before, during and after experiments
3. Develop methods for manufacturing replicas of real rock joints
4. Conduct direct shear tests on medium-scale rock joints and rock joint replica specimens at both constant normal stiffness (CNS) and constant normal load (CNL) loading conditions.

Three of these components (2-4 above) were completed in 2018. Back-analysis of preliminary direct shear test results of rock and replica materials in 3DEC began during 2019 and will continue into next year.

The main focus of the project in 2019 was completion of the large shear test device including i) confirming that the delivered manufactured and purchased components were according to specifications; ii) the design and manufacture of auxiliary equipment and assembling the equipment (see also below); iii) calibration and connection of all sensors to the control system; and iv) development of control programs for conducting shear tests under both CNL and CNS conditions.

The shear test equipment, with a length of 3.6 m and a mass of 16 metric tons, was integrated with the existing laboratory equipment (20 MN load frame) and control system. That required, for example, the design and manufacture of an adapter with an integrated spherical bearing for transmission of normal loads between the load frame and the shear test equipment. It also included the design of precise positioning systems between the workshop floor and bolster and between the bolster and the shear test equipment. All components were made with high tolerance and close fittings between the components in order to achieve high quality results from the tests. Consequently, the various handling and operation stages need to be precise. Therefore, the full demounting and mounting process required for part exchange, maintenance and operation was checked and successfully executed. A risk assessment was carried out and an operation manual was written and filed with other relevant documentation required for traceability and maintenance in parallel to this technical work.



**Figure 5-11: New Shear Testing Equipment Integrated with Existing Laboratory Load Frame**

A series of experiments on a steel reference specimen were conducted to assess that the control of a direct shear test works under constant normal stress and constant normal stiffness. Moreover, the normal stiffness of the components was measured in order to assemble data for a possible compensation of normal stiffness during CNS control in the same fashion as was conducted earlier for the small-scale shear test equipment. A journal publication (Larsson & Flansbjerg, 2019) was prepared documenting these experiments.

#### 5.1.7.4 Mont Terri FE-M Project

The FE-M experiment, long-term monitoring of the full-scale heater test, continues with the heating phase which commenced in December 2014. This experiment was designed to demonstrate the feasibility of: (1) constructing a full-scale 50 m long and 3 m in diameter deposition tunnel using standard construction equipment; (2) heater emplacement and backfilling procedures; (3) early post-closure monitoring to investigate repository-induced coupled thermo-hydro-mechanical (THM) effects on the backfill material and the host rock (i.e. Opalinus Clay); and (4) validation of THM models.

Field measurements include temperature, pore-water pressure, humidity/water content and suction, thermal conductivity, deformations, and stresses. The program is currently focused on the long-term monitoring of the THM processes confirming the technical readiness of the conceptual modelling framework pertinent to assessment of the long-term performance in the near field scale. Nagra has established a THM modelling task force consisting of Technical University of Catalonia (UPC), the École Polytechnique Fédérale de Lausanne (EPFL), and BGR/TUBAF/UFZ. In 2019, modelling activities comprised code and calculation verification of TH and THM model results amongst the three teams which used Code\_Bright, Code\_Aster and

OpenGeoSys, respectively. Future modelling will study the impacts of the underlying uncertainties on model predictions.

#### 5.1.7.5 Mont Terri GC-A Experiment

The main objective of this experiment is to understand the geomechanical in-situ response of the Opalinus clay during excavation at the transition from shaly to sandy facies.

This experiment consisted of multiple components including:

- Monitoring of the excavation convergence and pore pressure response;
- Laboratory and field geophysical measurement of static and dynamic elastic properties of the Opalinus clay; and
- In-situ stress measurements.

Interpretation of lab and field data continued in 2019. Moreover, following the previous over-coring trials, the University of Alberta conducted in-situ stress measurements using their reservoir geomechanical pressuremeter tool.

#### 5.1.7.6 Shear-Induced Pore Pressure Around Underground Excavations

Previous field tests at Mont Terri Underground Research Laboratory established that deformations in Opalinus Clay around underground openings are: 1) larger than predicted with available models; 2) not properly captured at tunnel face, and 3) coupled with pore pressure responses.

Early 2020, NWMO, NAGRA (Switzerland), and the University of Alberta plan to launch a new joint international collaboration in order to improve understanding of the coupled geomechanical processes relevant to nuclear waste disposal in argillaceous formations. This research program will include field measurements in a test tunnel at Mont Terri underground laboratory, experimental testing of Opalinus clay samples with the aim of measuring pore pressure internally inside the sample, and numerical modelling using experimental and field test results to analyze deformation and pore pressure in the test tunnel. It is hoped that the results of this program will help better understand the response of the Ordovician shales of southern Ontario to excavation processes.

#### 5.1.7.7 Numerical Modelling of Geomechanics

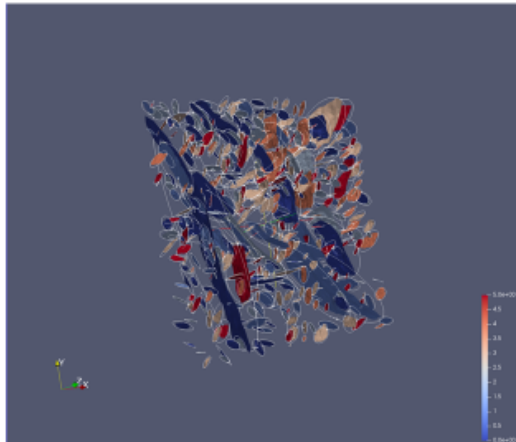
##### 5.1.7.7.1 *Rock Mass Effective Properties*

In 2016, POSIVA, SKB, and NWMO jointly sponsored a research program with ITASCA Consultants s.a.s. (ICSAS) and the Fractory (Joint Laboratory between ICSAS, CNRS and the University of Rennes, France) to improve our understanding of the role played by the fractures on rock mass mechanical behavior. In order to overcome the limitations of the available rock mass classification systems, numerical modelling using a Discrete Element Method is done with the final goal of developing guidelines and a numerical tool (PyRockMass) for in upscaling the mechanical properties of a rock mass containing Discrete Fracture Network (DFN).

The research program in 2019 focused on the following three main tasks:

The first task is to define and test a routine to integrate a DFN defined in MoFrac for use in the new effective rock mass methodology. This involved learning the definition of fractures with MoFrac, i.e. fractures as irregular surfaces, and defining equivalent underlying planes to obtain the geometrical parameters required for the application of the method.

## MoFrac DFN transformed in PyRockMassTool



### In PyRockMassTool

- \* Volume of rock into which DFN is defined
- \* DFN = collection of discrete fractures with mechanical properties
  - \* Each fracture : typical size (e.g. disk diameter), orientation, mechanical parameters

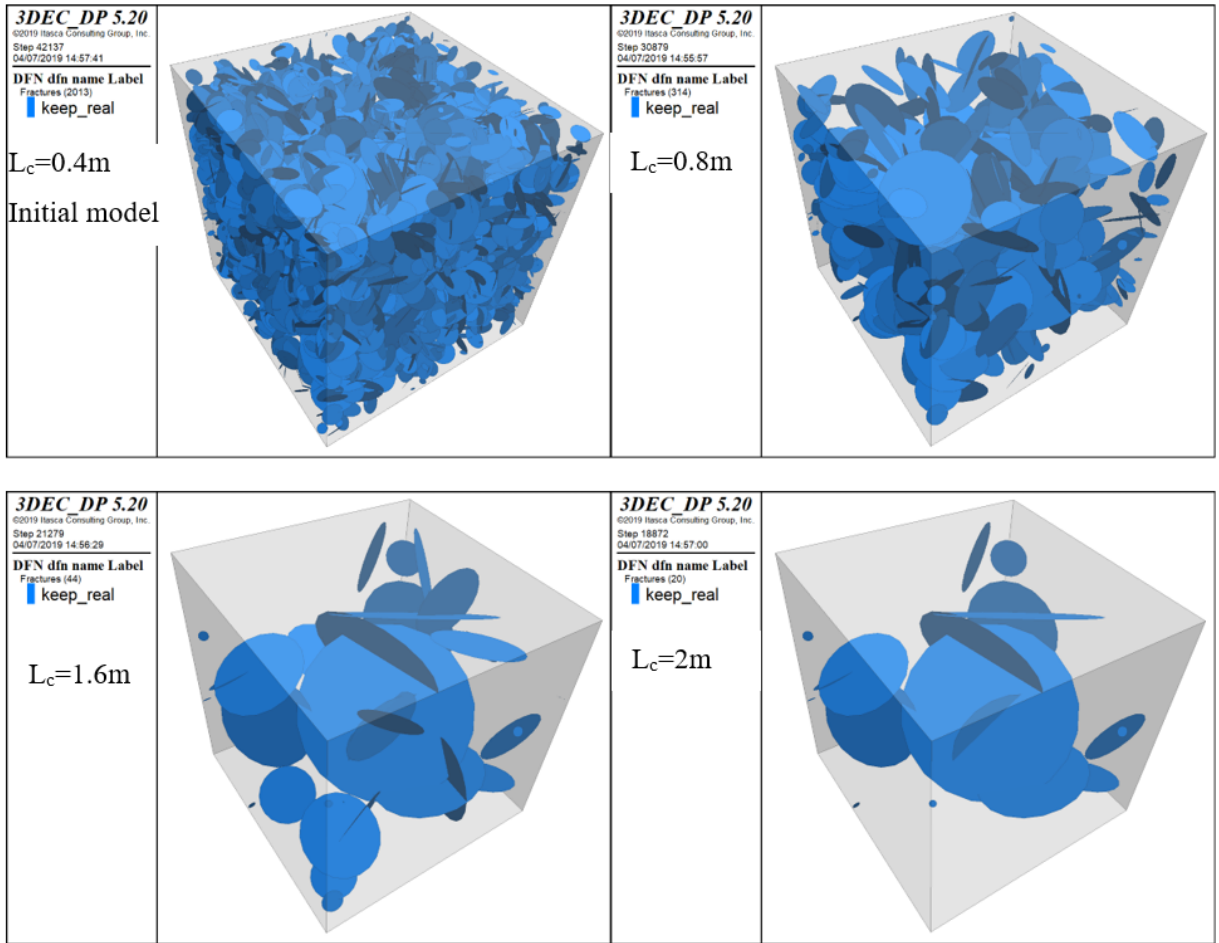
Each MoFrac-fracture is transformed into a fracture compatible with the PyRockMassTool input:

- \* Mean pole orientation by averaging over the in-plane facet orientations
- \* Equivalent size (diameter of a disc) either as
  - \* circumscribed disk (resulting area is larger than true area, largest fracture dimension is preserved), or
  - \* diameter of an effective disk of the same area (area is preserved)
- \* Fracture mechanical parameters are not defined in the MoFrac DFN, they can be defined independently

**Figure 5-12: MoFrac-DFN transformed in PyRockMass Tool Being Developed as Part of Rock Mass Effective Properties project.**

The second task is detailed analysis, based on 3DEC simulations, of stress redistribution around fractures to complement to the macroscopic definition of equivalent effective elastic properties. This was done specifically for DFN models with a power-law distribution of fracture sizes. Power-law based DFN models involve a hierarchical distribution of fracture sizes (governed by a power-law exponent), leading to a scaling organization with more and more fractures as their size decreases. One objective of this analysis was to check numerically that the developed methodology was robust for these more realistic DFN models (compared to DFN made of constant size fractures, as studied formerly in the project). A second objective was to insight into the relationship between the stress spatial variations and the geometrical properties of the DFN. The numerical experiments were defined to allow the incremental removal of smaller and smaller fractures of a DFN and hence to evaluate the consequences of replacing them by an equivalent effective matrix. These preliminary experiments constitute one basis to pursue the development of the DFN based Methodology towards stress distribution and damage modelling, as planed in the continuation plan of the project (i.e. phase 2).

The third task is to complete the final (SKB) report on Phase 1 of the project.



Note: the limit below which discrete fractures are removed from the DFN.

**Figure 5-13: One DFN realization with several values of  $L_c$**

**3DEC DP 5.20**

©2019 Itasca Consulting Group, Inc.

Step 42137

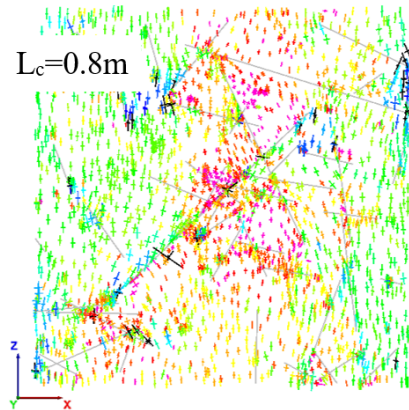
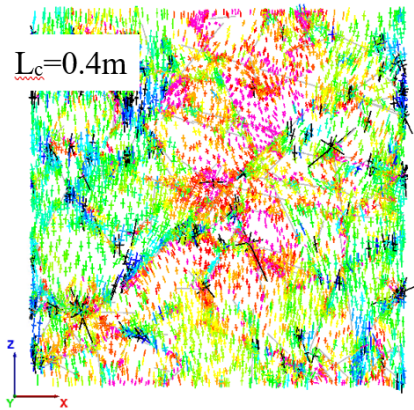
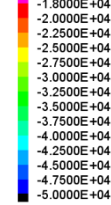
27/06/2019 14:58:58

**Stress**

Plane: active on

Scale: 4e-06

Minimum Prin.

**3DEC DP 5.20**

©2019 Itasca Consulting Group, Inc.

Step 21279

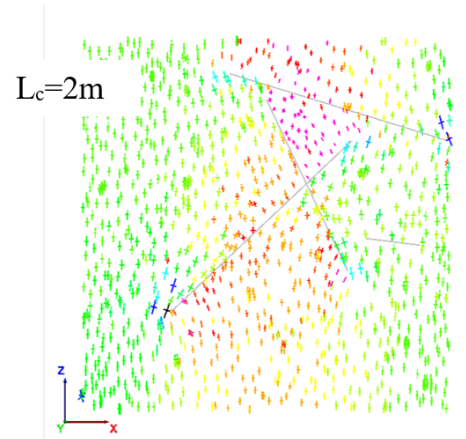
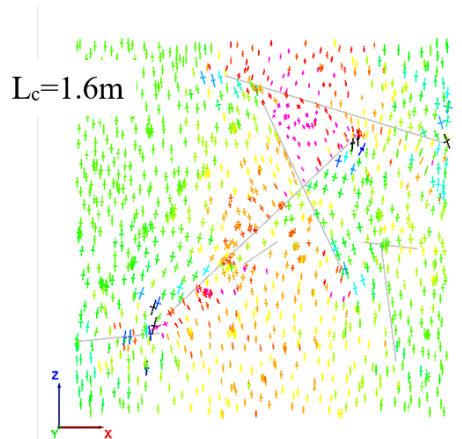
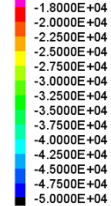
27/06/2019 16:00:10

**Stress**

Plane: active on

Scale: 4e-06

Minimum Prin.



Note: results calculated from one DFN realization whose small fractures are incrementally removed, from a limit  $L_c=0.4$  m to  $L_c=2$  m, and replaced by an effective elastic matrix.

**Figure 5-14: Local Stress Tensors**

During 2020, NWMO and SKB plan to initiate the second phase of this project.

#### 5.1.7.8 NSERC Energi Simulation Industrial Research Chair Program in Reservoir Geomechanics

NWMO has recently joined the renewal of a multi-sponsor NSERC/Energi Simulation Industrial Research Chair (IRC) in Reservoir Geomechanics at the University of Alberta. This IRC chair aims at advancing experimental and numerical methods as well as field studies to help mitigate operation risks and to optimize reservoir management as they pertain to the coupled processes in oil and gas reservoirs. Some of the findings are expected to be also applicable to crystalline settings.

Overall, participation in this multi-faceted IRC program is expected to advance our understanding of how intact rock and fractures at various scales respond to thermal-hydro-mechanical processes associated with a DGR.

## 5.2 LONG TERM GEOSPHERE STABILITY

### 5.2.1 Long Term Climate Change – Glaciation

#### 5.2.1.1 Surface Boundary Conditions

Glaciation associated with long-term climate change is considered the strongest external perturbation to the geosphere at potential repository depths. Potential impacts of glacial cycles on a deep geological repository include: 1) increased stress at repository depth, caused by glacial loading; 2) penetration of permafrost to repository depth; 3) recharge of oxygenated glacial meltwater to repository depth; and 4) the generation of seismic events and reactivation of faults induced by glacial rebound following ice-sheet retreat. The ability to adequately predict surface boundary conditions during glaciation is an essential element in determining the full impact of glaciation on the safety and stability of a DGR site and will be a necessary component supporting site characterization activities. For the purpose of the NWMO's studies into the impact of glaciation, such boundary conditions have been defined based on the University of Toronto's Glacial Systems Model (GSM) predictions (Peltier 2002, 2006, Stuhne and Peltier 2015, 2016). The GSM is a state-of-the-art model used to describe the advance and retreat of the Laurentide ice-sheet over the North American continent during the Late Quaternary Period of Earth history.

Following the update to the GSM methodology and subsequent validation described in Stuhne and Peltier (2015, 2016), a new phase of research was undertaken with the goal of refining the representation of the evolution of paleolakes and surface drainage basins within the model, as well as further analyses of fits to relative sea-level data in Southeastern Hudson's Bay region. Additional modelling capabilities to UofT GSM are currently being developed to deliver improvements to simulations of Laurentide ice sheet evolution. During 2019, research to understand the impact of glaciation on the Great lakes was advanced by further characterizing glacial meltwater in the UofT GSM, and by investigating the impact of glacial meltwater on the formation of proglacial lakes, as well as the evolution of the Great Lakes.

#### 5.2.1.2 Long-term Erosion

A new contract was initiated in 2019 between the NWMO and Dalhousie University to study the effects of glacial erosion within crystalline bedrock settings. The purpose of this contract is to produce a state-of-the-science review of published information relating to glacial erosion in crystalline bedrock settings (to be published in 2021). The current understanding of glacial erosional processes in crystalline settings will be reviewed, including i) recent advances in theoretical work on glacial erosion; ii) erosion studies involving numerical modelling of ice sheets; iii) any prior erosion rates from studies in the Canadian shield and other areas with similar lithology and glacial histories; iv) synthesis of factors that control glacial erosion and a ranking of their relative importance for crystalline bedrock settings in Ontario; v) descriptions and applications of cosmogenic radionuclides or other emerging approaches or measurement techniques to provide estimates of erosional processes and erosional rates and; vi) detailed sampling strategies for cosmogenic nuclide methods, as well as any special considerations for associated field and laboratory work.

#### 5.2.1.3 Greenland ICE Project

The NWMO collaborated with NAGRA, SKB and POSIVA on an ice drilling project (ICE) to establish constraints on the impact of ice sheets on groundwater boundary conditions at the ice-bed contact. The work used field studies of the Greenland ice sheet, collected as part of the

Greenland Analogue Project (2009-2012; final reports published in 2016) and as part of a larger National Science Foundation project focused on ice dynamics. This project focused on three aspects of boundary conditions that ice sheets place on groundwater systems: 1) transient high water-pressure pulses; 2) glacial-bed water-pressure gradients; and 3) constraining the flooding and transmissivity of water across the bed. The ICE project ran through the end of 2017, with a final report at project completion in 2019 (Harper et al. 2019).

#### 5.2.1.4 Glacial and Proglacial Environment – Numerical Modelling

##### 5.2.1.4.1 *CatchNet Project*

CatchNet (Catchment Transport and Cryo-hydrology Network) is a joint international program formed by international nuclear waste organizations and cold region hydrology researchers (URL: <https://www.skb.se/catchnet/>). It was established in 2019 to advance our understanding of hydrological and biogeochemical transport processes for a range of cold-climate conditions in the context of long-term, deep geological disposal of used nuclear fuel. CatchNet has identified three research packages (RP) to address important knowledge gaps:

- RP1: connecting the glacial and sub-glacial hydrology with the periglacial hydrological system on landscape scale;
- RP2: permafrost transition periods;
- RP3: biogeochemical cycling.

Currently CatchNet has three full members (SKB, NWMO and RWM) and one supporting member (COVRA). Each full member funds a PhD student or postdoctoral fellow to work on one of the research packages. NWMO is supporting a PhD student co-supervised by professors at McGill University and Dalhousie University to examine the impacts of permafrost transition on surface and subsurface hydrologic processes (RP2). The PhD students or postdoctoral will start their research during 2020.

##### 5.2.1.4.2 *University of Montana – Joint Work with SKB*

In 2019, NWMO and SKB initiated a new project to support researchers at the University of Montana (USA) to study coupled ice sheet, groundwater, and surface water hydrological processes through new data analysis and numerical modeling. This modelling study uses the field data previously collected from two international projects (GAP and GRASP) in the Kangerlussuaq area of western Greenland. This joint project will focus on the following two main areas:

- Evolution of the thermal state of the ice sheet bed;
- Ice-sheet processes influencing the ice sheet - bedrock boundary and underlying groundwater pressures near the ice sheet margin.

The researchers will work closely with the CatchNet program, participating in the CatchNet annual meeting and other activities regularly. In particular, the results of this study will be used as boundary conditions by CatchNet RP1.

## 5.2.2 Groundwater System Stability

### 5.2.2.1 Numerical Modelling Approaches

Reactive transport modelling is a useful approach for assessing long-term geochemical stability in geological formations. Reactive transport modelling is used to assess: 1) the degree to which dissolved oxygen in recharging waters may be attenuated within the proposed host rock; 2) how geochemical reactions (e.g., dissolution-precipitation, oxidation-reduction, and ion exchange reactions) may affect groundwater salinity (density) and composition along flow paths; and 3) how diffusive transport of reactive solutes may evolve in low-permeability geological formations.

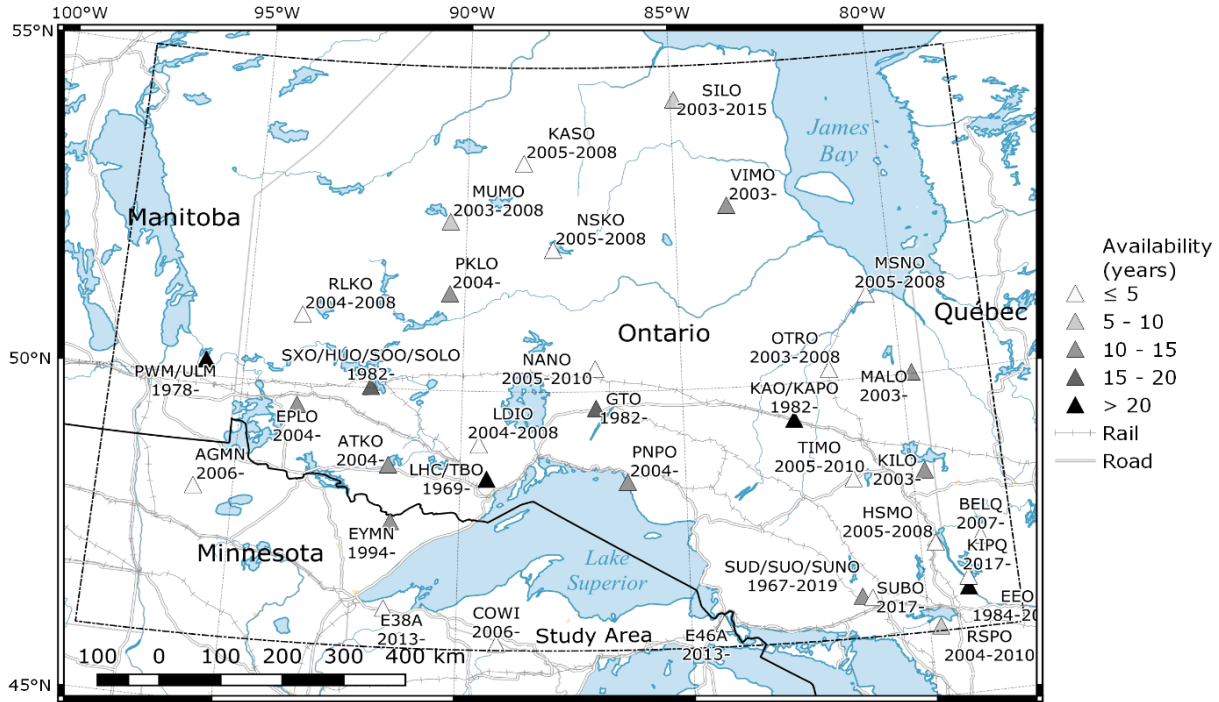
Research continued in 2019 to complete the implementation of unstructured grid capabilities into the multi-component reactive transport code MIN3P-THCm for 3-dimensional (3D) systems, including the parallelization of the unstructured grid functions. This development has been documented in journal publications (Su et al. 2019a, 2019b). A technical report providing additional details on the implementation of unstructured grids in MIN3P-THCm is expected in 2020. A 3D demonstration simulation based on the Michigan Basin is underway for the evaluation of MIN3P-THCm code capabilities for large-scale 3D flow and reactive transport simulations using unstructured meshes.

MIN3P-THCm was applied to investigate the formation mechanisms for sulfur water observed in the Michigan Basin (Xie et al. 2018). The simulations have been further improved using a more complete and realistic geochemical network including ferrous and ferric iron and associated redox and mineral dissolution/precipitation reactions. Simulated results show improved agreement with the available field data. The impact of paleo-glaciation on the formation and distribution of elevated sulphide is also being investigated through reactive transport simulations. A journal paper documenting the improved reactive transport simulation of sulfur water is expected to be submitted in 2020.

### **5.2.3 Seismicity**

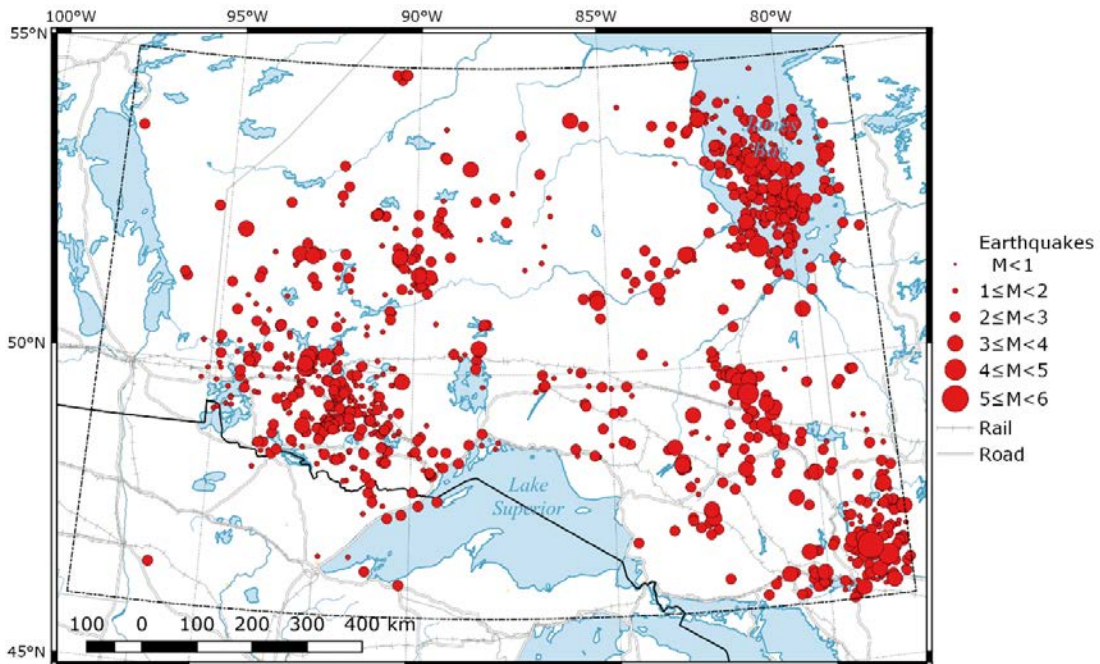
#### **5.2.3.1 Regional Seismic Monitoring**

The currently operating stations comprising the seismic network in northern Ontario can be seen below, along with stations that have since been closed. The distribution of seismicity for the calendar year of 2018 (reporting in 2019) falls in line with similar patterns, frequency and magnitudes of seismicity recorded for previous calendar years.



Note: study area is outlined with a dash-dotted line. Triangles are historical and currently active stations within the study area, shaded according to aggregate data availability 1995-2018. Stations are labelled with station code and nominal start and end dates of operation.

**Figure 5-15: Seismograph Stations in Northern Ontario, 1995-2018**



Note: Events and stations are plotted for the study area only.

**Figure 5-16: Earthquakes in Northern Ontario, 1982-2018**

### 5.2.3.2 Paleoseismicity

Due to the long life-cycle of a repository, potential perturbations from rare strong earthquakes ground motions requires consideration. No such earthquakes have occurred in Ontario in human-recorded history. However, the NWMO is carrying out research to look for evidence, or absence of evidence, of such events in the past as described below.

#### 5.2.3.2.1 *Event horizon correlation between lakes using palynomorphs*

Research applying the seismo-stratigraphic/chrono-stratigraphic approach to investigating mass transport signatures of paleoearthquakes in the southern area of the Western Quebec Seismic Zone near Ottawa continued during 2019. A study was initiated using the down-core content of selected palynomorphs (e.g. pollen, dinoflagellates, and green algae) to characterize the paleolimnological history and develop an age model for the lake sediments. Cores were collected from l'argile and McArthur lakes, Quebec, located about 25 km apart (Figure 5-17), in February-March 2019, to sample lacustrine and/or glaciomarine sediments overlying a pair of mass transport deposit (MTD) event horizons in both lakes. The cores were CT-scanned at the INRS facility in Quebec City, and digital CT-scanning data were processed. The images for the pair of coring sites collected from each lake were then laid out on a respective mosaic poster. The cores were shipped to the Department of Earth Sciences, Brock University, where analysis is underway by a M.Sc. student under the supervision of Professor F. McCarthy. To date, twenty-one and four samples have been processed from one of the two Lac de l'argile and McArthur Lake cores, respectively.

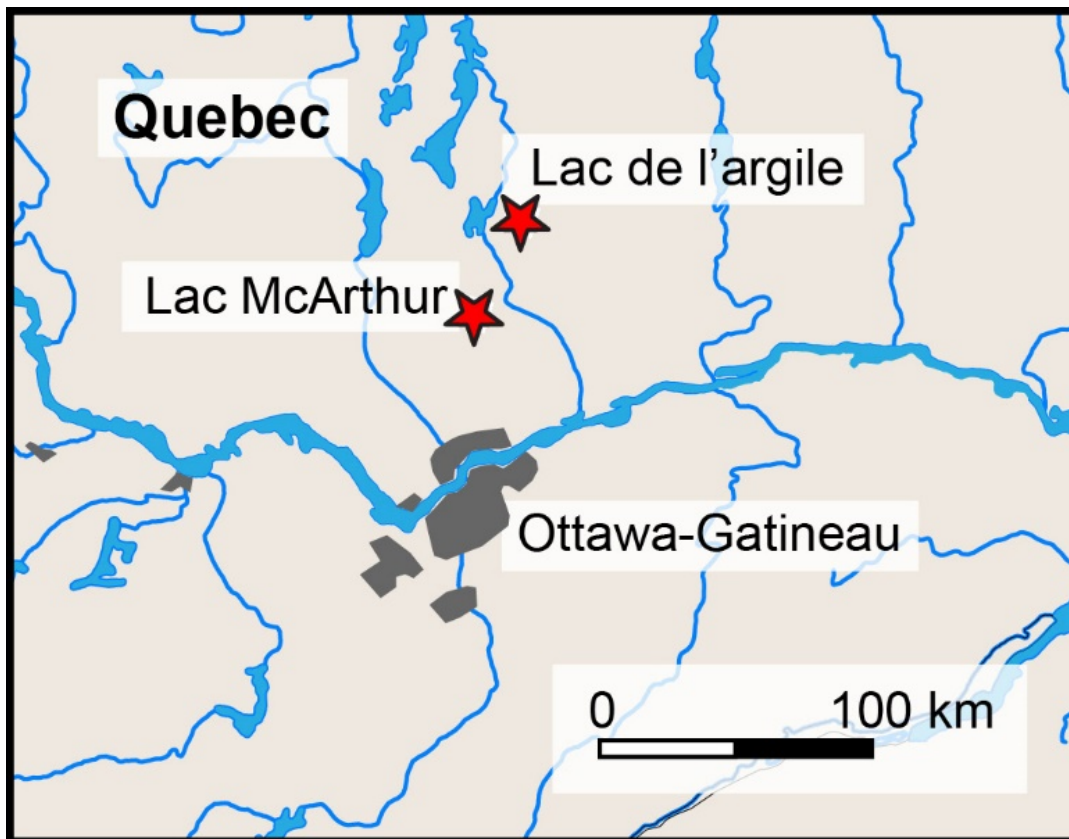


Figure 5-17: Map showing the locations of l'argile and McArthur lakes, Quebec

#### 5.2.3.2.2 *Profiling Lac Blouin, Val d'or, Quebec*

During 2019, profiling was conducted at the southern end of the Lac Blouin, Val d'or, Quebec, to follow-up reconnaissance profiling undertaken in 2016. The 2016 survey identified a series of shallow structures of late Holocene age that appear to represent a train of rotational failures developed on a low-angled failure plane. In July 2019, the full extent of the features was mapped, and a second set of similar structures was found to be located in an adjacent bay just to the north. Both sets of structures seemed promising for being low-angled failures that may have been triggered by late Holocene seismic shaking from an unknown earthquake. However, a conversation with a local resident revealed that rock and soil waste was previously dumped onto the frozen lake surface in the same area where the structures are located. The waste would have ended up on the lake floor during the spring melt. As a result, no additional work on these structures is planned.

#### 5.2.3.2.3 *Reconnaissance profiling in Lake Timiskaming, Ontario-Quebec*

During 2019, reconnaissance profiling was undertaken in the northern portion of Lake Timiskaming using a new, broadband, high-resolution, waterborne seismic reflection technique (see Pugin et al., 2019). This technique provides a higher energy source than the acoustic profiler, and can penetrate deeper into the lake sub-bottom. This profiling was used to test the technique in deep and shallow water settings overlying thick, fine-grained deposits. The profiling also provided a preliminary examination of Timiskaming East Shore fault, a possible neotectonic structure inferred to be present along the eastern side of Lake Timiskaming by Doughty et al. (2010, 2013). The presence of this fault is based on their interpretation of faulted glaciolacustrine deposits in the sub-bottom but is arguably conjectural because they do not objectively distinguish between neotectonic and glaciotectonic faulted sediments. Brooks and Pugin (2019) assessed the seismo-neotectonic origin of the New Liskeard-Thornloe scarp, Timiskaming Graben, Ontario. During 2020, new research will begin with the Geological Survey of Canada focusing on i) developing criteria to objectively distinguish between neotectonic and glaciotectonic faulted sediments; and, ii) assessing the inferred neotectonic origin of the Timiskaming East Shore fault. Similar reconnaissance profiling was also carried out in Tee and Kipawa lakes, Quebec.

### 5.2.4 **Geomechanical Stability of the Repository**

#### 5.2.4.1 Excavation Damaged Zones

The Queen's Geomechanics Group has been investigating the mechanics of, and developing predictive and characterization tools for, Excavation Damage Zone (EDZ) evolution around deep geological repositories in sedimentary and crystalline rock. Past research focussed on fundamental mechanics of EDZ, damage threshold definition, detection in laboratory testing, prediction and assessment of EDZ using continuum models, and secondary effects such as time dependency and saturation. The ongoing fourth phase of EDZ modelling has shifted the focus to discontinuum simulation of EDZ evolution and behaviour, including hydromechanical coupling, pre-existing discontinuities and internal defects and structure (intra-block structure). This advanced modelling puts increased demands on our ability to define relevant materials and structural properties in the laboratory and to log appropriate geomechanical details in the field. In addition, discontinuum models pose special challenges in verification, calibration and upscaling. In response, this research is based on the appreciation that conventional geotechnical characterization and analysis tools are not optimized for the demands of EDZ study. New geomechanics simulation approaches have been developed and adapted by

Queen's to allow for deeper mechanistic investigation of EDZ evolution. In parallel, Queen's research has updated conventional testing and investigation tools and developed new protocols for characterization.

The primary role of the Queen's Geomechanics Group is to improve the routine use of these advanced tools for the specific purpose of EDZ analysis in the DGR context and to develop protocols and guidelines for optimized model construction, calibration, verification and interpretation. An example of the numerical investigation of EDZ evolution using discontinuum tools is shown below.

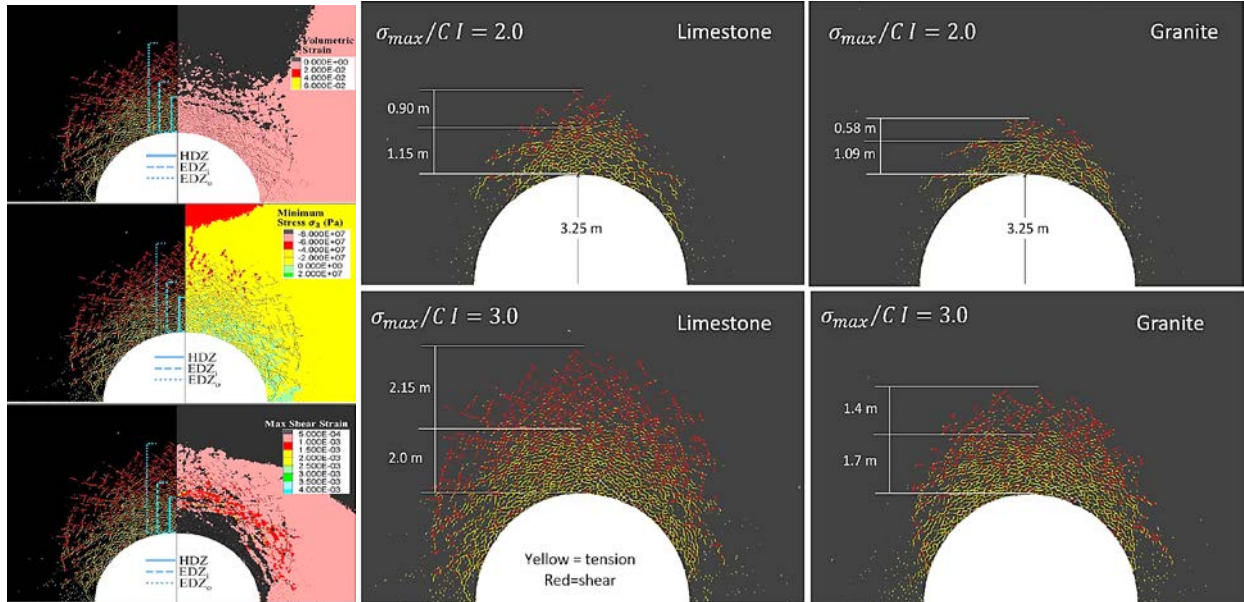


**Figure 5-18: (Left) Definition of EDZ Domains Using Discontinuum Model Indicators. (b) Sensitivity of EDZ Mode (Extension Vs Shear) and Extent, to Stress Level and Rock Properties**

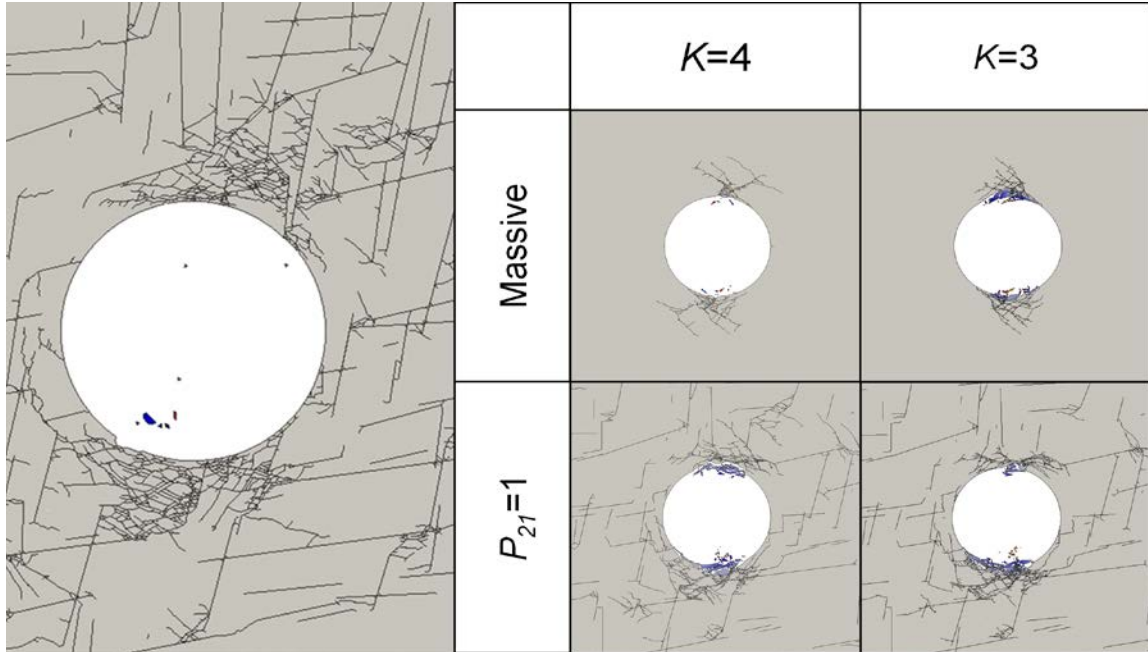


**Figure 5-19: Sensitivity of Discontinuum EDZ Development to Pre-existing Structure and Stress Ratio (Finite Element Discrete Element Hybrid Model).**

These advanced tools, however, also require advancements in the way that lab-scale testing and field sampling and logging is carried out. Past work has focussed on the mechanical properties of homogenous intact rock, relevant to EDZ development from damage initiation through accumulation to unstable propagation and macro-fracture development. Current work is aimed at improving and upgrading techniques for physical investigation of discontinuum components and property definition using the previously standardized compression, tensile, confined strength and direct shear testing methods (including boundary condition implications). Examples of some of the advancements underway are illustrated below.

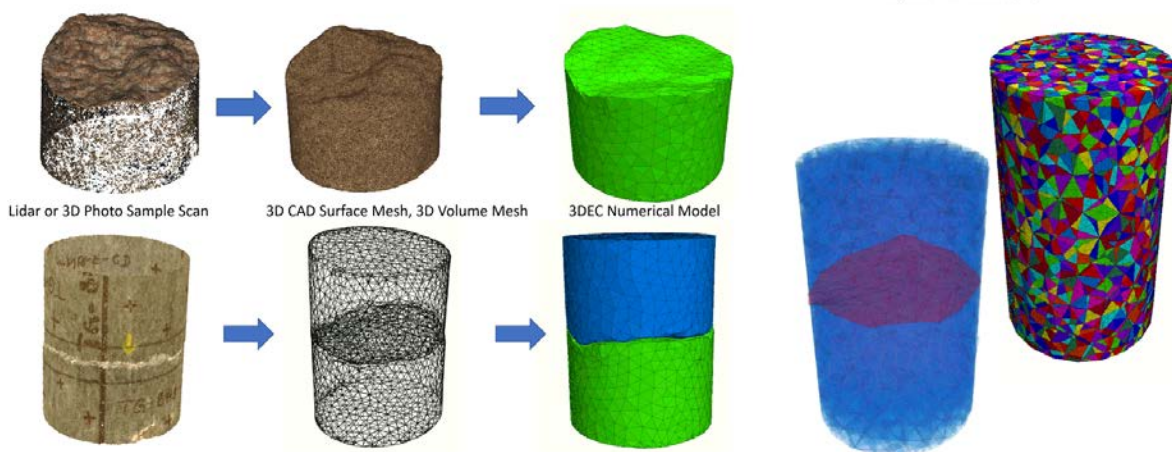


**Figure 5-20: Progression from Laser Or 3D Photoscans Of Direct Shear Discontinuity Samples, through to Geometrically Realistic 3D Discontinuum Model for Shear Test.**

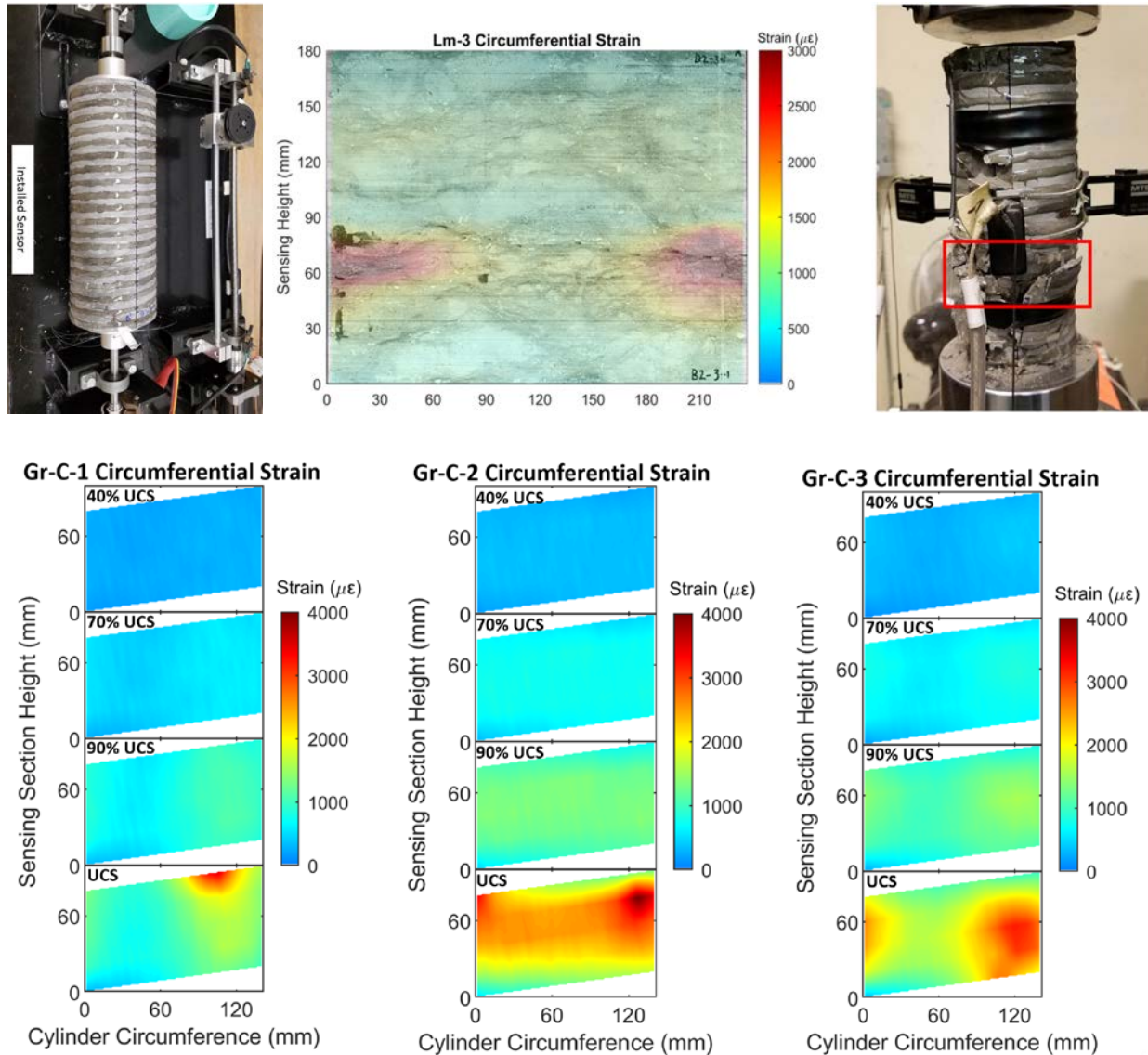


**Figure 5-21: (Top) Installation of Fibre-Optic Sensor for Full Sample Coverage of Lateral Strain - Strain Map At Yield For Limestone Sample Shown in the Middle Image. (Bottom) Strain Maps For Granite Samples at Different Stress Levels Showing Different Failure Modes Developing in the Test (from Platen Induced Chipping at Left, Spalling in the Middle and Shearing at Right).**

Other work during 2019 included the development of calibration and upscaling protocols for complex synthetic rockmass models in discrete element and hybrid finite-discrete element codes, investigation of saturation effects on damage thresholds in granite (limestone investigated previously), time-dependant degradation and creep in modelling and associated calibration, continuous logging of geomechanical parameters from rock core, boundary condition and testing parameter effects for direct shear testing and investigations of fully coupled hydromechanical modelling for discontinuum geomechanics.

## 5.2.4.2 Repository Design Considerations

### 5.2.4.2.1 *THM Analysis of Shaft and Cavern Stability*

The excavation of the underground openings (i.e. including placement rooms, shafts) for a repository, and the subsequent backfilling with heat-emitting UFCs as well as the buffer material, will induce coupled THM processes in-situ. NWMO has been conducting numerical analyses at near- and far-field scales to enhance our understanding of the response of the rock mass to hypothetical Canadian DGR configurations in both sedimentary and crystalline settings (ITASCA 2015a). These studies considered perturbations induced by the repository as well as the natural processes expected during a 1 Ma period. In the study by ITASCA (2015), the THM processes were one-way coupled, whereas an on-going THM modelling study (also by ITASCA) employed fully coupled THM analyses using refined input parameters. The sensitivity of the model predictions to some uncertain model input parameters (e.g. block-to-contact stiffness ratio for discontinuum modelling, poroelastic properties, and rock mass permeability) were also investigated.

All THM analyses were conducted for placement rooms consistent with the current conceptual APM repository design with 48-bundle canisters. THM modelling was conducted at two scales; near- and far-field scales, using a 3D continuum numerical code (FLAC3D) to generate evolving temperature, pore pressure, stress and deformation fields in the rock mass. In addition, 2D and 3D discrete element modeling was performed using UDEC and 3DEC to simulate evolution of damage around the repository rooms (i.e. near-field scale).

A number of conservative assumptions regarding geomechanical conditions were introduced in these analyses in order to provide bounding solutions for the various scenarios, including: time-dependent strength degradation; glaciations; low-probability seismic ground shaking; saturated rock mass and bentonite buffer. The effects of combinations of these loads and perturbations were also examined.

### 5.2.4.2.2 *Fault rupturing*

NWMO is conducting a study (by ITASCA) to numerically simulate a sizable seismic event resulting in the mobilization of surrounding fracture networks. Rupture of a seismogenic fault and its effect on the deformation of the off-fault fractures were examined. The purpose of the analysis was to determine the off-fault fracture displacements to inform the selection of respect distance within the repository horizon in crystalline rock.

Three different models were constructed to accommodate the fault size for moment magnitudes ( $M_w$ ) of 6.1, 6.6 and 6.9 seismic events occurring at the end of the glacial cycle when the vertical stress due to ice sheet is zero but glacially-induced horizontal stresses still remain. This base case analysis was conducted for five DFN realizations developed from the structural geology of Forsmark, Sweden. The modelling results revealed that for an earthquake with a moment magnitude,  $M_w$  of 6.1 and a dip angle of  $40^\circ$  (base case), the fault average shear displacement during the slip is about 1.6 m and the maximum shear displacement along the fault is 3.4 m. No DFN fractures slip more than 5 cm were observed in all DFN realizations except for a fault dip angle of  $30^\circ$ . Increasing the event magnitude while maintaining a dip angle of  $40^\circ$  (base case) resulted in a greater number of off-fault fractures with slippage over the 5 cm criterion and an increase in the distance to the fractures with such large displacements. Once site-specific DFN information is available, similar analyses will be conducted to support

repository engineering and design, as part of a complementary study during detailed site characterization.

## **5.2.5 Geoscientific Studies in Support of Geosynthesis**

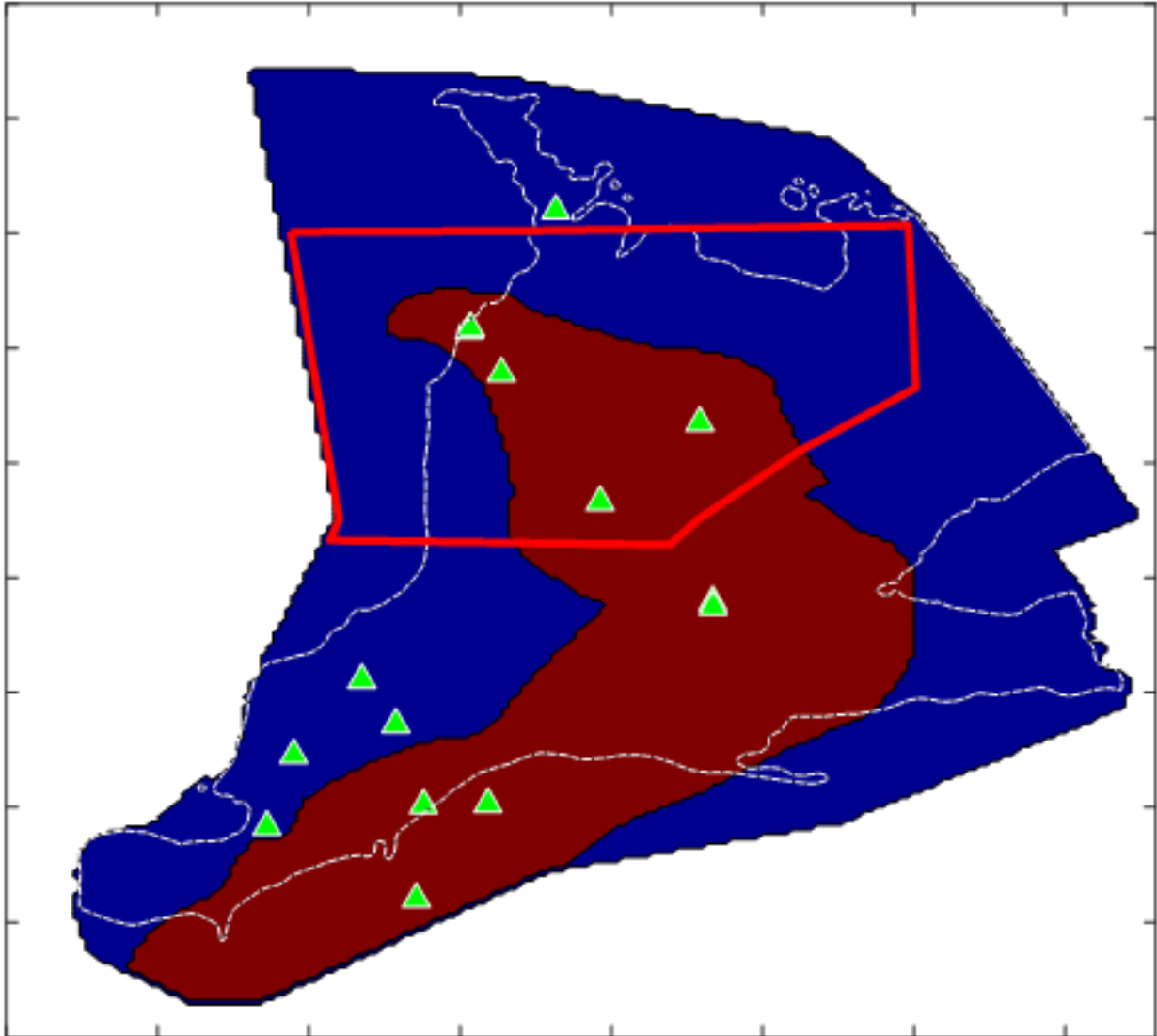
### **5.2.5.1 Natural Resources Assessment**

Initiated in 2017 and completed in 2019 (Chen et al. 2019), a hydrocarbon resource assessment for southern Ontario was produced for the NWMO by the Geological Survey of Canada (Alberta Office).

The resource assessment was comprised of two parts, an assessment of unconventional shale oil/gas resource potential in the organic-rich shales of the Collingwood Member of the Cobourg Formation and the Blue Mountain Formation within the Huron Domain of southern Ontario; and a quantitative assessment of conventional hydrocarbon potential within the Cambrian, Ordovician and Silurian strata of the Huron Domain of southern Ontario.

These represent an update of previously published work (Bailey and Cochrane 1984a &b; Golder, 2005), including the addition of supplemental information related to recent pool discoveries, history, size, and cumulative production rates. The results demonstrated that the geographic distribution of the predicted hydrocarbon resources of the Upper Ordovician Collingwood and Rouge River shale units, indicate that a large volume of the potential hydrocarbon resources of these two shale units occur in the Appalachian Basin portion of southern Ontario (Figure 5-22).

Only a small quantity of the reservoir-risked resource is predicted to occur in the southeastern part of the NWMO study area. The bulk of the potential hydrocarbons that are estimated to be trapped within the members is considered to be exceptionally low in the study area due to a combination of low permeability, contrasting lithologies, low formation pressures, low degrees of thermal maturation, high oil viscosity impeding hydrocarbon fluid flow, and poor oil show index  $S1/TOC < 1$ . When compared to similar analogous black shales, the Collingwood and Rouge River Members (combined) show a density (M BOE/sq km) that is several orders of magnitude lower than other oil producing shales, highlighting their unsuitability as an economic resource.



Note: Map showing study area around the formerly proposed L&ILW deep geological repository area (Red polygon) and areal extent of potential petroleum resources in the Collingwood and Rouge River members (reddish brown colored area). Green triangular symbols indicate well locations with log data for this study.

**Figure 5-22: Map of Potential Petroleum Resources in Southern Ontario**

## 6. REPOSITORY SAFETY

The objective of the repository safety program is to evaluate and improve the operational and long-term safety of any candidate deep geological repository. In the near-term, before a candidate site has been identified, this objective is addressed through case studies and through improving the understanding of important features and processes. Activities conducted in 2019 are described in the following sections.

The NWMO has completed studies that provide a technical summary of information on the safety of repositories located in a hypothetical crystalline Canadian Shield setting (NWMO 2012; 2017) and the sedimentary rock of the Michigan Basin in southern Ontario (NWMO 2013; 2018). The reports summarize key aspects of the repository concept and explain why the repository concept is expected to be safe in these locations (see Table 6-1).

**Table 6-1: Typical Physical Attributes Relevant to Long-term Safety**

Repository depth provides isolation from human activities  
 Site low in natural resources  
 Durable wasteform  
 Robust container  
 Clay seals  
 Low-permeability host rock  
 Spatial extent and durability of host rock formation  
 Stable chemical and hydrological environment

### 6.1 WASTE INVENTORY

#### 6.1.1 Physical Inventory

Currently there are about 2.9 million used CANDU fuel bundles. Based on the known plans for refurbishment and life extension, there could be about 5.5 million used CANDU fuel bundles (about 106,000 Mg heavy metal) from the current generation of nuclear power (Gobien and Ion 2019).

The CANDU fuel bundles are a mature product, with small design variations over the years primarily in the dimensions and the mass of each bundle, as well as variations in the number of elements per bundle by reactor type. The 37M bundle recently introduced in some stations has slightly different dimensions compared to the previous standard bundle.

In addition to the CANDU used fuel, AECL also has ~500 Mg of prototype and research reactor fuel fuels in storage at the Chalk River Laboratories and Whiteshell Research Laboratories. Most of this is UO<sub>2</sub> based fuel from the Nuclear Power Demonstration (NPD), Douglas Point and Gentilly-1 prototype reactors. AECL also holds a small amount (i.e., less than ~100 Mg) of various research fuel wastes with a variety of compositions and enrichments. There is also a very small amount of fuel still in service in low-power research reactors at McMaster University, Royal Military College of Canada and Polytechnique Montréal.

The Canadian used fuel inventory and forecast are updated annually by NWMO (Gobien and Ion 2019). A database with key information on fuel bundles produced to date is maintained by NWMO.

### 6.1.2 Radionuclide Inventory

Updating the 2000/2001 inventory continued throughout 2019. Calculations were carried out using the most recent Industry Standard Tool version of the ORIGEN-S code and the latest CANDU specific nuclear data (e.g., cross-sections, decay data, and fission product yields) for a range of used fuel burnups of interest to the safety assessment or design. Similar calculations were also performed for specific used fuel bundles with known burnups and power histories, for which radionuclide inventories have been experimentally measured. These latter calculations are for code validation and to provide confidence in the ORIGEN-S results. This work was completed in 2019. A report documenting the updated inventory and thermal power as a function of decay time for a reference CANDU fuel bundle will be published in 2020.

### 6.1.3 Chemical Composition

Measured data on main and trace elemental composition from 21 unirradiated CANDU fuel bundles (UO<sub>2</sub> pellets, Zircaloy end caps, Zircaloy tubing, Zircaloy tubing with a braze and spacer, and Zircaloy tubing with CANLUB coating), which encompassed a range of manufacturers, bundle types and manufacture dates, was previously completed to support the development of a recommended elemental composition value for UO<sub>2</sub> pellets and Zircaloy cladding (which includes the tubing as well as end caps, braze region and CANLUB).

In 2019, additional analysis was initiated in order to expand the material composition database and improve the method detection limits of select elements. In particular, the additional analysis focused on nitrogen and halogens in the fuel and Zircaloy cladding, and protactinium in the fuel, which are potential precursors of activation products.

### 6.1.4 Irradiation History

The NWMO maintains a statistical summary of the key parameters for the large majority of used CANDU fuel bundles: bundle type, source reactor, date of discharge, burnup and peak linear power. Burnup is important for determining the radionuclide content of a fuel bundle. Peak linear power is a secondary parameter that has small effect on radionuclide inventory, however it provides an indicator of the peak temperatures reached in the fuel. This in turn is relevant for the nature of the fuel microstructure and assessing the radionuclide distribution within a fuel pellet.

The Canadian stations all operate within a fairly consistent set of operating conditions, so have similar irradiation history. The burnup and peak linear power distributions for CANDU fuel discharged from the Bruce, Pickering and Darlington nuclear stations were determined for 1970 to 2006 (Wilk and Cantello 2006) and up to 2012 (Wilk 2013). The typical burnup of CANDU fuel ranges from about 130 to 220 MWh/kgU, with a mean burnup value from about 170 to 200 MWh/kgU between the stations, on a per station per decade basis. The 95<sup>th</sup> percentile values vary between about 220 MWh/kgU and 290 MWh/kgU (Wilk 2013).

This information is currently being updated for used fuel generated in the years since the last update, and also to evaluate older fuel records that are not available electronically, as fuel irradiation data from the first decade or so of the CANDU reactor program is not fully available on an individual bundle basis. These represent less than 10% of the current fuel bundle inventory. The report detailing the updated fuel irradiation data is expected to be available in 2021.

## 6.2 WASTEFORM DURABILITY

### 6.2.1 Used Fuel Dissolution

The first barrier to the release of radionuclides is the used fuel matrix. Most radionuclides are trapped within the  $\text{UO}_2$  grains and are only released as the fuel itself dissolves (which in turn only occurs if the container fails). The rate of fuel dissolution is therefore an important parameter for assessing long-term safety.

$\text{UO}_2$  dissolves extremely slowly under reducing conditions similar to those that would be expected in a Canadian deep geological repository. However, in a failed container that has filled with groundwater, used fuel dissolution may be driven by oxidants, particularly hydrogen peroxide ( $\text{H}_2\text{O}_2$ ) generated by the radiolysis of water.

Research on  $\text{UO}_2$  dissolution continued at Western University to further understand the mechanisms of a number of key reactions remaining unresolved, in particular the influence of  $\text{H}_2\text{O}_2$  decomposition and the reactions of the fuel with  $\text{H}_2$  produced either radiolytically or by corrosion of the steel vessel. The mechanistic understanding of the corrosion of  $\text{UO}_2$  under used fuel container conditions is important for long-term predictions of used fuel stability (Liu et al. 2017a, 2017b, 2017c, 2018, 2019). A study on the kinetics of  $\text{H}_2\text{O}_2$  decomposition on SIMFUELS (simulated spent nuclear fuels; doped  $\text{UO}_2$  specimens containing noble metal particles) has been conducted to determine the influence of noble metal particles on the reactions of  $\text{H}_2\text{O}_2$  with  $\text{UO}_2$  (i.e.  $\text{UO}_2$  corrosion and  $\text{H}_2\text{O}_2$  decomposition) by a combination of electrochemical, surface analytical and solution analytical methods (Zhu et al. 2019). It was observed that > 98% of the  $\text{H}_2\text{O}_2$  was consumed by  $\text{H}_2\text{O}_2$  decomposition.

The study of the kinetics of  $\text{H}_2\text{O}_2$  decomposition has been extended to standard CANDU fuel pellets to investigate variations in fuel reactivity due to differences in the manufacturing process. The characteristics of a series of standard  $\text{UO}_2$  pellets (1965-2017) has been investigated using electrical resistance measurements and Raman spectroscopy. Experiments on  $\text{H}_2\text{O}_2$  decomposition on the standard  $\text{UO}_2$  pellets are underway.

The kinetics of  $\text{H}_2\text{O}_2$  reduction on SIMFUEL,  $\text{RE}^{\text{III}}$ -doped  $\text{UO}_2$  and non-stoichiometric  $\text{UO}_2$  have been conducted using standard electrochemical methods at rotating disk electrodes. It was found the rate of  $\text{H}_2\text{O}_2$  reduction decreased in the order of SIMFUEL > Gd-doped  $\text{UO}_2$  > Dy-doped  $\text{UO}_2$  with the rate suppressed on the  $\text{RE}^{\text{III}}$ -doped  $\text{UO}_2$ . The slightly faster rate on the SIMFUEL may be attributable to the catalysis of reduction on the noble metal particles. The  $\text{H}_2\text{O}_2$  reduction on all three specimens was found to be suppressed by the presence of the ground water anion  $\text{HCO}_3^-/\text{CO}_3^{2-}$ . The results of the research on the kinetics of  $\text{H}_2\text{O}_2$  reduction on SIMFUEL and  $\text{RE}^{\text{III}}$ -doped  $\text{UO}_2$  will be presented in a journal publication.

The  $\text{H}_2$  effect in suppressing the corrosion behavior of  $\text{UO}_2$  (un-doped and  $\text{RE}^{\text{III}}$ -doped  $\text{UO}_2$ ) without catalysis of noble metal particles has been studied by producing H radicals electrochemically and radiolytically to simulate radiation effects on  $\text{UO}_2$  corrosion when  $\text{H}_2$  is present. It was observed that the combination of gamma radiation and  $\text{H}_2$  was required to reduce the  $\text{UO}_2$  matrix, and the reduction of  $\text{U}^{\text{V}}$  was reversible for specimens close to stoichiometric ( $\text{UO}_{2+x}$  with  $x < 0.005$ ) but only partially reversible for  $\text{RE}^{\text{III}}$ -doped  $\text{UO}_2$  with a much higher  $\text{U}^{\text{V}}$  content. At high gamma dose rates and dissolved  $\text{H}_2$  concentrations the matrix reduction appeared to be irreversible. The results of the research on the  $\text{H}_2$  effect in suppressing the corrosion behavior of  $\text{UO}_2$  without catalysis of noble metal particles will be described in a journal publication.

## 6.2.2 Solubility

The maximum concentration of a radionuclide within or near a failed container will be limited by the radionuclide solubility. Radionuclide solubilities are calculated by geochemical modelling using thermodynamic data under relevant geochemical conditions. These data are compiled in quality-controlled thermodynamic datasets.

NWMO continues to support the joint international Nuclear Energy Agency (NEA) effort on developing thermodynamic databases for elements of importance in safety assessment (Mompeán and Wanner 2003). Phase VI of the project which was started in 2019 will provide (1) an update of the chemical thermodynamics of complexes and compounds of U, Np, Pu, Am, Tc, Zr, Ni and Se with selected organic ligands, (2) a review of the chemical thermodynamics of lanthanides, and (3) a state-of-the-art review on thermodynamics at high temperatures.

The review of the thermodynamic data for iron Part 2 expects to be published in 2020. The second update of the actinides and technetium thermodynamic data is expected for publication in 2020. The reviews of molybdenum thermodynamic data, the state-of-the-art reports on the thermodynamics of cement materials and high-ionic strength systems (Pitzer model) are underway. The implementation of the new interactive TDB electronic database was completed in 2018 and a PHREEQC format thermodynamic database was available. The PHREEQC format thermodynamic database will be updated to include all the new reactions from the iron Part 2 book and the second update of the actinides book.

The NEA TDB project provides high-quality datasets. This information is important, but is not sufficient on its own, as it does not address the full range of conditions of interest. For example, the NEA TDB project has focused on low-salinity systems in which activity corrections are described using Specific Ion Interaction Theory (SIT) parameters. Due to the high salinity of porewaters observed in some deep-seated sedimentary and crystalline rock formations in Canada, a thermodynamic database including Pitzer ion interaction parameters is needed for radionuclide solubility calculations.

The state-of-the-art report on high-ionic strength systems (Pitzer model) will be useful to identify the data gap for Pitzer ion interaction parameters. The THEREDA (THERmodynamic REference DAtabase) Pitzer thermodynamic database (Altmair et al. 2011) is a relevant public database for high-salinity systems. It has been assessed by the NWMO and found to provide a good representation of experimental data for many subsystems.

The NWMO is also co-sponsoring the NSERC/UNENE Senior Industrial Research Chair in High Temperature Aqueous Chemistry at the University of Guelph, where there is capability to carry out various thermodynamic measurements at high temperatures and high salinities. This Chair program initiated in 2016. Progress has been made in several areas: (1) the equilibrium constants and transport properties for uranyl with sulfate from 25 to 350 °C determined by Raman spectroscopy approach (Alcorn 2019); and (2) the equilibrium constants and transport properties of lanthanum with halides from 25 to 250 °C determined by Raman spectroscopy and conductivity approach. A journal paper documenting the thermodynamic properties of lanthanum with halides is expected to be submitted in 2020. Measurements of equilibrium constants for uranyl with halides is underway.

## 6.3 BIOSPHERE

### 6.3.1 General Approach – Post-closure Biosphere Modelling and Data

The biosphere is a complex system, and will change over the one million year timescales considered in a safety assessment. In the context of deep geologic repositories, biosphere models are developed to obtain a useful estimate of the potential dose and non-radiological consequences through consideration of dominant or representative pathways.

In 2019, the NWMO continued the development of a new system modelling tool known as the Integrated System Model or ISM (Gobien and Medri 2019). One of the components of the ISM tool is a dynamic biosphere model, ISM-BIO which was implemented using the AMBER software. The model simplifies the biosphere as a series of compartments which can each receive, accumulate and transfer contaminants. Transfer between some compartments is dynamically modelled, while others are modelled by ratios that assume the compartments are in quasi-equilibrium over the time scales of interest. The ISM-BIO will continue to evolve in an interactive approach as the sites are characterized and the assessment objectives evolve.

### 6.3.2 Participation in BIOPROTA

BIOPROTA is an international collaborative forum created to address key uncertainties in long-term assessments of contaminant releases into the environment arising from radioactive waste disposal. Participation is aimed at national authorities and agencies with responsibility for achieving safe radioactive waste management practices. Overall, the intent of BIOPROTA is to make available the best sources of information to justify modelling assumptions made within radiological assessments constructed to support radioactive waste management. In 2019, the NWMO continued to participate in the C-14 and the BIOMASS 2020 update projects.

#### C-14 Project

Over the past decade, BIOPROTA has undertaken several projects relating to the behavior of C-14 in the biosphere. In 2014, refereed paper on this work was published in the Radiocarbon Journal (Limer et al. 2013). In 2016, a workshop was held to discuss model-data and model-model comparisons for three C-14 scenarios covering atmospheric deposition, release to sub-soil and modelling of contamination from an historical near-surface disposal. This led to a new project being initiated in 2017 to encompass model-data and model-model comparisons for two scenarios (one relating to C-14 from a historical near-surface disposal facility at Duke Swamp at the Chalk River Laboratory Site in Canada and the second to C-14 behaviour in a Finnish boreal forest).

The project also included a task to review the behaviour of carbon and C-14 in aquatic environments, with particular focus on where fish obtain their carbon from. Specifications for the data sets were circulated and modelling participation was invited. A fish review specification was also circulated. Reports on these studies were published in 2018 (Thorne et al. 2018). A workshop was held April 2019 to share understanding of C-14 behaviour when released in aquatic environments, from the sub-surface and in the atmosphere. The workshop findings are summarized in Limer (2019).

## BIOMASS 2020 Update

The International Atomic Energy Agency (IAEA) BIOMASS report on reference biospheres for solid radioactive waste disposal was published in 2003. BIOPROTA has undertaken to review and enhance the BIOMASS methodology. The work programme is being co-ordinated with IAEA MODARIA II working group 6 (WG6). BIOPROTA held workshops during 2016-2017, and published workshop reports identifying key areas of review and update of the BIOMASS methodology (Smith 2016, 2017a, 2017b). In 2018, an interim report on the BIOPROTA / BIOMASS project was published, along with three workshop reports and a journal publication on climate change and landscape development with respect to the BIOMASS update (Lindborg et al. 2018). In 2019 the draft report detailing the revised BIOMASS methodology was finalized and is expected to be published in 2020. A supplementary report is planned to develop to include detailed material and examples to support the enhanced BIOMASS guidance.

## **6.4 SAFETY ASSESSMENT**

### **6.4.1 Pre-closure Safety**

The pre-closure period includes site preparation, construction, operation, decommissioning, monitoring and closure. Topics include normal operations safety (public and worker dose), and malfunctions and accidents. In the context of a geological repository and related facilities for used fuel, these topics were addressed as part of AECL's Environmental Impact Statement (AECL 1994, OHN 1994), and reviewed as part of the NWMO options study (NWMO 2005). The pre-closure safety assessment will be updated in parallel with the ongoing work to develop more detailed plans for operations and surface facilities.

#### 6.4.1.1 Normal Operations

A preliminary dose assessment of the facility was carried out in 2014 to guide ALARA (As Low As Reasonable Achievable) development of the repository concepts (Reijonen et al. 2014).

Recently, a preliminary normal operations analysis was initiated for the DGR conceptual design. It assesses potential radiological doses to the public from airborne and waterborne emissions during normal operations of a DGR and its related surface processing facilities, as well as direct and skyshine external radiation doses from used fuel to public or non-nuclear energy worker (non-NEW) receptors. The results are for a generic site and consider exposure to receptors at a potential fence line location. During normal operations, airborne radioactivity can be released during handling of the used fuel from surface contamination that is generally present on all the used fuel bundles and from cladding failures in the fuel element. Waterborne emissions can result from cell washdowns and decontamination of used fuel modules, used fuel transportation packages, and containers. Simple, conservative models are used to estimate the dispersion of airborne and waterborne emissions released from the Used Fuel Packaging Plant (UFPP). Radiological doses to the public are calculated using the methodology described in the Canadian Standards Association (CSA) N288.1-14 (CSA 2014) for a reference case, as well as sensitivity cases used to bound uncertainties associated with input parameters. Used fuel bundles will be handled and temporarily stored in the UFPP during re-packaging operations. The potential external gamma radiation dose rates due to direct and sky-scattered (skyshine) external radiation to a public or non-NEW receptor standing at a potential fence line location are calculated. This study continues to 2020.

In 2019, an initial assessment of the radon hazard was performed to determine whether there is health hazard to workers during construction and operation of the DGR, and a need for radon monitoring or development of any action levels in order to be in compliance with the applicable regulatory requirements. The study is for a generic crystalline or sedimentary rock site and continues to 2020.

#### 6.4.1.2 Abnormal Events and Accidents

A preliminary study was carried out to identify potential internal accident scenarios that may arise during the operations phase for the repository, based on a conceptual design of the UFPP and repository (Reijonen et al. 2016). In this preliminary study, a failure modes and effects analysis (FMEA) was used to identify potential internal hazards resulting from, for example, failure of equipment, failure of vehicles, failure of the shaft hoist system, loss of electric power, ventilation and filtration system failure, and human error. The estimates of the internal initiating event frequencies were obtained based on data from the nuclear industry and from earlier used fuel management studies (AECL 1994). The potential external events were also identified for a generic site based on literature review.

Recently, a preliminary analysis was initiated to assess the potential public dose consequences for the accident scenarios identified in the previous hazard identification study (Reijonen et al. 2016) for a generic site. The study considers exposure to a person standing at various distances from the fence line under conservative atmospheric conditions. Atmospheric dispersion factors are derived based on the Gaussian dispersion model described in CSA N288.2-M91 (CSA 2003). Radiological doses to the public are calculated for accidents that are classified as Possible Events (occurring at least once every 100 years of operation) or Unlikely Events (occurring less frequent than Possible Events). The presence or absence of ventilation system High Efficiency Particulate Air filters is also considered in combination with specific accident scenarios. The results to-date indicate that the calculated public doses for inhalation, air immersion and ground exposure pathways remain below the interim dose criterion of 0.5 mSv for Possible Events and 20 mSv for Unlikely Events for all accidents considered. This study also looks at the minimum site boundary distance by calculating public doses at various distances from the UFPP, Ventilation Shaft, and Main Shaft. Sensitivity cases are carried out to determine the effect of stack release height, the effluent exit velocity, and the release orientation on the calculated minimum site boundary distance. This study will be completed in 2020.

The potential external hazard events are dependent on the site. As part of the site characterization phase, the external hazard events will be evaluated. Two specific important external events are seismicity and flooding. The work related to the seismic hazard potential is being assessed under site characterization. The potential impact of climate change on flood risk also needs to be considered given the operating timeframe for the repository and is described below.

#### 6.4.1.3 Climate Change Impacts Study

A study was initiated in 2018 to review anticipated climate change impacts on climate conditions (e.g., temperature and precipitation) and develop a methodology to incorporate these climate changes into probable maximum precipitation (PMP) estimation appropriate for the DGR study areas in Ontario. A report documenting the study was issued in 2019 (Wood 2019).

In 2019, the preferred method by Wood (2019) has been applied to assess the climate change impacts on the PMP and Intensity-Duration-Frequency (IDF) amounts for the Ignace study area.

The approach follows the key steps in Figure 6-1. Of these steps, the approach to evaluating future climate impacts on precipitation uses the state of science and publicly available climate projections to complete the climate change impact assessment on the PMP and the IDF values. The multi-model ensemble approach is used to describe the probable range of results and potential climate changes to PMP and IDF amounts expressed as percentiles, so that the level of acceptable risk can be selected by using the desired percentile. The study considered projected changes in climate over three separate time periods – mid-century (2041 to 2070); end-of-century (2071-2100); and beyond 2100. These periods coincide with the different phases for a possible deep geological repository, including site preparation and construction; the operational period; extended post-closure monitoring; and decommissioning. There is a level of inherent uncertainty when projecting future climate; however, the approach taken in this study aims to address this uncertainty by relying on a multi-model ensemble and providing percentiles. The work for both Ignace and Southern Ontario study areas will be completed in 2020.

The next steps are to estimate the flood potentials and associated climate change impacts for the Ignace and Southern Ontario study areas. It is expected that the climate change impacts would be periodically updated in the future as part of the safety assessment / licensing review.

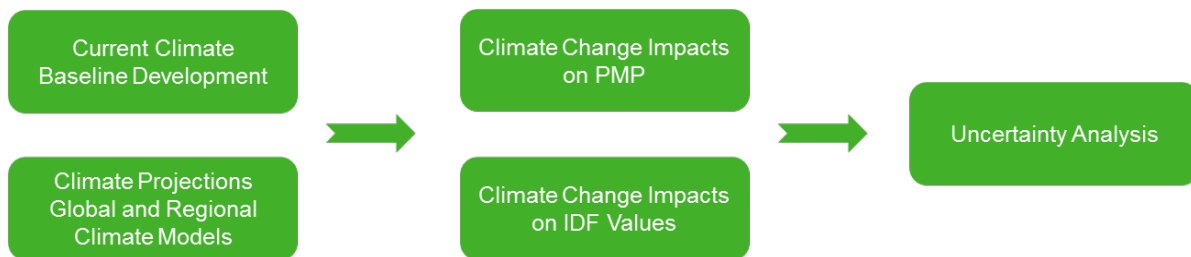


**Figure 6-1: High Level Step-Wise Approach in Climate Change Impacts Study**

#### 6.4.1.4 Site-Specific Properties for Safety Assessment

Pre-closure safety assessment in Sections 6.4.1.1 and 6.4.1.2 employs an environmental transfer model to calculate potential dose to the public from the airborne and aqueous releases from a nuclear facility under normal and accident conditions. CSA provides guidelines for the model calculations (CSA 2003, 2008 and 2014). CSA (2014) also provides regional default values for some parameters for southern Ontario, western Ontario, eastern Ontario, Quebec and Maritimes. However, there are no default values provided for aqueous dilution factors (AqDF). Site specific data will be needed to determine the AqDF.

Depending on the site location, additional site-specific data may be needed and integrated with regional or other relevant generic data. These site-specific data will be acquired as parts of baseline monitoring program, e.g., installation of a meteorology tower at the Ignace study area.

#### 6.4.1.5 Behaviour of Used Fuel / Packages under Normal and Accident Conditions

A key aspect of the pre-closure safety assessment is the behaviour of the used fuel and packages under normal and accident conditions. CANDU fuel is a solid waste form, non-volatile and contained within Zircaloy sheathing. All used fuels have small amount of surface contamination. However, some used fuels may be damaged during transport to the DGR, or

during handling within the UFPP. These could result in some release of particulate, gases, or volatile elements from the used fuel. These releases would be handled within the surface facilities as part of the design basis (e.g., particulates captured on a High Efficiency Particulate Air (HEPA) filter system).

From a pre-closure safety assessment perspective, uncertainties in fuel integrity will be handled by conservative assumptions. Normal operations and accident assessments are discussed in Section 6.4.1.1 and 6.4.1.2 respectively. Of interest from a pre-closure safety assessment perspective are cases where the fuel is not yet sealed in a container, or the container itself is not fully closed. The NWMO are looking for opportunities to learn from others' used fuel handling experience such as participation in the NEA Expert Group on Operational Safety and data available in literature (for example, from U.S. Idaho National Laboratory (INL) 2005). Used fuel handling experiences at Canadian Nuclear Laboratories and at Ontario Power Generation's Dry Storage facilities will also be sought for.

In order to estimate the radiological release source terms during a potential accident, the preliminary assessment as discussed in Section 6.4.1.2 follows the U.S. Department of Energy (DOE)'s five factor formula - material at risk, damage ratio, airborne release fraction, respirable fraction, and leakpath factor. The assigned values for the five factors in this study are based mostly on the U.S. DOE Handbook (U.S. DOE 1994) and the subsequent U.S. DOE standard (U.S. DOE 2007), as well as values used in the Yucca Mountain assessment (U.S. DOE 2009).

For preliminary normal operation assessment, as discussed in Section 6.4.1.1, radionuclide release from intact fuel bundles and fuel bundles with an intentionally defected fuel element are based on experimental data (Chen et al. 1986, 1989). A range of radionuclide release rates are reported in literature, and the highest measured release rates are conservatively used for the reference case. The fuel bundle failure rates during transportation and handling are considered to be relatively low, as the fuel processing facilities in the UFPP will be designed to minimize the impact on the used fuel. Conservative assumptions are made to bound the uncertainty in the fuel bundle failure rates. These source term values are considered overall conservative, taking into account in part differences in used fuel characteristics, container and handling requirements (e.g., the lower burnup of CANDU bundles).

The NWMO will continue to monitor the literature and international practices, and experience in Canadian fuel handling to support these values.

## **6.4.2 Post-closure Safety**

### **6.4.2.1 Post-closure Safety Assessment Methods**

The purpose of a post-closure safety assessment is to determine the potential effects of the repository on the health and safety of persons and the environment during the post-closure timeframe.

The ability of the repository to safely contain and isolate used nuclear fuel is achieved by multiple barriers, these being the ceramic used fuel pellet, the fuel sheath, the robust long-lived container, a series of clay-based seals and backfill material, and the site-specific geology.

Preliminary work towards site-specific assessments of post-closure safety included:

- 1) Interpretation and processing of geoscience data such as digital elevation data from LiDAR surveys, GIS data for surface waters and cultural features, discrete fracture networks, and hydraulic conductivity profiles;
- 2) Construction of groundwater flow and transport models, building on the approaches developed in previous case studies (e.g., Kremer et al. 2019). Special attention was given to fracture networks and how improved understanding can be taken into account as site characterization continues. This included a review of the literature on the various approaches to modelling faults, fractures, and their properties;
- 3) Preliminary modelling exercises such as postulated failure scenarios, the hypothetical release of contaminants, the performance of the multiple barriers, and determining the most consequential locations for water-supply wells. Additional effort was given to exploring potential complementary metrics for assessing site suitability.

Post-closure assessment methodology was based on guidance from the Canadian Nuclear Safety Commission (CNSC 2018).

#### 6.4.2.1.1 *Integrated System Model*

In late 2018, the NWMO initiated development of a new system modelling tool known as the Integrated System Model (ISM). The ISM consist of a connected series of models developed in commercially available codes each representing a specific portion of the repository system. The ISM-NF model developed using COMSOL describes the waste form, containers, engineered barrier system, and excavation damaged zone surrounding the placement room. It assumes the failure of some containers, degradation of the used fuel by water, and transport of species out of the container and through the engineered barrier system and excavation damaged zone. The ISM-GEO model developed using HGS describes the movement of species from the repository via the groundwater through the rock mass and fractures, to the surface environment. The ISM-BIO model developed using AMBER determines the concentration of species in environmental media (e.g., surface water, groundwater, sediments, soils, air) and estimates the consequent radiological dose to a critical group living near the repository.

The NWMO continues to develop and test the ISM consistent with NWMO technical computing software procedures, and with the CSA Standard N286.7-16 (CSA 2016). The ISM model theory is described in (Gobien et al. 2019). Additional software documentation is expected to be complete in 2020. Validation of the ISM is an ongoing task, with further validation of specific process models or overall system-level comparisons performed when suitable opportunities arise.

In addition to the development of the ISM component models the NWMO is developing a scope of work to produce a pre-processing, linking and post-processing tool that will couple together the component ISM models. Ultimately the ISM is expected to be computationally tractible for deterministic simulations, and potentially for probabilistic analysis. The work program to develop the ISM linking tool is expected to start in 2020.

#### 6.4.2.2 Acceptance Criteria

Acceptance criteria for radiological and non-radiological contaminants applicable to post-closure safety assessments are used to judge the acceptability of analysis results for the protection of

humans and the environment. Currently, criteria are referred to as “interim” because they have not been formally approved for use in a used fuel repository licence application.

Interim acceptance criteria for the radiological protection of persons, expressed as an annual dose rate target, are based on the recommendations of the ICRP (2007) and IAEA (2006) and aligned with the reference risk value of ICRP (2013), Health Canada (2010), and IAEA (2006).

Protection policies for non-human biota are not as mature as those for humans. As such, there are not internationally agreed upon environmental benchmarks of dose rate criteria against which to assess radiological effects to non-human biota. In the most recent post-closure safety assessment (NWMO 2018), the NWMO used a two-tiered criteria system, which includes proposed criteria from ERICA (Garnier-Laplace et al. 2006), PROTECT (Andersson et al. 2008) and the ICRP’s Derived Consideration Reference Levels (ICRP 2008). This approach is consistent with the approach proposed by BIOPROTA, an international forum which seeks to address key uncertainties in long-term assessments of contaminant releases into the environment arising from radioactive waste disposal (see Section 6.3).

With respect to the protection of persons and the environment from non-radiological contaminants, a set of interim criteria which span all environmental media (i.e., surface water, groundwater, soil sediment and air) and relevant elements in a used fuel repository are documented in Medri 2015. Work was initiated in 2016 to develop interim non-radiological acceptance criteria for relevant elements missing from Medri (2015): gold, bismuth, bromine, iodine, indium, osmium, palladium, platinum, rhodium, ruthenium, tellurium and tungsten. Criteria for these elements were developed using a comprehensive literature search, as well as aquatic and terrestrial toxicity tests for rhodium and ruthenium. These additional interim acceptance criteria were published in 2019 (Fernandes et al. 2019).

## **6.5 MONITORING**

### **6.5.1 Knowledge Management**

The NEA Repository Metadata (RepMet) Management project was a four year initiative aimed to create sets of metadata that can be used by national programmes to manage their repository data, information and records in a way that is harmonized internationally and suitable for long-term management. RepMet focused on the period before repository closure. The NWMO participated in this program since its start. An overview of the project, including deliverables produced since 2014, is presented in NEA (2018).

The NEA initiative on the Preservation of Records, Knowledge and Memory (RK&M) across Generations was a multi-year initiative looking to minimise the risk of losing records, knowledge and memory, with a focus on the period of time after repository closure. The NWMO participated in this program since its start. Three reports of the RK&M initiative were published in 2019, including the report describing the Key Information File concept for a repository (NEA 2019a), the report describing the Set of Essential Records concept for a repository (NEA 2019b), and the RK&M final report (NEA 2019c).

## 7. SITE ASSESSMENT

As of the end of 2019, potential repository siting areas were being considered within two regions in Ontario: the Ignace Wabigoon area in northwestern Ontario, and South Bruce/Huron-Kinloss in southern Ontario. The status of the geological and environmental studies underway in these regions is described below.

### 7.1 IGNACE

#### 7.1.1 Geological Investigation

By the end of 2019, the Geoscience Site Assessment team and their contractors completed the drilling of 3 kilometre-long boreholes in the crystalline rock of the Revell Batholith west of Ignace, Ontario. The drilling of a fourth borehole was underway as of late 2019. Drilling, coring and testing of each borehole takes several months in the field (followed by several months of laboratory testing of rock and water samples). During drilling and coring, each 3 m core run retrieved underwent a standard work flow that included core photography, core sampling, as well as geological and geotechnical logging of lithology, alterations and structures into an acQuire GIM Suite borehole data management system.

The borehole drilling plan included taking water samples opportunistically from any locations where flowing groundwater was intersected.



Figure 7-1: Borehole IG\_BH02 Site, Summer 2019

Down-hole geophysical logging of the boreholes was completed (i.e. measurements taken within the borehole). Many geophysical logs were collected, including logs such as Optical & Acoustic Televiwer, Flowing Fluid Electrical Conductivity (FFEC), Natural Gamma, Gamma-Gamma Density, and Neutron and Borehole Deviation. Geophysical logging, specifically the optical and acoustic televiwer logs, were used to orient structures logged in the unoriented core. Natural Gamma, Neutron, and Density logs provided additional information to refine the distribution and characterization of lithological units and alteration. Other down-hole geophysical logs (e.g., FFEC) provided inputs into the planning of subsequent borehole tests including hydraulic testing and the installation of a long-term WestBay monitoring system.

Hydraulic testing of the boreholes was carried out using a double inflatable packer tool with a 20 m interval. Testing was carried out at selected intervals along the length of the boreholes. Tests were designed to test both intervals of intact rock, and also areas where structures and potential water flow were indicated by core and geophysical logs.

Following the hydraulic testing, boreholes are either temporarily sealed with packers, or a Westbay MP38 Multi-Level system is installed. The Westbay system typically comprise 20 packered intervals where pressure and temperature can be measured. These systems will allow for the monitoring of the evolution of formation pressures, for potential to sample groundwater, and will provide information on vertical gradients at the site.

Rock core samples collected during drilling and coring are sent to offsite laboratories for various analyses including Geomechanics (strength), Petrophysics (density, porosity, permeability and effective diffusion), Geochemistry (porewater composition, sorption) and Microbiology. In addition, a suite of general archive samples are collected and preserved from each borehole, to be available for future testing.

Planning is underway for the next boreholes (boreholes 5 and 6), as well as additional geological work in the area, including geological mapping, installation of microseismic monitoring stations, 2D seismic survey and installation of shallow groundwater monitoring wells.



**Figure 7-2: Examining Core from Ignace Boreholes**

## 7.1.2 Environmental Assessment

In 2019, the NWMO and its contractor (Tulloch Engineering Inc.) along with members of the Wabigoon Lake Ojibway Nation (WLO) community undertook its fourth year of field studies to collect abiotic and biotic data in the Ignace Wabigoon siting area. The 2019 environmental sampling program focused primarily on the study area within the Revell batholith where siting activities have been occurring for the past several years. Previously established surface water sampling locations were chosen to represent near-field and far-field receptors for the potential future DGR and current drilling activities. See below the attached figure showing locations sampled during the 2019 field season.

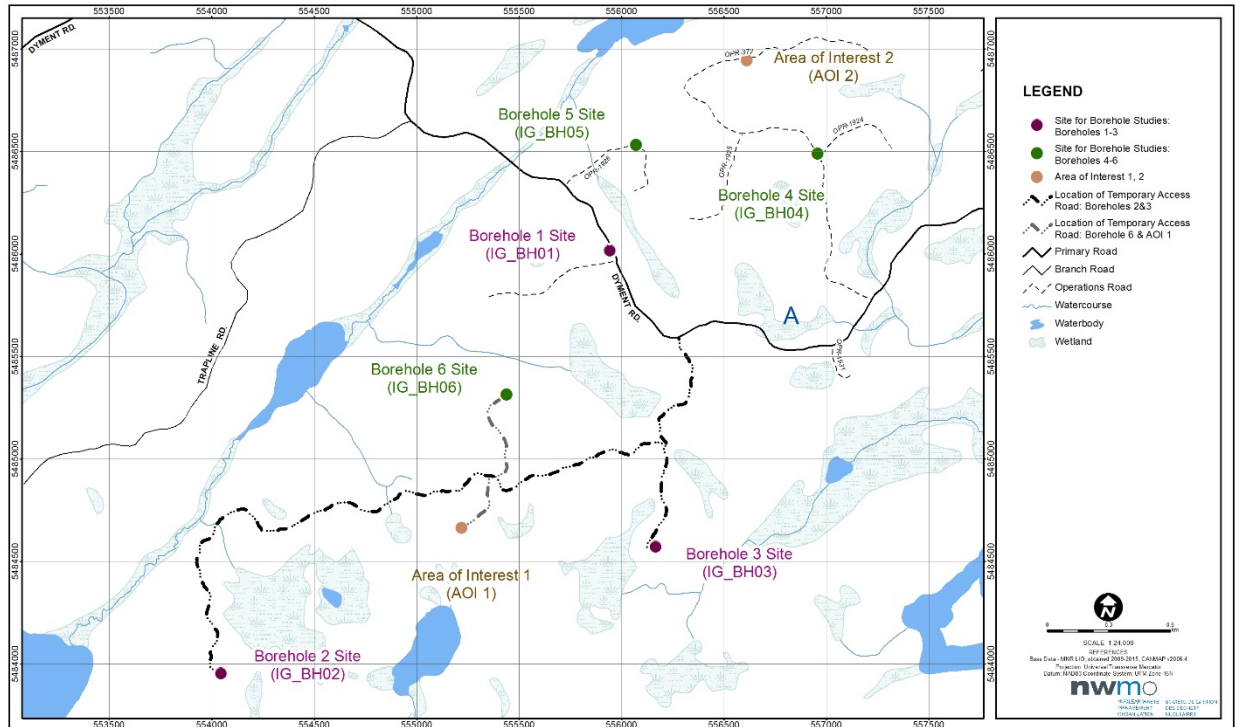


**Figure 7-3: Ignace Wabigoon - Location of Borehole Sites 1 to 6 and Area of Interest 1 and 2**

Environmental monitoring studies conducted in 2019 included the continuation of water and sediment monitoring, soil sampling at Boreholes 2, 3, 4, 5, and 6 pad locations as well as a fish usability assessment on Mennin Lake. In addition, significant wildlife habitat, nesting bird, bat habitat and aquatic features studies were conducted prior to tree clearing and road/drill pad building in support of Borehole 6 pad construction.

All surface water sampling sites from 2018 were revisited in 2019. In-situ water measurements and surface water sample collection occurred in June, August and October 2019. Sediment sampling occurred at all surface water sites in October 2019.

Soil samples in 2019 were collected at Borehole 2 and 3 sites as well as at borehole 4, 5 and 6 sites. All soils sampling followed discrete sampling methodology with a 3 x 3 grid pattern located on either the constructed pad or planned pad location with 2 reference samples located downgrade from the pad footprint. Borehole 2 and 3 pad soil sampling occurred in August and

June 2019, respectively. Sampling at these sites was considered post pad construction and completed by Tulloch and WLON guides. Sampled soils consisted of imported pit run gravel used to establish the pad and natural soils for the two reference samples located off the pad. Borehole 4, 5 and 6 site soil sampling was conducted by trained WLON guides supervised by either NWMO or Tulloch Environmental staff. These sampling events took place in October 2019 for boreholes 4 and 5 and November 2019 for borehole 6. Sampling at these three sites was considered pre-disturbance and was meant to serve as a baseline prior to importing material to construct the drill pads. Sampled material consisted of native soil both on the pad and outside of the pad footprint.

Two separate fish usability assessments were conducted on Mennin Lake in 2019. Mennin Lake was targeted for a fish usability study due to the fact that it is the main aquatic receptor downstream of the siting area and is heavily used by local community members and tourists as a prime fishing location. Fish sampling consisted of collecting standard fisheries assessment attributes from each lethally sampled specimen and submitting boneless, skinless tissue samples for analysis of total metals (including total mercury and methyl mercury) and % moisture. The first sampling event targeted walleye exclusively and took place under winter conditions in February 2019. Effort consisted of three days of under ice angling and yielded 3 walleye. The second of the two sampling events was more extensive and took place over a three day period in August 2019. During this time walleye and northern pike of varying sizes as well as bait fish were targeted. Standard angling and minnow trapping efforts yielded the sampling of 20 walleye, 12 northern pike and 14 composite samples consisting of baitfish sized yellow perch.

In October 2019, Tulloch environmental accompanied by a WLON guide completed a sweep of the undisturbed borehole 6 access road and pad. The purpose of this initiative was to identify any potentially significant wildlife habitat, nesting birds, bat habitat or aquatic features that may be affected by site establishment activities. During this sweep no significant habitat or watercourse crossings were identified. It was recommended that the clearing and road building work take place on the proposed route outside of the time sensitive breeding seasons for birds and bats in the area and with implementation of proper mitigation techniques to minimize any potential impacts on local flora and fauna.

## **7.2 SOUTH BRUCE/HURON-KINLOSS**

In 2019, NWMO's land access process was initiated. Site assessment activities in South Bruce/Huron-Kinloss mainly related to planning for drilling of initial boreholes in the area.

Regionally, information on the geology is available from the deep boreholes and detailed studies undertaken at the Bruce nuclear site in the adjacent Municipality of Kincardine. Ongoing studies of the southern Ontario geology have been noted in the previous Section 5.

**REFERENCES**

- Abrahamsen-Mills, L. and J. Small. 2019. State of Science Review: Modelling microbial effects to assess long-term performance of a DGR. Nuclear Waste Management Organization Report NWMO-TR-2019-15. Toronto, Canada.
- Ackerley, N., M. Kolaj, V. Peci and J. Adams. 2019. Recent Advances In Long-Term Seismic Monitoring And Hazard Assessment In Northern Ontario. 4<sup>th</sup> Canadian Conference on Nuclear Waste Management, Decommissioning and Environmental Restoration. Ottawa, Canada.
- AECL. 1994. Environmental Impact Statement on the concept for disposal of Canada's nuclear fuel waste. Atomic Energy of Canada Limited Report AECL-10711, COG-93-1. Chalk River, Canada.
- Al, T., I. Clark, L. Kennell, M. Jensen and K. Raven. 2015. Geochemical evolution and residence time of porewater in low-permeability rock of the Michigan Basin, Southwest Ontario. *Chemical Geology*, **404**, 1-17.
- Al-Asam, I.S. and R. Crowe. 2018. Fluid compartmentalization and dolomitization in the Cambrian and Ordovician successions of the Huron Domain, Michigan Basin. *Marine and Petroleum Geology*, **92**, 160-178.
- Alcorn, C.D., J.S. Cox, L. Applegarth and P. Tremaine. 2019. Investigation of uranyl sulfate complexation under hydrothermal conditions by quantitative Raman spectroscopy and density functional theory, *J. Physical Chemistry B* **123**, 7385-7409.
- Altmaier, M., V. Brendler, C. Bube, V. Neck, C. Marquardt, H.C. Moog, A. Richter, T. Schrage, W. Voigt, S. Wilhelm, T. Willms and G. Wollmann. 2011. THEREDA Thermodynamische Referenz-Datenbasis. Abschlussbericht (dt. Vollversion).
- Andersson, P., K. Beaugelin-Seiller, N.A. Beresford, D. Copplestone, C. Della Vedova, J. Garnier-Laplace, B. J. Howard, P. Howe, D.H. Oughton, C. Wells, P. Whitehouse. 2008. Deliverable 5: Numerical benchmarks for protecting biota from radiation in the environment: proposed levels, underlying reasoning and recommendations. PROTECT. Stockholm, Sweden.
- Armand, G., F. Bumbieler, N. Conil, R. de la Vaissière, J.-M. Bosgiraud and M.-N. Vu. 2017. Main outcomes from in situ thermo-hydro-mechanical experiments programme to demonstrate feasibility of radioactive high-level waste disposal in the Callovo-Oxfordian claystone. *J. Rock Mech. Geotech. Eng.* **9**, 415-427.
- Aquanty Inc. 2018. HydroGeoSphere User Manual, Aquanty Inc., Waterloo, Canada.
- Bailey Geological Services Ltd. and R.O. Cochrane. 1984a. Evaluation of the conventional and potential oil and gas reserves of the Cambrian of Ontario; Ontario Geological Survey, Open File Report 5499. Ontario, Canada.

- Bailey Geological Services Ltd. and R.O. Cochrane. 1984b. Evaluation of the conventional and potential oil and gas reserves of the Ordovician of Ontario; Ontario Geological Survey, Open File Report 5498. Ontario, Canada.
- Bastola, S., L. Fava and M. Cai. 2015. Validation of MoFrac 2.0 using the Äspö dataset. Nuclear Waste Management Organization Report NWMO TR-2015-25. Toronto, Canada.
- Birkholzer, J.T., C.F. Tsang, A.E. Bond, J.A. Hudson, L. Jing and O. Stephansson. 25 years of DECOVALEX - scientific advances and lessons learned from an international research collaboration in coupled subsurface processes. *Int J Rock Mech Min Sci.* 2019; 122: 103995.
- Booker, J.R. and C. Savvidou. 1985. Consolidation around a point heat source. *Int. J. Numerical Analytical Meth. Geomechanics* 9:173-185.
- Bradbury, M.H. and B. Baeyens. 2005. Modelling the sorption of Mn(II), Co(II), Ni(II), Zn(II), Cd(II), Eu(III), Am(III), Sn(IV), Th(IV), Np(V) and U(VI) on montmorillonite: Linear free energy relationships and estimates of surface binding constants for some selected heavy metals and actinides. *Geochimica et Cosmochimica Acta* 69, 875-892.
- Brooks, G.R. and A.J.-M. Pugin. 2019. Assessment of a seismo-neotectonic origin for the New Liskeard-Thornloe scarp, Timiskaming graben, northeastern Ontario. *Canadian Journal of Earth Sciences.* doi.org/10.1139/cjes-2019-0036.
- Carter, T.R., Brunton, F.R., Clark, J.K., Fortner, L., Freckelton, C., Logan, C.E., Russell, H.A.J., Somers, M., Sutherland, L. and Yeung, K.H. 2019. A three-dimensional geological model of the Paleozoic bedrock of southern Ontario; Geological Survey of Canada, Open File 8618, <https://doi.org/10.4095/315045>, Ontario Geological Survey, Groundwater Resources Study 19.
- Chen, J. M. Behazin, J. Binns, K. Birch, A. Blyth, S. Briggs, J. Freire-Canosa, G. Cheema, R. Crowe, D. Doyle, F. Garisto, J. Giallonardo, M. Gobien, R. Guo, S. Hirschorn, M. Hobbs, M. Ion, J. Jacyk, H. Kasani, P. Keech, E. Kremer, C. Lawrence, H. Leung, K. Liberda, T. Liyanage, J. McKelvie, C. Medri, M. Mielcarek, L. Kennell-Morrison, A. Murchison, A. Parmenter, M. Sanchez-Rico Castejon, U. Stahmer, Y. Sui, E. Sykes, M. Sykes, T. Yang, X. Zhang, B. Zhao. 2019. Technical Program for Long-Term Management of Canada's Used Nuclear Fuel - Annual Report 2018. Nuclear Waste Management Organization Report NWMO-TR-2019-01. Toronto, Canada.
- Chen, J.D., A.H. Kerr, E.A. Hildebrandt, E.L. Bialas, H.G. Delany, K.M. Wasywich, and C.R. Frost. 1989. Radiochemical Analysis of CANDU Used Fuel Stored in Concrete Canisters in Moist Air at 150°C. *Proceedings Second International Conference on CANDU Fuel.* pp. 337 – 351. Pembroke, Canada, October 1-5, 1989. (Also available at <https://inis.iaea.org>).
- Chen, J.D., P.A. Seeley, R. Taylor, D.C. Hartrick, N.L. Pshhyshlak, K.H. Wasywich, A. Rochon and K.I. Burns. 1986. Characterization of Corrosion Deposits and the Assessment of Fission Products Released from Used CANDU Fuel. *Proceedings 2<sup>nd</sup> International*

- Conference on Radioactive Waste Management. Winnipeg, Canada, 7-11 September 1986. Canadian Nuclear Society, Canada.
- Chen, Z., P. Hannigan, T. Carter, X. Liu, R. Crowe and M. Obermajer. 2019. A petroleum resource assessment of the Huron Domain. Nuclear Waste Management Organization Report NWMO-TR-2019-20. Toronto, Canada.
- Clark, I.D., T. Al, M. Jensen, L. Kennell, M. Mazurek, R. Mohapatra and K. Raven. 2013. Paleozoic-aged brine and authigenic helium preserved in an Ordovician shale aquiclude. *Geology*, 41, 9, 951-954.
- CNSC. 2018. Assessing the Long-Term Safety of Radioactive Waste Management. Canadian Nuclear Safety Commission Regulatory Document CNSC REGDOC-2.11.1 Volume III, Ottawa, Canada.
- CSA. 2003. Guidelines for Calculating Radiation Doses to the Public from a Release of Airborne Radioactive Material under Hypothetical Accident Conditions in Nuclear Reactors. Canadian Standards Association CSA N288.2-M91. Toronto, Canada.
- CSA. 2008. Guidelines for Calculating Derived Release Limits for Radioactive Material in Airborne and Liquid Effluents for Normal Operation of Nuclear Facilities. Canadian Standards Association CSA Guideline N288.1-08. Toronto, Canada.
- CSA. 2014. Guidelines for Calculating the Radiological Consequences to the Public of a Release of Airborne Radioactive Material for Nuclear Reactor Accidents. Canadian Standards Association CSA N288.2-14. Toronto, Canada.
- Davis, D.W., C.N. Sutcliffe, A.M. Thibodeau, J. Spalding, D. Schneider, A. Cruden, J. Adams, A. Parmenter, M. Jensen and Z. Zajacz. 2019. Hydrochronology of a proposed deep geological repository for low- and intermediate-level nuclear waste in southern Ontario from U–Pb dating of secondary minerals: response to Silurian and Cretaceous events. Submitted to *Canadian Journal of Earth Sciences*.
- Dixon, D. 2019. Review of the T-H-M-C Properties of MX-80 Bentonite. Nuclear Waste Management Organization Report NWMO-TR-2019-07. Toronto, Canada.
- Doughty, M., N. Eyles and L. Daurio. 2010. Ongoing neotectonic activity in the Timiskaming-Kipawa area of Ontario and Québec. *Geoscience Canada*, 37: 109-116.
- Doughty, M., N. Eyles and C.H. Eyles. 2013. High-resolution seismic reflection profiling of neotectonic faults in Lake Timiskaming, Timiskaming graben, Ontario-Quebec, Canada. *Sedimentology*, 60: 983-1006.
- Engel K., S. Coyotzi, M.A. Vachon, J.R. McKelvie and J.D. Neufeld. 2019a. Validating DNA Extraction Protocols for Bentonite Clay. *mSphere* 4(5). doi: 10.1128/mSphere.00334-19.

- Engel K., S. Ford, S. Coyotzi, J. McKelvie, N. Diomidis, G. Slater and J. Neufeld. 2019b. Stability of Microbial Community Profiles Associated with Compacted Bentonite from the Grimsel Underground Research Laboratory. *mSphere*, 4(6). doi: 10.1128/msphere.00601-19.
- Fernandes, S., K. Woolhouse and N. Thackeray. 2019. Supplementary Non-Radiological Interim Acceptance Criteria for the Protection of Persons and the Environment. Nuclear Waste Management Organization Report NWMO-TR-2017-05. Toronto, Canada.
- Freire-Canosa, J. 2019. The Impact of Used CANDU Fuel Exposure to 400°C Temperature during the Lid Closure Welding of the Used Fuel Container (UFC) for a DGR. CNS 4th Nuclear Waste Management Decommissioning and Environmental Remediation Conference. Ottawa, Canada.
- Garnier-Laplace, J., R. Gilbin, A. Agüero, F. Alonzo, M. Björk, Ph. Ciffroy, D. Copplestone, M. Gilek, T. Hertel-Aas, A. Jaworska, C-M. Larsson, D. Oughton and I. Zinger. 2006. Deliverable 5: Derivation of Predicted-No-Effect-Dose-Rate values for ecosystems (and their sub-organisational levels) exposure to radioactive substances. ERICA.
- Gobien, M. and M. Ion. 2019. Nuclear fuel waste projections in Canada – 2019 Update. Nuclear Waste Management Organization Report NWMO-TR-2019-14. Toronto, Canada.
- Gobien, M., S. Briggs, J. Chen, and C. Medri. ISM v1.0 Theory Manual. Nuclear Waste Management Organization Report NWMO-TR-2019-06. Toronto, Canada.
- Golder Associates Ltd. 2005. Hydrocarbon resource assessment of the Trenton-Black River hydrothermal dolomite play in Ontario; Ontario Oil, Gas and Salt Resources Library. Canada.
- Guo, R. 2017. Thermal response of a Canadian conceptual deep geological repository in crystalline rock and a method to correct the influence of the near-field adiabatic boundary condition. *Engineering Geology* 218 (2017) 50-62.
- Guo, R. 2019a. Coupled thermo-hydro-mechanical modelling of the multi-scale heating experiments – DECOVALEX–2019 Task E: Step 1, Step 2 and Step 3. Nuclear Waste Management Organization Report NWMO-TR-2019-11. Toronto, Canada.
- Guo, R. 2019b. Prediction of the Thermal-Hydraulic-Mechanical Response of a geological repository at large scale and sensitivity analyses – DECOVALEX-2019 Task E: Step 4. Nuclear Waste Management Organization Report NWMO-TR-2019-12. Toronto, Canada.
- Harper, J., T. Meierbachtol and N. Humphrey. 2019. Greenland ICE Project. Nuclear Waste Management Organization Report NWMO-TR-2019-16. Toronto, Canada.
- Health Canada. 2010. Part IV Guidance on Human Health Detailed Quantitative Radiological Risk Assessment. Ottawa, Canada.

- IAEA. 2006. Safety Requirements: Geological Disposal of Radioactive Waste. International Atomic Energy Agency Safety Requirements WS-R-4. Vienna, Austria.
- ICRP. 2007. The 2007 Recommendations of the International Commission on Radiological Protection. International Commission on Radiological Protection Publication 103, Annals of the ICRP (W2-4). Vienna, Austria.
- ICRP. 2008. Environmental Protection: the Concept and Use of Reference Animals and Plants. ICRP Publication 108. Vienna, Austria.
- ICRP. 2013. Radiological Protection in Geological Disposal of Long-lived Solid Radioactive Waste. International Commission on Radiological Protection Publication 122, Annals of the ICRP 42(3). Vienna, Austria.
- Jacobsson L. 2016. Parametrisation of Fractures - Direct Shear Tests on Calcite and Breccia infilled Rock Joints from Äspö HRL under Constant Normal Stiffness Condition, Posiva WR 2016-19, Posiva OY, Eurajoki, Finland.
- Junkin, W., E. Ben-Awuah and L. Fava. 2019a. DFN variability analysis through voxelization. Proc. ARMA 2019, 53<sup>rd</sup> US Rock Mechanics/Geomechanics Symposium, New York, USA.
- Junkin, W., E. Ben-Awuah and L. Fava. 2019b. Incorporating DFN analysis in rock engineering systems blast fragmentation models. Proc. ARMA 2019, 53<sup>rd</sup> US Rock Mechanics/Geomechanics Symposium, New York, USA.
- Junkin, W., L. Fava, E. Ben-Awuah and R.M. Srivastava. 2018. Analysis of MoFrac-generated deterministic and stochastic Discrete Fracture Network models. Proc. DFNE 2018, 2<sup>nd</sup> International Discrete Fracture Network Engineering Conference, Seattle, USA.
- Junkin W., D. Janeczek, S. Bastola, X. Wang, M. Cai, L. Fava, E. Sykes, R. Munier and R.M. Srivastava. 2017. Discrete Fracture Network generation for the Äspö TAS08 tunnel using MoFrac. Proc. ARMA 2017, 51<sup>st</sup> US Rock Mechanics/Geomechanics Symposium, San Francisco, USA.
- Kremer, E.P., J.D. Avis, J. Chen, P.J. Gierszewski, M. Gobien, R. Guo and C.L.D. Medri. 2019. Postclosure Safety Assessment of a Canadian Used Fuel Repository. 4th Canadian Conference on Nuclear Waste Management, Decommissioning and Environmental Restoration. Ottawa, Canada.
- Larsson, J. and M. Flansbjerg. 2019. An Approach to Compensate for the Influence of the System Normal Stiffness in CNS Direct Shear Tests. *Submitted to Rock Mechanics and Rock Engineering*.
- Lawrence, C., D. Doyle, A. Murchison and C. Boyle. 2019. Overview of Canada's Plan for the Long-Term Management of Used Nuclear Fuel. Waste Management Symposia 2019. Phoenix, USA.

- Lawrence, C., D. Doyle, A. Murchison and C. Boyle. 2019. Overview of the Development and Proof Testing of the Engineered Barrier System and Emplacement Technologies for the Long Term Management of Canada's Used Nuclear Fuel. 4th Canadian Conference on Nuclear Waste Management, Decommissioning and Environmental Restoration. Ottawa, Canada.
- Limer, L., R. Klos, R. Walke, G. Shaw., M. Nordén, S. Xu. 2013. Soil-plant-atmosphere modeling in the context of releases of  $^{14}\text{C}$  as a consequence of nuclear activities. *Radiocarbon* 55(2-3), 804-813.
- Limer, L. (Ed). 2019. C-14 in the Biosphere: Report of an International Workshop. BIOPROTA project report, Version 2.0. BIOPROTA, UK.
- Lindborg, T., M.Thorne, E.Andersson, J.Becker, J.Brandefelt, T.Cabianca, M.Gunia, A.T.K.Ikonen, E.Johansson, V.Kangasniemi, U.Kautsky, G.Kirchner, R.Klos, R.Kowe, A.Kontula, P.Kupiainen, A.-M.Lahdenperä, N.S.Lord, D.J.Lunt, J.-O.Näslund, M.Nordén, S.Norris, D.Pérez-Sánchez, A.Proverbio, K.Rieki, A.Rübel, L.Sweeck, R.Walke, S.Xu, G.Smith, G.Pröhl. 2018. Climate change and landscape development in post-closure safety assessment of solid waste disposal: Results of an initiative of the IAEA. *Journal of Environmental Radioactivity*. 183: 41-83.
- Liu, N., H. He, J.J Noël and D.W. Shoesmith. 2017a. The electrochemical study of  $\text{Dy}_2\text{O}_3$  doped  $\text{UO}_2$  in slightly alkaline sodium carbonate/bicarbonate and phosphate solutions, *Electrochimica Acta* 235, 654-663.
- Liu, N., J. Kim, J. Lee, Y-S. Youn, J-G. Kim, J-Y. Kim, J.J Noël and D.W. Shoesmith. 2017b. Influence of Gd doping on the structure and electrochemical behavior of  $\text{UO}_2$ , *Electrochimica Acta* 247, 496-504.
- Liu, N., Z. Qin, J.J Noël and D.W. Shoesmith. 2017c. Modelling the radiolytic corrosion of a-doped  $\text{UO}_2$  and spent nuclear fuel, *Journal of Nuclear Materials* 494, 87-94.
- Liu, N., Z. Zhu, J.J Noël and D.W. Shoesmith. 2018. Corrosion of nuclear fuel inside a failed waste container, *Encyclopedia of Interfacial Chemistry*, 2018, 172–182.
- Liu, N., Z. Zhu, L. Wu, Z. Qin, J.J Noël and D.W. Shoesmith. 2019. Predicting radionuclide release rates from spent nuclear fuel inside a failed waste disposal container using a finite element model, *Corrosion Journal* 75, 302-308.
- Malmberg. D. and K. Birch. 2019. Thermo-hydro-mechanical Modelling of NWMO Placement Room. 4th Canadian Conference on Nuclear Waste Management, Decommissioning and Environmental Restoration. September, 2019.
- Martin C.D. and N.A. Chandler. 1994. The progressive failure of Lac du Bonnet granite, *Int. J Rock Mech Min Sci*, 31, 643-659.
- Marty, N.C.M., P. Blanc, O. Bildstein, F. Claret, B. Cochapin, D. Su, E.C. Gaucher, D. Jacques, J.-E. Lartigue, K. U. Mayer, J.C.L Meeussen, I. Munier, I. Pointeau, S. Liu and C.

- Steeffel. 2015. Benchmark for reactive transport codes in the context of complex cement/clay interactions, *Computational Geosciences, Special Issue on: Subsurface Environmental Simulation Benchmarks*, doi: 10.1007/s10596-014-9463-6.
- Mayer, K.U., E.O. Frind and D.W. Blowes. 2002. Multicomponent reactive transport modelling in variably saturated porous media using a generalized formulation for kinetically controlled reactions. *Water Resources Research* 38, 1174, doi: 10.1029/2001WR000862.
- Mayer, K.U. and K.T.B. MacQuarrie. 2010. Solution of the MoMaS reactive transport benchmark with MIN3P - Model formulation and simulation results, *Computational Geosciences* 14, 405-419, doi: 10.1007/s10596-009-9158-6.
- Medri, C. 2015. Non-radiological interim acceptance criteria for the protection of persons and the environment. Nuclear Waste Management Organization Report NWMO-TR-2015-03. Toronto, Canada.
- Medri, C. and G. Bird. 2015. Non-Human Biota Dose Assessment Equations and Data. Nuclear Waste Management Organization Report NWMO TR-2014-02 R001. Toronto, Canada.
- Mompeán, F.J and H. Wanner. 2003. The OECD Nuclear Energy Agency thermodynamic database project. *Radiochimica Acta*, 91: 617-622.
- NEA. 2018. Metadata for Radioactive Waste Management. Report NEA# 7378. OECD Nuclear Energy Agency. Paris, France.
- NEA. 2019a. Preservation of Records, Knowledge and Memory across Generations: Developing a Key Information File for a Radioactive Waste Repository. Report NEA#7377. OECD Nuclear Energy Agency. Paris, France.
- NEA. 2019b. Preservation of Records, Knowledge and Memory (RK&M) across Generations: Compiling a Set of Essential Records for a Radioactive Waste Repository. Report NEA#7423. OECD Nuclear Energy Agency. Paris, France.
- NWMO. 2005. Choosing a Way Forward – The Future Management of Canada’s Nuclear Fuel – Final Study. Toronto, Canada.
- NWMO. 2019. RD 2019 – NWMO’s Program for research and development for long term management of used nuclear fuel. Nuclear Waste Management Organization Report NWMO-TR-2019-18. Toronto, Canada.
- NEA. 2019c. Preservation of Records, Knowledge and Memory across Generations: Final Report. Report NEA#7421. OECD Nuclear Energy Agency. Paris, France.
- NWMO. 2017. Postclosure Safety Assessment of a Used Fuel Repository in Crystalline Rock. Nuclear Waste Management Organization. NWMO-TR-2017-02. Toronto, Canada.
- NWMO. 2018. Postclosure Safety Assessment of a Used Fuel Repository in Sedimentary Rock. Nuclear Waste Management Organization. NWMO-TR-2018-08. Toronto, Canada.

- OHN. 1994. The disposal of Canada's nuclear fuel waste: Preclosure assessment of a conceptual system. Ontario Hydro Nuclear Report N-03784-940010 (UFMED), COG-93-6. Toronto, Canada.
- Pugin, A. J.-M., Brewer, K. and Brooks, G.R., 2019. Broadband waterborne hammer seismic source for imaging river and lake sub-bottoms. SEG International Exposition and 89th Annual Meeting, p. 2750-2754. <https://doi.org/10.1190/segam2019-3202612.1>.
- Racette, J., A. Walker, T. Yang and S. Nagasaki. 2019. Sorption of Se(-II): Batch Sorption Experiments on Limestone and Multi-site Sorption Modelling on Illite and Montmorillonite. Proceedings of 39<sup>th</sup> Annual Conference of the Canadian Nuclear Society and 43<sup>rd</sup> Annual CNS/CAN Student Conference, Ottawa, Canada.
- Reijonen, H., T. Karvonen and J.L. Cormenzana. 2014. Preliminary ALARA dose assessment for three APM DGR concepts. Nuclear Waste Management Organization Report NWMO TR-2014-18. Toronto, Canada.
- Reijonen, H., J.L. Cormenzana and T. Karvonen. 2016. Preliminary hazard identification for the Mark II conceptual design. Nuclear Waste Management Organization Report NWMO-TR-2016-02. Toronto, Canada.
- Selvadurai APS. 2019a. The Biot coefficient for a low permeability heterogeneous limestone, *Continuum Mechanics and Thermodynamics*, 31: 939–953.
- Selvadurai APS. 2019b. A multi-phasic perspective of the intact permeability of the heterogeneous argillaceous Cobourg limestone, *Scientific Reports*, 9: 17388, <https://doi.org/10.1038/s41598-019-53343-7>.
- Selvadurai APS and S. Rezaei Niya (2019c). Effective thermal conductivity of an intact heterogeneous limestone, *Rock Mech and Geotech Eng* (In press).
- Selvadurai APS, Selvadurai PA (2010). Surface permeability tests: Experiments and modelling for estimating effective permeability, *Proceedings of the Royal Society, Mathematical and Physical Sciences Series A*, 466: 2819-2846.
- Selvadurai PA, Selvadurai APS (2014). On the effective permeability of a heterogeneous porous medium: the role of the geometric mean, *Philosophical Magazine*, 94: 2318-2338.
- Siren T, Hakala M, Valli J, Christiansson R, Mas Ivars D, Lam T, Mattila J, Suikkanen J. 2017. Parametrisation of Fractures - Final Report, Posiva Report 2017-1, Posiva OY, Eurajoki, Finland.
- Smith, K. 2016. Update and Review of the IAEA BIOMASS-6 Reference Biosphere Methodology. Report of the first programme workshop. BIOPROTA, UK.

- Smith, K. 2017a. Update and Review of the IAEA BIOMASS Methodology. Report of the second workshop held in parallel with the first meeting of MORARIA II Working Group 6. BIOPROTA, UK.
- Smith, K. 2017b. Update and Review of the IAEA BIOMASS Methodology. Summary of the third workshop held in parallel with the first interim meeting of MORARIA II Working Group 6. BIOPROTA, UK.
- Smith, D.W. and J.R. Booker. 1993. Green's functions for a fully coupled thermoporoelastic material. *Int. J. Numerical Analytical Meth. Geomechanics* 17:139-163.
- Snowdon, A.P., J.F. Sykes and S.D. Normani. 2019. Topography scale effects on groundwater-surface water exchange fluxes in a Canadian Shield setting. *Submitted to Journal of Hydrology*.
- Stroes-Gascoyne, S., C.J. Hamon, P. Maak and S. Russell. 2010. The effects of the physical properties of highly compacted smectitic clay (bentonite) on the culturability of indigenous microorganisms. *Appl. Clay Sci.* 47:155-162.
- Sutcliffe, C.N., A.M. Thibodeau, D.W. Davis, I. Al-Aasm, A. Parmenter, Z. Zajacz and M. Jensen. 2019. Hydrochronology of a proposed deep geological repository for low- and intermediate-level nuclear waste in southern Ontario from U–Pb dating of secondary minerals: response to Alleghanian events. *Submitted to the Canadian Journal of Earth Sciences*.
- Su, D., K. U. Mayer and K.T.B. MacQuarrie, 2019a. Numerical investigation of flow instabilities using fully unstructured discretization for variably saturated flow problems. *Submitted to Advances in Water Resources*.
- Su, D., K. U. Mayer and K.T.B. MacQuarrie, 2019b. MIN3P-HPC: a high performance unstructured grid code for subsurface flow and reactive transport simulation. *Submitted to Mathematical Geosciences*.
- Suvorov AP, Selvadurai APS. 2019. The Biot coefficient for an elasto-plastic material, *Int J Eng. Sci.* 145: 103166.
- Thorne, M., K. Smith, I. Kovalets, R. Avila and R. Walke. 2018. Terrestrial model-data comparisons and review of carbon uptake by fish. BIOPROTA Report, Henley-on-Thames, UK.
- Tomonaga, Y., N. Giroud, M. S. Brennwald, E. Horstmann, N. Diomidis, R. Kipfer, P. Wersin. 2019. On-line monitoring of the gas composition in the Full-scale Emplacement experiment at Mont Terri (Switzerland). *Applied Geochemistry*, 100, 234-243. doi:10.1016/j.apgeochem.2018.11.015
- Tortola, M. 2019. Petrographic and Geochemical Attributes of Silurian and Devonian Dolomitized Formations in the Huron Domain, Michigan Basin. Master's Thesis, University of Windsor, Canada.

- US DOE. 1994. Airborne release fractions/rates and respirable fractions for non-reactor nuclear facilities. U.S. Department of Energy DOE-HDBK-3010-94. USA.
- US DOE. 2007. Preparation of safety basis documents for transuranic waste facilities. U.S. Department of Energy, DOE-STD-5506-2007. USA.
- US DOE. 2009. Yucca Mountain Repository SAR. U.S. Department of Energy, DOE/RW-0573, Rev. 1. USA.
- US INL. 2005. Damaged spent fuel at U.S. DOE Facilities, experience and lessons learned. Idaho National Laboratory Report INL/EXT-05-00760. Idaho, USA.
- Wilk, L. and G. Cantello. 2006. Used fuel burnups and power ratings for OPG owned used fuel. Ontario Power Generation Report 06819-REP-01300-10121. Toronto, Canada.
- Wilk, L. 2013. CANDU fuel burnup and power rating 2012 update. Nuclear Waste Management Organization Report NWMO TR-2013-02. Toronto, Canada.
- Vilks, P. 2011. Sorption of Selected Radionuclides on Sedimentary Rocks in Saline Conditions - Literature Review. Nuclear Waste Management Organization Report NWMO TR-2011-12, Toronto, Canada.
- Walker, A., J. Racette, J. Goguen and S. Nagasaki. 2018. Ionic Strength and pH Dependence of Sorption of Se(-II) onto Illite, Bentonite and Shale. Proceedings of 38th Annual Conference of the Canadian Nuclear Society and 42nd Annual CNS/CAN Student Conference, Saskatoon, SK, Canada, June 3-6, 2018.
- Wood. 2019. Climate Change Impacts Review and Method Development. NWMO-TR-2019-05. Toronto, Canada.
- Wu, M, M. Behazin, J. Nam and P. Keech. 2019. Internal Corrosion of Used Fuel Container. Nuclear Waste Management Organization Report NWMO-TR-2019-02. Toronto, Canada.
- Xie, M., P. Rasouli, K.U. Mayer and K.T.B. MacQuarrie. 2014. Reactive Transport Modelling of Diffusion in Low Permeable Media – MIN3P-THcm Simulations of EBS TF-C Compacted Bentonite Diffusion Experiments. Nuclear Waste Management Organization Report NWMO TR-2014-23. Toronto, Canada.
- Xie, M., D. Su, K.U. Mayer and K.T.B. MacQuarrie. 2018. Reactive Transport Modelling Investigation of Elevated Dissolved Sulphide Concentrations in Sedimentary Basin Rocks. Nuclear Waste Management Organization Report NWMO-TR-2018-07, Toronto, Canada
- Yu, B., J. Tam, W. Li, H.J. Cho, J.-G. Legoux, D. Poirier, J.D. Giallonardo and U. Erb, 2019. Microstructural and Bulk Properties Evolution of Cold Sprayed Copper Coatings after Low Temperature Annealing, *Materialia*, Vol. 7, p.100356.

Zhang, X., L. Lang, D. Doyle and C. Boyle. 2019. Development of the structural design basis of the long-term storage container for Canada's used nuclear fuel. 4th Canadian Conference on Nuclear Waste Management, Decommissioning and Environmental Restoration. Ottawa, Canada.

Zhu, Z., L. Wu, J.J Noël and D.W. Shoesmith. 2019. Anodic reactions occurring on simulated spent nuclear fuel (SIMFUEL) in hydrogen peroxide solutions containing bicarbonate/carbonate – The effect of fission products. *Electrochimica Acta* 320, 134546.

**APPENDIX A: NWMO TECHNICAL REPORTS AND REFEREED JOURNAL ARTICLES**

## A.1 NWMO TECHNICAL REPORTS

Abrahamsen-Mills, L. and J. Small. 2019. State of Science Review: Modelling microbial effects to assess long-term performance of a DGR. Nuclear Waste Management Organization Report NWMO-TR-2019-15. Toronto, Canada.

Chen, J. M. Behazin, J. Binns, K. Birch, A. Blyth, S. Briggs, J. Freire-Canosa, G. Cheema, R. Crowe, D. Doyle, F. Garisto, J. Giallonardo, M. Gobien, R. Guo, S. Hirschorn, M. Hobbs, M. Ion, J. Jacyk, H. Kasani, P. Keech, E. Kremer, C. Lawrence, H. Leung, K. Liberda, T. Liyanage, J. McKelvie, C. Medri, M. Mielcarek, L. Kennell-Morrison, A. Murchison, A. Parmenter, M. Sanchez-Rico Castejon, U. Stahmer, Y. Sui, E. Sykes, M. Sykes, T. Yang, X. Zhang, B. Zhao. 2019. Technical Program for Long-Term Management of Canada's Used Nuclear Fuel - Annual Report 2018. Nuclear Waste Management Organization Report NWMO-TR-2019-01. Toronto, Canada.

Chen, Z., P. Hannigan, T. Carter, X. Liu, R. Crowe and M. Obermajer. 2019. A petroleum resource assessment of the Huron Domain. Nuclear Waste Management Organization Report NWMO-TR-2019-20. Toronto, Canada.

Dixon, D. 2019. Review of the T-H-M-C Properties of MX-80 Bentonite. Nuclear Waste Management Organization Report NWMO-TR-2019-07. Toronto, Canada.

Gobien, M., S. Briggs, J. Chen and C. Medri. ISM v1.0 Theory Manual. Nuclear Waste Management Organization Report NWMO-TR-2019-06. Toronto, Canada.

Gobien, M. and M. Ion. 2019. Nuclear Fuel Waste Projections in Canada – 2019 Update. Nuclear Waste Management Organization Report NWMO-TR-2019-14. Toronto, Canada.

Guo, R. 2019a. Coupled thermo-hydro-mechanical modelling of the multi-scale heating experiments – DECOVALEX–2019 Task E: Step 1, Step 2 and Step 3. Nuclear Waste Management Organization Report NWMO-TR-2019-11. Toronto, Canada.

Guo, R. 2019b. Prediction of the Thermal-Hydraulic-Mechanical Response of a geological repository at large scale and sensitivity analyses – DECOVALEX-2019 Task E: Step 4. Nuclear Waste Management Organization Report NWMO-TR-2019-12. Toronto, Canada.

Harper, J., T. Meierbachtol and N. Humphrey. 2019. Greenland ICE Project. Nuclear Waste Management Organization Report NWMO-TR-2019-16. Toronto, Canada.

NWMO. 2019. RD 2019 – NWMO's Program for research and development for long term management of used nuclear fuel. Nuclear Waste Management Organization Report NWMO-TR-2019-18. Toronto, Canada.

Wood. 2019. Climate Change Impacts Review and Method Development. Nuclear Waste Management Organization Report NWMO-TR-2019-05. Toronto, Canada.

Wu, M., M. Behazin, J. Nam and P. Keech. 2019. Internal Corrosion of Used Fuel Container. Nuclear Waste Management Organization Report NWMO-TR-2019-02. Toronto, Canada.

## A.2 REFEREED JOURNAL ARTICLES

- Alcorn, C.D., J.S. Cox, L. Applegarth and P. Tremaine. 2019. Investigation of uranyl sulfate complexation under hydrothermal conditions by quantitative Raman spectroscopy and density functional theory, *Journal of Physical Chemistry B* 123, 7385-7409.
- Engel K., S. Coyotzi, M.A. Vachon, J.R. McKelvie and J.D. Neufeld. 2019. Validating DNA Extraction Protocols for Bentonite Clay. *mSphere* 4(5). doi: 10.1128/mSphere.00334-19
- Engel K., S. Ford, S. Coyotzi, J. McKelvie, N. Diomidis, G. Slater and J. Neufeld. 2019. Stability of Microbial Community Profiles Associated with Compacted Bentonite from the Grimsel Underground Research Laboratory. *mSphere*, 4(6). doi: 10.1128/msphere.00601-19.
- Guo, M., J. Chen, T. Martino, M. Biesinger, J.J. Noël, D.W. Shoesmith. 2019. The susceptibility of copper to pitting corrosion in borate-buffered aqueous solutions containing chloride and sulphide. *J. Electrochem. Society*, 166:C550-C558.
- Järvine, A., A.G. Murchison, P.G. Keech, M.D. Pandey. 2019. A probabilistic model for estimating the life expectancy of used nuclear fuel containers in a Canadian geological repository: baseline model. *Nuclear Eng. Design*, 352:110202.
- Martino, T., J. Smith, J. Chen, Z. Qin, J.J. Noël, and D.W. Shoesmith. 2019. The properties of electrochemically-grown copper sulfide films. *J. Electrochemical Society*, 166:C9-C18.
- Necib, S., M.L. Schlegel, C. Bataillon, S. Daumas, N. Diomidis, P. Keech, D. Crusset. 2019. Long-term Corrosion Behaviour of Carbon Steel and Stainless Steel in Opalinus Clay: Influence of Stepwise Temperature Increase. *Corrosion Eng. Science Techn.* 54:516.
- Poirier, D., J.G. Legoux, P. Vo, B. Blais, J.D. Giallonardo, P.G. Keech. 2019. Powder Development and Qualification for High-Performance Cold Spray Copper Coatings on Steel Substrates. *J. Thermal Spray Tech.* doi.org/10.1007/s11666-019-00833-9
- Selvadurai, P. 2019a. The Biot coefficient for a low permeability heterogeneous limestone. *Continuum Mechanics and Thermodynamics* 31(5):939-953. doi: 10.1007/s00161-018-0653-7
- Selvadurai P. 2019b. A multi-phasic perspective of the intact permeability of the heterogeneous argillaceous Cobourg limestone, *Scientific Reports*, 9: 17388, <https://doi.org/10.1038/s41598-019-53343-7>.
- Senior, N.A., R.C. Newman, D. Artymowicz, W.J. Binns, P.G. Keech and D.S. Hall. 2019. A Method to Measure Extremely Low Corrosion Rates of Copper Metal in Anoxic Aqueous Media, *J. Electrochemical Society* 166:C3015-C3017.
- Standish, T.E., L.J. Braithwaite, D.W. Shoesmith and J.J. Noël. 2019. Influence of area ratio and chloride concentration on the galvanic coupling of copper and carbon steel. *J. Electrochemical Society*, 166:C3448-C3455.

- Suvorov, A.P., and A.P.S. Selvadurai. 2019. The Biot coefficient for an elasto-plastic material, *Int J Eng. Sci*, 145: 103166.
- Vazaios, I., M. Diederichs and N. Vlachopoulos. 2019. Assessment of strain bursting in deep tunnelling by using the finite-discrete element method. *J Rock Mechanics and Geotechnical Engineering*, 11:12-37. doi:10.1016/j.jrmge.2018.06.007
- Vazaios, I., N. Vlachopoulos and M. Diederichs. 2019. Assessing fracturing mechanisms and evolution of excavation damage zone of tunnels in interlocked rock masses at high stresses using a finite-discrete element approach. *J Rock Mechanics and Geotechnical Engineering*. 11(4):701-722. doi:10.1016/j.jrmge.2019.02.004
- Vazaios, I., N. Vlachopoulos and M. Diederichs. 2019. The mechanical analysis and interpretation of the EDZ formation around deep tunnels within massive rockmasses using a hybrid finite-discrete element approach: The case of the AECL URL Test Tunnel. *Canadian Geotechnical J*, 56(1):35-59. doi:10.1139/cgj-2017-0578
- Yu B., J. Tam, W. Li, H.J. Cho, J.G. Legoux, D. Poirier, J.D. Giallonardo and U. Erb. 2019. Microstructural and Bulk Properties Evolution of Cold-Sprayed Copper Coatings after Low Temperature Annealing, *Materialia*, 7:100356.
- Zhu, Z., L. Wu, J.J. Noël, and D.W. Shoesmith. 2019. Anodic reactions occurring on simulated spent nuclear fuel (SIMFUEL) in hydrogen peroxide solutions containing bicarbonate/carbonate—The effect of fission products. *Electrochimica Acta*, 320, 134546.